Structural and Functional Analysis of FLOWERING LOCUS T in *Arabidopsis thaliana*

Dissertation

der Mathematisch-Naturwissenschaftlichen Fakultät

der Eberhard Karls Universität Tübingen

zur Erlangung des Grades eines

Doktors der Naturwissenschaften

(Dr. rer. nat.)

vorgelegt von

William Wing Ho HO

aus Hong Kong S.A.R., China

Tübingen

2013

Tag der mündlichen Qualifikation:	25.02.2013
Dekan:	Prof. Dr. Wolfgang Rosenstiel
1. Berichterstatter:	Prof. Dr. Detlef Weigel
2. Berichterstatter:	Prof. Dr. Friedrich Schöffl

Table of Contents

Summary

In plant life cycle, onset of flowering is an important event controlled by a complex network of interacting pathways. In plants such as *Arabidopsis thaliana*, in which flowering is promoted under long days, day-length pathways play an important role. Inductive conditions lead to the production of FLOWERING LOCUS T (FT) protein in leaves. This protein then travels through the phloem to the shoot apex. There, it interacts via GENERAL REGULATORY FACTOR (GRF/14-3-3) proteins with the FD transcription factor to directly activate different flower-identity genes. The floral promoting activity of FT is, however, antagonized by floral repressing TERMINAL FLOWER 1 (TFL1), expressed specifically at the shoot apex. Though opposite in function, both FT and TFL1 are members of the PEBP (phosphatidylethanolamine binding protein) family.

Previous studies have shown that TFL1 can function similarly to the floral promoting FT via a single amino acid change (H88Y), but the corresponding mutation on the FT backbone (Y85H) cannot convert FT into a floral repressing molecule (Hanzawa et al., 2005). Later, exonic swapping between *FT* and *TFL1* demonstrated that the motif encoded by exon 4B and 4C is required for FT function, while either exon 4B or 4C is sufficient for TFL1 activity (Ahn et al., 2006). However, swapping of exon 4B between a floral repressing *BvFT1* and floral promoting *BvFT2* (*FT* paralogs in sugar beet) can only convert BvFT1 into BvFT2 (Pin et al., 2010). Data supporting the conversion from BvFT2 to BvFT1 was not conclusive. In spite of these findings, it is still unclear if residues other than Y85 and the motif encoded by exon 4B and 4C would contribute to the floral promoting function of FT. Also, recent findings postulated the existence of a coactivator of FT, such additional regulatory modules of FT have been found in the flowering network of other plant species, implying apparent gaps in FT studies.

After the introductory Chapter 1, in Chapter 2 of this thesis, I present the first part of my work targeted at identifying and characterizing the functional determinants of the florigenic identity of FT. By creating and examining hundreds of mutated versions of the FT protein, I could show that six amino acid residues encoded by exon 4 are critical to FT function. Among them, four residues (E109, Q140, N152 and L128) play an essential role for maintaining the charge of two localized regions coined as Binding Pocket Peripheral (BPP) and exon 4B and 4C encoded Lobe (BCL). As shown by my overexpression and complementation studies, when mutation of these residues retains the localized charge, FT function is not affected, but mutations that introduce positive charge to the regions are sufficient to convert FT into a fully functional TFL1. In addition, two other residues (W138 at BPP and Y134 at BCL) with protruding aromatic side groups were also found to be critical for maintaining FT florigenic identity. However, they are independent of charge and do not tolerate most kinds of substitutions. Together with the aromatic Y85 located in the previously described anion binding pocket (ABP) of PEBP, a role for their potential involvement in the intermolecular binding with a functionally critical ligand is proposed. Further, the ABP

is negative in charge. However, based on the latest findings, ABP does bind with negatively charged ligands (Tavel et al., 2012), implying that the specific charge and bondings maintained by the six residues may be responsible for opposing a repulsive force during the docking of ligand. Such a “repulsive lock” is believed to add one more layer of selectivity to the ligand binding, thereby increasing the stringency of control for this crucial developmental switch.

To identify the potential coactivator of FT that could bind to the promoting function-defining regions (such as the negatively charged BPP), in Chapter 3 of this thesis, I present the second part of my work that made use of interaction assays in yeast and *in planta* to test whether the previously identified FT interactors might selectively bind to FT, while neither binding to TFL1, nor to FT with charge reverted at the region BPP. Surprisingly, both the transcription factor FD and the bridging molecule, GRF/14-3-3 protein, are bound to FT, TFL1 and the charge-reverted FT. In contrast, selected members of the TCP (TEOSINTE BRANCHED1, CYCLOIDEA, PCF) family of transcription factors could distinguish between FT and both TFL1 and the charge-reverted FT. This finding suggests that TCPs might potentially serve as FT-specific factors in flowering time control. As shown by the analysis of the single insertion lines and combinations of T-DNA insertion lines of *TCP*s, individual TCP-clades may act redundantly on flowering time control. Further, by means of systematic knockdown of *TCP* by artificial microRNA (amiRNA), I demonstrated the involvement of the TCP5 clade, specific members of the TCP8 clade and TCP4 alone in modulating flowering time, implying the potential of TCPs for serving as an FT coactivator during the floral transition.

In summary, my work identified and characterized novel elements constituting the FT florigenic identity. Together with the additional findings supplementing the previously identified determinants, I provide an integral viewpoint on factors determining FT florigenic identity. Further, the uncovering of specific requirements, such as charge maintenance, for the function-defining residues suggested their role in recruiting an important FT coactivator. Indeed, I could identify several TCP transcription factors that can interact preferentially with the non-mutated FT, but not with the charge-reverted version of FT. As amiRNA knockdown mutants of specific *TCP* candidates showed defects in flowering time control, TCP proteins are good candidates for the postulated coactivator involved in the FT-mediated floral transition.

Zusammenfassung

Die Induktion des Blühens ist ein wichtiges Ereignis im Lebenszyklus einer Pflanze. Sie wird von einem komplexen Netzwerk interagierender Signalwege kontrolliert. In Pflanzen wie *Arabidopsis thaliana*, in welchen das Blühen durch lange Tage induziert wird, spielen Signalwege, die Tageslängen übermitteln, eine wichtige Rolle. Induzierende Bedingungen führen zur Produktion des FLOWERING LOCUS T (FT) Proteins in Blättern. Dieses Protein wandert dann durch das Phloem an den Sproß-Apex. Dort interagiert es über GENERAL REGULATORY FACTOR (GRF/14-3-3) Proteine mit dem Transkriptionsfaktor FD, wodurch auf direktem Weg Blüten-Identitätsgene aktiviert werden. Der Aktivität von FT wirkt jedoch das TERMINAL FLOWER 1 (TFL1) Protein entgegen, welches spezifisch am Sproß-Apex produziert wird. Trotz ihrer gegensätzlichen Funktion sind sowohl FT als auch TFL1 Teil der PEBP (phosphatidylethanolamine binding protein) Protein-Familie.

Frühere Studien haben gezeigt, dass der Austausch einer einzigen Aminosäure (H88Y) ausreicht, um TFL1 in ein das Blühen induzierende FT umzuwandeln. Die vergleichbare Mutation in FT hingegen (Y85H) konnte FT nicht in einen Blüh-Repressor verwandeln (Hanzawa et al., 2005). Später wurde mittels Austausch von Exonen zwischen *FT* und *TFL1* gezeigt, dass ein Motif, das von Exon 4B und 4C kodiert wird, für die Funktion von FT absolut erforderlich ist. Hingegen ist jedes einzelne der beiden Exon-Teile ausreichend, um die TFL1-Funktion zu vermitteln (Ahn et al., 2006). Ähnlich in der Zuckerrübe, wo der Austausch von Exon 4B das blühreprimierende *FT1* in das blühfördernde *FT2* Paralog verwandeln kann (Pin et al., 2010), während die Daten zur Umwandlung von *FT2* in *FT1* nicht schlüssig waren. Trotz dieser Ergebnisse ist noch immer unklar, ob außer Y85 und dem Exon4-Motif noch andere Aminosäuren zur blühinduzierenden Funktion von FT beitragen. Zusätzlich haben neue Erkenntnisse zur Postulierung eines Ko-Aktivators von FT geführt; solche zusätzlichen regulatorischen Elemente wurden schon in den Blühnetzwerken in anderern Pflanzen gefunden, was impliziert, dass es noch immer offensichtliche Lücken in den FT-Studien gibt.

Nach einem einleitenden Kapitel, beschreibe ich im zweiten Kapitel dieser Arbeit den ersten Teil meines Projekts, dessen Absicht es war, Faktoren zu identifizieren und zu charakterisieren, die FT seine blühinduzierende Funktion verleihen. Mittels exzessiver Mutagenese Analyse und elektrostatischer Analyse in silico wurden hunderte mutierter Versionen von FT generiert. Ich konnte zeigen, dass sechs Aminosäuren, die in Exon 4 kodiert werden, essentiell für die Funktion von FT sind. Von diesen sind vier (E109, Q140, N152 und L128) wichtig, um die Ladung in zwei begrenzten Regionen zu erhalten, der ‘Binding Pocket Peripheral’ (BPP) und der ‘Exon 4B and 4C encoded Lobe’ (BCL). Durch meine Überexpressions- und Komplementations-Studien konnte ich zeigen, dass Änderungen dieser Aminosäure-Reste die FT-Funktion nicht beeinträchtigen, solange sie die lokale Ladung erhalten. Mutationen, die eine positive Ladung in die Regionen einbringen, sind hingegen ausreichend, um FT in ein voll funktionales TFL1 Protein umzuwandeln. Zusätzlich wurden noch zwei weitere Aminosäure-Reste (W138 in der BPP-Region und Y134 in der BCL-Region) mit aromatischen Seitengruppen an kritischen Stellen identifiziert, die für die blühinduzierende Funktion von FT wichtig waren. Diese Positionen waren

jedoch unabhängig von ihrer Ladung und konnten keinerlei Mutationen tolerieren. Unter Berücksichtigung der aromatischen Y85 Position an der beschriebenen ‘Anion Binding Pocket’ (ABP) der PEBP Proteine wurde eine Rolle für diese aromatischen Aminosäuren in der intermolekularen Bindung eines potentiell relevanten Liganden vorgeschlagen. Hinzu kommt, dass die ABP eine negativ geladene Oberfläche bildet, während neuste Erkenntnisse die ABP mit negativ geladenen Liganden in Verbindung bringt (Tavel et al., 2012). Dies lässt vermuten, dass die spezifische Ladung und die Bindungen, die von den sieben Aminosäuren gebildet werden, zu einer abstoßenden Kraft während der Interaktion mit Liganden führen könnte. Von solch einem ‘repulsive lock’ wird angenommen, dass es eine zusätzliche Spezifitätskontrolle bei der Liganden-Bindung darstellt und so die Stringenz erhöht, mit der dieser wichtige Entwicklungs-Schritt kontrolliert wird.

Um den potentiellen Ko-Aktivator von FT zu identifizieren, der an die beschriebenen Regionen, wie zum Beispiel die negative geladene BPP, binden kann, beschreibe ich im dritten Kapitel meine Ergebnisse, die ich mit Hilfe von Interaktions-Studien in Hefe und *in planta* generiert habe. Hierbei wurden schon beschriebene FT-Interaktoren darauf getestet, ob sie selektiv an FT binden konnten, aber weder an TFL1 noch an die mutierten FT Proteine, in denen die Ladung an der BPP verändert wurde. Überraschenderweise interagierten sowohl der Transkriptionsfaktor FD und die Brückenmoleküle GENERAL REGULATORY FACTOR (GRF/14-3-3) sowohl mit FT als auch mit TFL1 und dem ladungsveränderten FT. Hingegen konnten Mitglieder der TCP (TEOSINTE BRANCHED1, CYCLOIDEA, PCF) Transkriptionsfaktor-Familie zwischen FT und TFL1/verändertem FT unterscheiden. Dies impliziert, dass TCP Proteine potentiell als FT-spezifische Faktoren in der Blühkontrolle agieren könnten. Die Analyse von einzelnen *tcp* T-DNA Mutanten erster und dritter Ordnung, und auch Kombinationen von Mutanten höherer Ordnung hat gezeigt, dass einzelne Zweige eng verwandter TCP Proteine redundante Funktionen einnehmen können. Durch den systematischen knock-down von TCP Proteinen durch artifizielle microRNAs konnte ich zeigen, dass sowohl der TCP5-Zweig also auch Mitglieder des TCP8-Zweigs und TCP4 eine Rolle in der Blühinduktion spielen und dadurch potentiell als Ko-Faktoren von FT während der Blühinduktion dienen könnten.

Zusammengefasst habe ich in meiner Arbeit Elemente identifiziert und charakterisiert, die zur blühinduzierenden Funktion von FT beitragen. Unter Berücksichtigung der schon vorher bekannten Elemente liefert diese Arbeit einen wesentlichen Beitrag unserem Verständnis zur der Blühinduktion via FT. Die Aufdeckung spezieller Anforderungen, wie der Ladungs-Erhaltung an den funktionell relevanten Aminosäuren im FT Protein, hat dazu geführt, eine potentielle Rolle dieser Aminosäuren in der Rekrutierung von wichtigen Ko-Faktoren anzunehmen. In der Tat konnte ich mehrere TCP Transkriptionsfaktoren identifizieren, die exklusiv mit FT, aber nicht mit den ladungsveränderten Versionen von FT interagieren konnten. Der knock-down von *TCP* Kandidaten-Proteinen Genen über artifizielle microRNAs hat Veränderungen im Blühzeitpunkt ergeben, weshalb TCP Proteine nun gute Kandidaten für den postulierten Ko-Aktivator in der FT-bedingten Kontrolle der Blühinduktion darstellen.

Chapter 1 General Introduction

1.1. Flowering

During their life cycle, plants undergo several developmental transitions. The first one is germination, which is the transition from an embryonic to a post-embryonic mode of growth. Subsequently, seedlings pass through a juvenile vegetative phase, where nutrients, and thus biomass, are accumulated. Then, it is followed by a transition to the adult vegetative phase, where plants can respond to floral inductive signals. With such capacity, mature plants can then enter a reproductive phase, where shoot apical meristem start to produce flowers instead of leaves. Such transition is known as the initiation of flowering (Bäurle and Dean, 2006).

Sophisticated regulatory networks monitoring such discrete environmental cues as day length and winter temperature control the timing of flowering (Lang, 1952). In response to these cues, expression of diverse environmentally responsive transcription factors are modulated and converged to a small number of floral integrator genes that initiate the early stages of flowering (Corbesier and Coupland, 2006). With such strict regulation, flowering can occur under conditions most likely to maximize reproductive success while seed production can be ensured (Purugganan and Fuller, 2009). In the model plant species *Arabidopsis thaliana*, around 180 genes have been implicated in flowering time control (Fornara et al., 2010). Depending on the type of cues they responded to, most of these genes can be categorized into five floral regulatory pathways known as: photoperiodic pathway, vernalization pathway, autonomous pathway, gibberellic acid pathway, and age pathway.

1.2 Flowering Control in *Arabidopsis thaliana*

1.2.1 Photoperiodic Pathway

Flowering of *Arabidopsis* is promoted by exposure to long days (LD), but repressed by short days (SD). The day-length dependent flowering is regulated by photoperiodic pathway. Activation of the photoperiodic pathway leads to the transcriptional activation of florigen FLOWERING LOCUS T (FT), which occurs only under long days (Kardailsky, 1999; Kobayashi, 1999). This LD-dependent activation of FT requires the triggering by the zinc-finger transcriptional regulator CONSTANS (CO) (Putterill et al., 1995) that is tightly regulated at both transcriptional and post-translational levels.

1.2.1.1 Transcriptional Regulation of *CO*

A range of DOF transcription factors known as CYCLING DOF FACTORs (CDFs) repress flowering by down-regulating *CO* expression in leaves. However, at the end of LD, light promotes the interaction between the circadian regulated GIGANTEA (GI) and a family of F-box ubiquitin ligases, such as FLAVIN-

BINDING KELCH REPEAT F-BOX 1 (FKF1) protein. These interactions stabilize the F-box proteins, allowing them to promote the degradation of CDFs (Figure 1A). On the contrary, under SD conditions, *GI* and *FKF1* expression peak at the dark phase preventing the formation of a stable GI-FKF1 complex. The CDF proteins are therefore required to repress *CO* transcription (Fornara et al., 2009; Sawa et al., 2007).

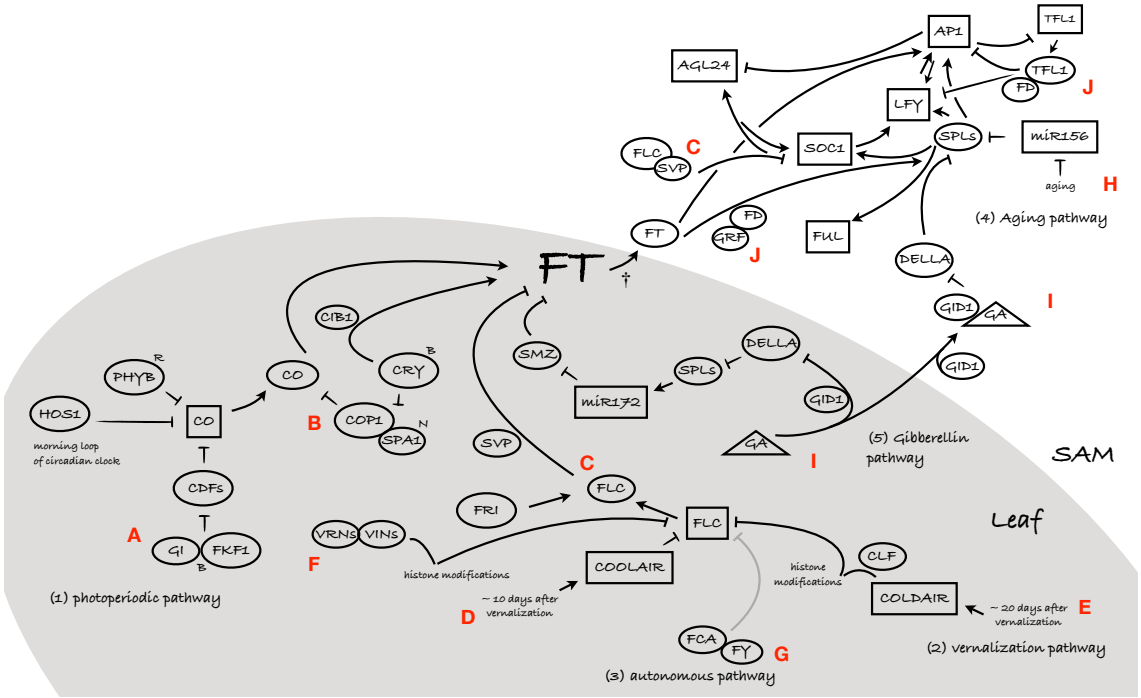

Figure 1. Control of flowering in *Arabidopsis thaliana*. **(A)** Transcriptional regulation of *CO* expression. CYCLING DOF FACTORS; GI, GIGANTEA; FKF1, FLAVIN-BINDING KELCH REPEAT F-BOX1; B, blue light input at the end of LD. **(B)** Post-translational regulation of CO protein. PHYB, phytochrome B; R, red light input during the morning phase; HOS1, HIGH EXPRESSION OF OSMOTICALLY RESPONSIVE GENE 1 (HOS1); COP1, CONSTITUTIVE PHOTOMORPHOGENIC 1; SPA1, SUPPRESSOR OF PHYTOCHROME A; N, activity predominant during the night, light during the daytime reduces its activity; CRYTOCHROME2 (CRY2). Remark: light-activated CRY2 can physically interact with cryptochrome-interacting basic-helix-loop-helix (CIB1) to promote *FT* expression (Liu et al., 2008a). **(C)** Transcriptional regulation by FLC-SVP complex. FLC, FLOWERING LOCUS C; SVP, SHORT VEGETATIVE PHASE (SVP); SOC1, SUPPRESSOR OF OVEREXPRESSION OF CONSTANS 1. Remark: FRIGIDA (FRI) is a coiled-coiled protein that promotes *FLC* transcription (Johanson, 2000). **(D)** Initial repression of *FLC* transcription. **(E)** Initiation of extended *FLC* repression. CLF, CURLY LEAF. **(F)** Stabilization of *FLC* repression. VIN3, VERNALIZATION INSENSITIVE 3, VRN2, VERNALIZATION 2. **(G)** Regulation of *FLC* expression by FCA-FY complex of the autonomous pathway. **(H)** Regulation of MADS box floral patterning network at SAM by aging pathway. SPL, SQUAMOSA PROMOTER BINDING PROTEIN-LIKE; miR156, microRNA 156; SAM, shoot apical meristem. **(I)** Gibberellic acid-mediated control of flowering in leaves and in SAM. GA, gibberellic acid; GID1, GIBBERELLIN INSENSITIVE DWARF1; miR172, microRNA172; SMZ, SCHLAFMUTZE. **(J)** Repression of meristem identity gene by TFL1-FD and antagonistic action of FT-GRF-FD in SAM. AP1, APETALA1; LFY, LEAFY; TFL1, TERMINAL FLOWER 1; GENERAL REGULATORY FACTOR (GRF); FRUITFULL (FUL). Symbol † represents the long distance movement of FT protein from phloem companion cells of leaves to SAM. Arrow indicates positive interaction; perpendicular line indicates negative interaction; grey lines represent uncertain interactions. Genes or RNAs are in rectangular shape, proteins are in circle, while hormones are in triangular shape (Figure modified based on Fornara et al., 2010).

1.2.1.2 Post-Translational Regulation of CO

Besides the morning degradation of *CO* mediated by photoreceptor Phytochrome B (PHYB) and HIGH EXPRESSION OF OSMOTICALLY RESPONSIVE GENE 1 (HOS1) (Lazaro et al., 2012; Valverde, 2004), CO protein is ubiquitylated by a ubiquitin ligase complex constituted by CONSTITUTIVE PHOTOMORPHOGENIC 1 (COP1) and SUPPRESSOR OF PHYTOCHROME A (SPA1) (Figure 1B). Such modification of CO facilitates its degradation mediated by 26S proteosome (Jang et al., 2008; Laubinger et al., 2006; Liu et al., 2008b). Activity of the COP1-SPA1 complex is repressed by light. At the time *GI*, *FKF1*, and *CO* peak their expression (at around 10 hours after dawn under SD), any CO protein formed is degraded by the COP1-SPA1. In contrast, under LD, the occurrence of a light phase can reduce the activity of the COP1-SPA1 complex, leading to CO not being efficiently degraded. Together with the fact that light-activated CRYPTOCHROME 2 (CRY2) can physically interact either with SPA1 or COP1 to stabilize any CO protein formed at the end of the LD, catalytic activity of COP1–SPA1 is weakened and CO protein can thus accumulate (Briggs and Olney, 2001; Zuo et al., 2011).

On the whole, circadian patterns of *GI* and *FKF1* transcription together with the post-translational modulation create the diurnal rhythms of *CO* expression. Whether the rhythm coincides with the exposure to light determines the accumulation of CO proteins and thus flowering.

1.2.2 Vernalization Pathway

FLOWERING LOCUS C (FLC) is a MADS-box transcription factor that acts as a potent repressor of flowering. FLC action is mediated by physically interacting with another MADS box protein, SHORT VEGETATIVE PHASE (SVP). SVP is proposed to have the ability to recruit chromatin modifiers that block transcription of floral promoting genes, such as *SUPPRESSOR OF OVEREXPRESSION OF CONSTANS 1* (*SOC1*), in shoot apical meristem (SAM) and *FT* in vasculature of leaves (Figure 1C) (Fujiwara et al., 2008; Lee et al., 2007; Li et al., 2008).

Activity of FLC differs among varieties of *Arabidopsis* and is responsible for much of the variation in flowering time observed among these plants. The vernalization pathway activates flowering by silencing *FLC* in response to prolonged exposure to low temperatures, allowing transcriptional induction of *FT* and its paralog, *TWIN SISTER OF FT* (*TSF*), by CO under subsequent long days. *FLC* repression in response to vernalization can be considered in three phases: (1) initial repression of *FLC* transcription, (2) initiation of extended *FLC* repression and (3) stabilization of *FLC* repression (Gendall et al., 2001; Michaels and Amasino, 1999).

1.2.2.1 Initial Repression of *FLC* Transcription

Repression of *FLC* transcription at the beginning of the vernalization correlates with the expression of a non-coding RNA. At around 10 days after the start of vernalization, the expression of the antisense non-coding RNA *COOLAIR* reaches a peak and then subsides to low levels (Swiezewski et al., 2009). This peak of *COOLAIR* expression correlates with the beginning of decrease of *FLC* mRNA abundance (Figure

1D). *COOLAIR* is expressed from a promoter found at the 3′ end of the *FLC* gene. Insertion of this promoter at the 3′ end of *GFP* marker gene expressed from the heterologous cauliflower mosaic virus 35S causes a cold-dependent reduction in *GFP* mRNA.

1.2.2.2 Initiation of Extended *FLC* Repression

At around 20 days after the start of vernalization, a second non-coding RNA, *COLDAIR*, reaches a peak in expression. This sense RNA is transcribed from the genomic sequences, that also give rise to the first intron of *FLC* sense transcript and appears to be expressed from a vernalization response element. *COLDAIR* functions by recruiting a component of Polycomb repressive complex 2 (PRC2), known as CURLY LEAF (CLF) protein, to the *FLC* locus (Figure 1D). Formation of PRC2 can in turn introduce histone H3 lysine 27 trimethylation (H3K27me3) and lead to histone modification at the *FLC* locus (De Lucia et al., 2008; Goodrich et al., 1997; Heo and Sung, 2011). In the first four weeks of vernalization, the chromatin mark increases around the transcriptional start site and the first exon of *FLC*, and later in vernalization further spreads across the first intron. In this way, H3K27me3 remains enriched at the locus and continues to spread across the whole coding sequence (Angel et al., 2011; Finnegan and Dennis, 2007).

1.2.2.3 Stabilization of *FLC* Repression

Maintenance of *FLC* repression, even after plants are returned to warmer temperatures, requires further histone modifications at the chromatin of the *FLC* locus. In Col-0 reference background, these modifications involve the PHD finger protein VERNALIZATION INSENSITIVE 3 (VIN3) and a POLYCOMB REPRESSIVE COMPLEX 2 (PRC2) that includes VERNALIZATION 2 (VRN2) (He and Amasino, 2005) (Figure 1F). At around 40 days after the start of vernalization when *COLDAIR* and *FLC* mRNA fall in expression, transcription of *VIN3* gene is induced. *VIN3* encodes a protein required for silencing of *FLC* that may interact with PRC2, creating a Polycomb complex that specifically silences gene expression after vernalization (Sung and Amasino, 2004).

1.2.3 Autonomous Pathway

Mutants of the autonomous pathway are late flowering but still responsive to photoperiodic cues and are sensitive to vernalization. To date, seven autonomous pathway genes have been cloned, including *FVE*, *FLOWERING LOCUS D* (*FLD*), *FPA*, *FLOWERING LATE WITH KH MOTIFS* (*FLK*), *LUMINIDEPENDENS*, *FCA,* and *FY*. Although roles for serving as chromatin-associated proteins, as potentially RNA binding or processing factors have been proposed, autonomous pathway is one of the least known flowering time related control in *Arabidopsis*, while the understanding of the functional roles of these genes is still at a preliminary stage.

FVE encodes a multi-copy suppressor of *ira* 1 (MSI1) homolog (Ausín et al., 2004; Kim et al., 2004), while FLD is an amine oxidase homolog (He et al., 2003). FVE as well as FLD have been implicated in the formation of histone deacetylation complexes (Ausín et al., 2004; He et al., 2003). Both FPA and

FLK contain putative RNA binding domains. The FPA protein, however, contains an RNA recognition motif (RRM) (Macknight et al., 1997; Schomburg et al., 2001) in comparison with the three K homology (KH) domains contained by FLK (Lim et al., 2004; Mockler et al., 2004). FY is homologous to Pfs2p that was found to be an essential polyadenylation and 3′ end-processing factor from yeast (Simpson et al., 2003), while *LUMINIDEPENDENS* encodes a homeodomain protein with unknown function (Lee et al., 1993).

The best understood members in this group are FCA and FY. FCA contains the putative RNA binding and RRM domains and is therefore proposed as an RNA processing factor. FCA physically interacts with FY through its C-terminal WW domain, which is a well-known protein-protein interaction module (Simpson et al., 2003). By promoting the use of an internal polyadenylation site in the *FCA* transcript, FCA can negatively regulate its own expression in an FY-dependent manner (Macknight, 2002; Quesada et al., 2003).

Genetic data has shown that genes of the autonomous pathway are likely to form a series of semi-redundant sub-pathways all targeting *FLC* (Koornneef et al., 1991; Michaels and Amasino, 2001; Sheldon et al., 2000). Therefore, the autonomous pathway represents a second *FLC* repressing mechanism that can in turn modulate *FT* expression (Figure 1G).

1.2.4 Age Pathway

Age pathway is an endogenous pathway centered at the microRNA156-targeted *SQUAMOSA PROMOTER BINDING PROTEIN-LIKE* (*SPL*) genes acting downstream of FT-FD.

SPLs promote flowering by initiating the expression of several other transcription factors, such as LEAFY (LFY), FRUITFUL (FUL), and SOC1. However, expression of SPLs is negatively regulated by the microRNA156, whose cellular levels are higher in younger plants and progressively decrease as the plant ages. Therefore, in young plants precocious flowering is prevented by high levels of microRNA156. But as plants age, a subsequent day length-independent decline in microRNA156 abundance paralleled by a rise in *SPL* levels can provide a permissive environment for flowering (Figure 1H) (Wang et al., 2009).

1.2.5 Gibberellic Acid Pathway

Gibberellic acid (GA) is a diterpene hormone discovered in the 1930s. Since its discovery, GA has been shown to play diversified roles in plant growth and development, including seed germination, cell elongation, fruit senescence, and flowering time control (Davies, 2010). Only until recently, have the regulatory mechanisms underlying the GA-mediated control of flowering begun to be understood.

During the vegetative phase, the regulatory protein, DELLA, represses flowering via direct interaction with the microRNA156-targeted SPL proteins. Such binding inhibits SPL transcriptional activation of microRNA172 in leaves and the MADS box protein family in shoot apical meristem (SAM) (Yu et al., 2012). Then, during floral induction, GA is perceived by its nuclear receptor, GIBBERELLIN INSENSITIVE DWARF1 (GID1), which undergoes conformational changes after binding with bioactive GA. These changes facilitate the interaction between GID1 and DELLA proteins, subsequently leading to the

degradation of DELLAs mediated by ubiquitin-proteasome pathway (Fu, 2004; Griffiths et al., 2006; Harberd, 2003; Schwechheimer and Willige, 2009). Upon removal of the transcriptional repression exerted by DELLAs, on the one hand, microRNA172 can be expressed and targets *SCHLAFMUTZE* (*SMZ*) transcripts in leaves. Repression of SMZ lifts the blockage of *FT* expression and makes plants responsive to the photoinductive period (Galvao et al., 2012; Mathieu et al., 2009). On the other hand, SPLs are key players in the age pathway regulated by mircoRNA156 (Wang et al., 2009). As a plant ages, elimination of the DELLAs allows SPLs to activate MADS box genes like *FRUITFUL* (*FUL*) and *LEAFY* (*LFY*) and thus triggers flowering (Figure 1I). Further, besides serving as upstream activators of the floral-promoting MADS box genes, SPLs also act as downstream targets of the MADS box family. This interlocking positive feedback loop may contribute to the rapid and irreversible floral transition in *Arabidopsis* (Yu et al., 2012).

Altogether, GA pathway represents an additional layer of endogenous regulation of periodic and age pathways; the crosstalk resulted implies the intimate interrelationships between different floral regulatory pathways.

1.2.6 The Florigen FT

Photoperiod and vernalization pathways control flowering in response to seasonal changes in day length and temperature. Age, autonomous, and gibberellin pathways act more independently of environmental stimuli and work endogenously to modulate the developmental shift. Among them, four out of five of the flowering pathways converge to trigger the expression of *FT* (Figure 1). However, perception of environmental cues, like photoperiod, and thus *FT* expression take place in leaf vasculature, while floral transition occurs at SAM. How can the floral transition be achieved? Over 70 years ago, grafting experiments led to the proposal of a mobile, graft-transmissible signal that was produced in leaves, which traveled to the shoot apex where it induces flower formation (Kobayashi and Weigel, 2007). This signal was coined “florigen”. Despite the proposal of florigen decades ago, its identity was only discovered recently.

FT is only transcribed in leaves, but the protein acts through FD, which is expressed only at the apex (Wigge et al., 2005). Also, fusion of FT and three yellow fluorescence proteins (3xYFP) around the Tobacco Etch Virus protease recognition site ($TEVP^{rs}$) hinders FT movement. Therefore, phloem companion cell (PCC)-specific expression of the *FT:TEVP^{rs}:3xYFP* by SUC2 promoter cannot promote flowering. However, crossing of SUC2: FT:$TEVP^{rs}$:3xYFP with the SUC2:TEVP line that can release the FT protein from 3xYFP was found to be sufficient to induce flowering (Mathieu et al., 2007). Further supporting this notion, in *Arabidopsis thaliana* and rice, green fluorescence protein-fused FT or FT-like proteins expressed in the companion cells were detected at the shoot meristem (Aki et al., 2008; Corbesier et al., 2007), suggesting FT is in agreement with the properties of the graft-transmissible signal and is thereby proposed as the florigen. Recently, a FT ligand, FT-INTERACTING PROTEIN 1 (FTIP1), has found to be present in the plasmodesmata of the phloem companion cells of *Arabidopsis thaliana* and

shown to be required for active transport of FT protein into the phloem sieve elements (Liu et al., 2012). This provided further evidence for the conclusion drawn.

1.2.7 Floral Transition at SAM

In young floral primordia, expression of meristem identity genes, such as *APETALA1* (*AP1*) and *LEAFY* (*LFY*), are repressed by an FT homolog named TERMINAL FLOWER 1 (TFL1) (Liljegren et al., 1999; Shannon and Meeks-Wagner, 1993) (Figure 1J). But upon FT arrival at SAM, FT antagonizes TFL1 and initiates flower development by interacting with a basic leucine zipper (bZIP) domain transcription factor known as FD, potentially via the bridging molecules GENERAL REGULATORY FACTOR (GRF) or 14-3-3 proteins as in case of rice (Taoka et al., 2011). The resulting floral activating complex (FAC) triggers transcription of the MADS box factor *AP1* (Wigge et al., 2005) and of *SPL* transcription factors (including SPL3, 4, 5 and 9), which in turn promote the expression of *AP1*, *LFY*, MADS box genes *FRUITFULL* (*FUL*), and another floral integrator known as *SOC1*. Through interaction with AGL24, SOC1 activates *LFY* expression while feedback promotes the *SPL* transcription, together initiating the flower development at SAM (Jung et al., 2011; Lee et al., 2008; Wang et al., 2009; Yamaguchi et al., 2009).

1.3 Flowering Control in Other Plant Species

Different plant species show precise but distinct seasonal patterns of flowering, implying different ways of control underspun. Recent advancement of crop genomics allows isolation and role characterization of numerous amounts of genes controlling flowering in species other than *Arabidopsis thaliana*. This includes long day plants (wheat and barley), short day plants (rice, Japanese morning glory, and potato), domesticated plants (sunflower), biennial (sugar beet) and perennial plants (poplar) (Dubcovsky et al., 2006; Hayama et al., 2003; Hayama et al., 2007; Navarro et al., 2011; Blackman et al., 2010; Pin et al., 2010; Hsu et al., 2011).

Surprisingly, in most cases, the floral inducing role of FT-like proteins is highly conserved. Only the mechanisms controlling transcription of *FT*-like genes vary during evolution, allowing their diversified seasonal responses. In contrast, FT-like paralogs of some species evolved an antagonistic function that goes against the original FT-like proteins. Interplay of these antagonistic FT pairs confers plants with the ability to respond to environmental clues differently.

1.3.1 FT-like Proteins as Floral Inducer

1.3.1.1 HD3A in Short-Day Rice

Despite their different responses to day length, initial identification of genes required to confer a short-day flowering response in *Oryza sativa* (rice) identified CO and FT homologs HEADING DATE 1 (HD1) and HEADING DATE 3A (HD3A) respectively, suggest the photoperiod pathway is likely to be highly conserved between *Arabidopsis* and rice (Hayama et al., 2003).

Although HD1 represses flowering under LD by inhibiting transcription of the *HD3A* gene, under SD, it promotes the transcription of the FT-like genes *HD3A* and its paralog *RICE FT-LIKE 1* (*RFT1*). HD3A and RFT1 in turn promote flowering in a manner similar to FT and TSF in *Arabidopsis* (Figure 2B). Moreover, the conserved mechanism between rice and *Arabidopsis* was complicated by the identification of rice genes that do not have counterparts in *Arabidopsis thaliana* but that have important functions in photoperiodic responses. In particular, *EARLY HEADING DATE 1* (*EHD1*), which encodes a B-type response regulator and activates transcription of *HD3A* and *RFT1* under SD independent of HD1 (Andres et al., 2009; Doi, 2004). Further, the rice protein encoded by *GHD7* (*GRAIN NUMBER PLANT HEIGHT AND HEADING DATE 7*) has a crucial role in photoperiodic response by serving as a floral repressor of *EHD1* transcription under LD conditions (Xue et al., 2008).

On the whole, three key regulatory genes for the photoperiodic control of flowering are conserved between the long-day *Arabidopsis* and short-day rice, but regulation of the *FT* gene by CO was reversed resulting in the suppression of flowering in rice under LD conditions. (Hayama et al., 2003). In addition, two extra gating mechanisms exerted by the floral promoter EHD1 and the floral repressor GHD7 result in a different wiring of the photoperiod pathway in rice (Itoh et al., 2010).

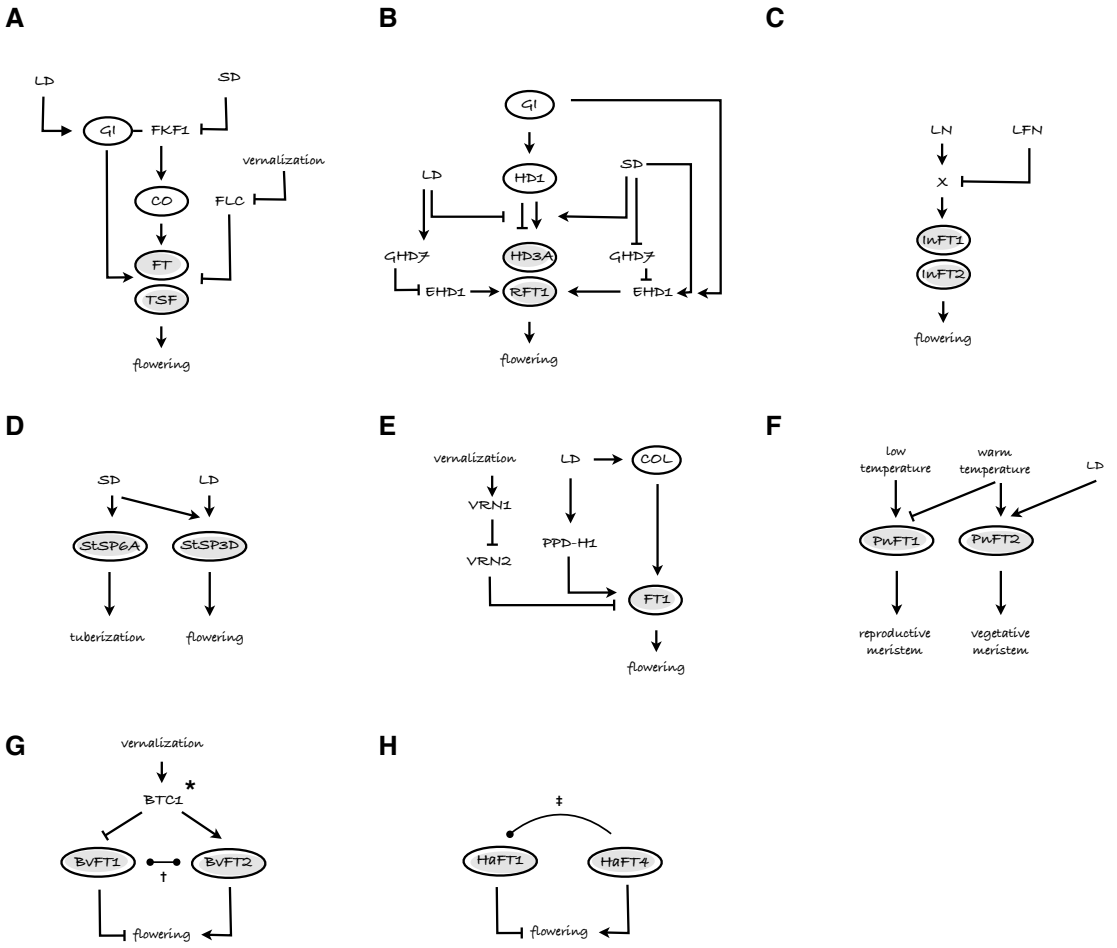

Figure 2. Comparison of *FT* homologs or paralogs expression regulated by environmental clues in different plant species. **(A)** Long-day *Arabidopsis thaliana*. LD; long day; SD, short day; GI, GIGANTEA; FKF1, FLAVIN-BINDING KELCH REPEAT F-BOX1; CO, CONSTANS; FLC, FLOWERING LOCUS C; FT, FLOWERING LOCUS T; TSF, TWIN SISTER OF FT. **(B)** Short-day rice. Rice do not require vernalization to promote flowering. HD1, HEADING DATE 1; HD3A, HEADING DATE 3A; RFT1, RICE FT-LIKE 1; GHD7, GRAIN NUMBER PLANT HEIGHT AND HEADING DATE 7; EHD1, EARLY HEADING DATE 1. **(C)** Short-day Japanese morning glory. Expression of *InFTs* is independent of *InCO* expression, but highly dependent of night length. LN, long night (longer than 11 hours); FL, light flashes given during the night; X, putative transcription factor regulating expression of InFTs. **(D)** Day-neutral potato. StSP6A/3D, SELF-PRUNING 6A/3D of *Solanum tuberosum*. **(E)** Long-day wheat and barley. COL, CONSTANS-LIKE PROTEIN; VRN1/2, VERNALIZATION1/2. **(F)** Perennial poplar. PnFT1/2, FLOWERING LOCUS T 1/2 of *Populus spp*. **(G)** Biennial sugar beet. In annual sugar beet, BTC1 can repress *BvFT1* while promote *BvFT2* to induce flowering without experiencing vernalization. In contrast, in biennial sugar beet, the recessive *btc1* allele would become active for repressing *BvFT1* while promoting *BvFT2* expression only after vernalization. Therefore, the biennial variety would not flower in the first year. BvFT1/2, FLOWERING LOCUS T 1/2 of *Beta vulgaris*. **†** BvFT1 and BvFT2 differ by three amino acid residues at their exon 4B. **(G)** Domesticated Sunflower. ‡ Floral repressing *HaFT1* is originated from the floral promoting *HaFT4*, where after gene duplication, a single frameshift mutation (TG to C at exon 3) resulted as the dominant negative allele *HaFT1*. Arrow indicates positive interaction; perpendicular line indicates negative interaction; grey lines represent uncertain interactions. Floral regulatory components highly conserved or found in more than one plant species are in circles. *FT* homologs or paralogs are shaded. (Figure modified based on Andrés and Coupland, 2012)

1.3.1.2 InFT in Short-Day Japanese Morning Glory

In the classical SD model species *Ipomoea nil* (Japanese morning glory), two putative orthologs of FT, InFT1 and InFT2, promote flowering specifically under SD, where light flashes during the night phase reduce their expression and prevent flowering. Also, as demonstrated by the fact that *Ipomoea* accessions that differ in their critical night-length responses express *InFT* at different times after dusk independent of *InCO* expression, suggesting that expression of *InFT* may be regulated by a different transcription factor in *Ipomoea* (Figure 2C). Therefore, SD response in Ipomoea is controlled by a dedicated light sensitive clock set by dusk, that in turn activates *InFT* transcription in darkness. Only if the night is sufficiently long (longer than 11 hours) it can induce *InFT* expression and thus flowering in SD (Hayama et al., 2007). This demonstrates that floral inducing function of InFT is conserved, but that *Ipomoea* adopted a different mechanism for measuring day length and control of *InFT* expression as described for *Arabidopsis* and rice.

1.3.1.3 StSP6A in Day-Neutral Potato

Seasonal fluctuation in day length regulates important aspects of plant development such as the flowering transition. But apart from flowering, *FT*-like genes were also shown to control other seasonal developmental responses. In *Solanum tuberosum* (potato), the formation of tubers is also known as tuberization. In Andean varieties of potato, tuberization is induced under SD. This response is controlled by transport of the FT-like protein named SELF-PRUNING 6A (SP6A), which is only expressed under short days, from the leaves to the roots (Navarro et al., 2011). By contrast, the protein encoded by the paralogous gene *SELF-PRUNING 3D* (*SP3D*) promotes flowering and is expressed under all day lengths, leading to a contrasting day-neutral flowering with SD-dependent tuberization (Figure 2D).

This example demonstrates that, depending on the regulatory context, even for *FT*-like paralogs from the same species, they can respond to environmental cues differently during their mediation of different developmental transitions.

1.3.1.4 FT1 in Long-Day Wheat and Barley

In the temperate cereals, such as wheat and barley, flowering is promoted by LD. CO-like proteins are involved in the activation of *FT*-like genes in their LD responses (Campoli et al., 2012). However, three additional factors that are not found in *Arabidopsis* determine the transcriptional activation of the *FT*-like genes of these species.

Firstly, in barley, pseudo-response regulator *PPD-H1* gene promotes early flowering in response to long days and encodes a pseudo-response regulator protein containing a CCT domain (Figure 2E). Cultivation of barley originated in the Middle East and accessions in this region tend to carry active *PPD-H1* alleles causing flowering to occur rapidly in spring in response to long days and before summer drought. Barley crop varieties used in northern Europe, however, mainly carry mutant *ppd-H1* alleles that

reduce the response to long days, thereby allowing the plant to grow throughout the milder summers of the region generating higher seed yields (Turner, 2005).

Secondly, similar to *Arabidopsis*, promotion of flowering through long days is blocked until exposed to winter temperatures. The interaction between the photoperiod responses and vernalization is mediated by a protein known as VERNALIZATION 2 (VRN2), which is not found in *A. thaliana*. Under LD, VRN2 blocks the expression of at least one of the *FT*-like genes found in cereals (Dubcovsky et al., 2006; Yan et al., 2004). Transcription of VRN2 is repressed after exposure to vernalization by the MADS box transcription factor VERNALIZATION 1 (VRN1) that is expressed in response to vernalization exposure (Yan et al., 2003). Thus, at the onset of spring, as day length is extended, transcription of *FT*-like genes (such as *FT1*) is activated through the photoperiodic flowering pathway and thereby promotes flowering (Campoli et al., 2012; Turner, 2005). Therefore, as in *A. thaliana*, the vernalization and photoperiod pathways are tightly interlinked in cereals, though transcription of *FT*-like genes is regulated differently.

All in all, these examples demonstrate that the floral inducing role of *FT*-like genes appears to be highly conserved in many plants. However, there are differences in the upstream control, allowing for transcription of *FT*-like genes in response to different day lengths. However, exceptions do exist.

1.3.2 FT-like Proteins as Floral Inducer and Repressor

1.3.2.1 PnFT1 and PnFT2 in Perennial Poplar

Long-lived trees, such as poplar species, have evolved a unique seasonal control of flowering. In these plants, a single-shoot meristem cycles from vegetative growth to flowering and back to vegetative growth. Nevertheless, this cycle is strictly seasonal (Yuceer et al., 2003). During winter, when poplar species are exposed to low temperatures, reproduction is initiated, whereas the floral buds are formed and open in spring. By contrast, during summer, when the plants are exposed to long days and warm temperatures, vegetative growth occurs (Hsu et al., 2011). Such synchronization of flowering and vegetative growth is conferred by different *FT*-like genes.

Low temperature that is typical of winter promotes *PnFT1* expression, that in turn triggers the formation of a limited number of reproductive buds. By contrast, warm temperature typical of spring and early summer suppresses *PnFT1* transcription. Together with the long-day photoinductive period, *PnFT2* expression is induced, which promotes vegetative growth (Figure 2F) (Hsu et al., 2011). In this way, interplay of the two antagonistic *FT*-like gene paralogues can modulate the meristemic function in perennial poplar species appropriately in response to seasonal change.

1.3.2.2 BvFT1 and BvFT2 in Biennial Sugar Beet

In sugar beet, genetic analysis of the *FT*-like gene family identified two members correlating with flowering, in which BvFT1 confers a block on flowering, while BvFT2 induces flowering (Pin et al., 2010).

Their orchestration with the molecule BTC1, a vernalization-sensitive repressor, determines flowering in sugar beet.

In annuals, the dominant *BTC1* allele promotes flowering under LD by repressing *BvFT1* and activating *BvFT2*. On the contrary, biennial sugar beet carries a recessive *btc1* allele, which does not block expression of the floral repressor *BvFT1* in the first year. Only after experiencing low temperatures in winter, *btc1* becomes active enough to repress *BvFT1* and to induce *BvFT2*, thereby promoting floral initiation (Pin et al., 2012). So in this way, vernalization is required before the biennials can flower (Figure 2G). Such variation in the vernalization requirement makes the biennials become agriculturally significant. Premature flowering of the sugar beets before the annual harvest reduces the yield of the sugar-containing beets and complicates harvesting. However, such limitation can be overcome by sowing biennial varieties in the early spring and harvesting them in autumn before flowering. Notably, regardless of their totally opposite function, sequence of BvFT1 and BvFT2 proteins differ only by three amino acids at motif encoded by their exon 4 (Pin et al., 2010).

1.3.2.3 HaFT4 and HaFT1 in Domesticated Sunflower

Different floral regulatory mechanisms have evolved independently in different families of flowering plants. In some cases, gene duplication mediates the rise of evolutionary novelties to act on the native mechanism within a species. For instance, in *Helianthus annuus* (sunflower) flowering is promoted by *HaFT4*. However, a recent gene duplication lead to the rise of another mutated copy named *HaFT1*. Genetic and functional analysis demonstrate that a frameshift mutation (TG to C at exon 3) resulting from a selective sweep during early domestication of sunflower underlies a major quantitative trait locus (QTL) for the floral delaying ability of *HaFT1* (Blackman et al., 2010). Notably, this dominant-negative *HaFT1* allele delays flowering through interference with action of its paralog *HaFT4* (Figure 2H).

Altogether, this example indicates, on the one hand, how the interactions evolving between new gene family members may play an important role for fostering plant phenotypic changes. On the other hand, similar to the case of sugar beet, it demonstrates the ease and possibility of the floral inducing role of FT-like protein can be reversed via minor amino acid or nucleotide changes.

1.4 Mystery of FT

Despite extensive studies of over a decade on dissecting the FT function, our understanding on the critical determinants for determining FT florigenic identity is still limited. Also, how such determinants of FT function can mediate the floral transition remains unclear. Further, as implied by the other plant species such as rice and barley, it is the question if FT in *Arabidopsis* would also require yet-to-be-known ligand(s) for its floral promoting function. All of these questions have remained unsolved making FT one of the most mysterious molecules in the field of plant research.

Chapter 2

Determinants of FT Florigenic Identity

2.1 CONTRIBUTIONS

Unless otherwise specified, I performed all experiments presented in this chapter, with the help of Pauline Ip for plant work.

Detlef Weigel[1], Friedrich Schoeffl[2], Sascha Laubinger[2], Jiawei Wang[3], Yasushi Kobayashi[4], Rebecca Schwab[1], and Roosa Laitinen[5] provided critical advices on defining the direction of my research. I designed the experiments with the help of Detlef Weigel and Markus Schmid[1].

[1]Max Planck Institute for Developmental Biology, Tuebingen, Germany

[2]Center for Plant Molecular Biology (ZMBP), Eberhard-Karls University, Tuebingen, Germany.

[3]National Key Laboratory of Plant Genetics, Institute of Plant Physiology and Ecology, Shanghai Institutes for Biological Sciences, Shanghai, China

[4]Department of Botany, Graduate School of Science, Kyoto University, Japan

[5]Max Planck Institute of Molecular Plant Physiology, Potsdam, Germany

2.2 INTRODUCTION

2.2.1 Phosphatidylethanolamine Binding Protein PEBP

Phosphatidylethanolamine binding protein, in short PEBP, is a protein family conserved throughout every kingdom of species (Bollengier and Mahler, 1988; Cornwall et al., 1991; Perry et al., 1994; Seddiqi et al., 1994). Apart from their widespread and featured small size (mostly of around 23kDa), PEBP is also characterized by its uniqueness in structural topology, with which, so far, none of the identified protein families have shown to have any similarities (Schoentgen et al., 1987). As we know, structural ubiquity and uniqueness usually imply a distinctive role and machinery. So, what is the function, and how is the functioning of this family of proteins?

2.2.2 Animal PEBP versus Plant PEBP

In animals, based on the presence of a C-terminal α-helix, an adjacent loop and a bulky side-group for tightly controlling the access to an anion binding pocket (ABP) of animal PEBPs, a role for this pocket in accommodating the headgroup of phospholipids during transmembrane signaling has been proposed (Banfield and Brady, 2000). However, all of the three regulatory features are absent and there is no evidence on phospholipid binding in plants. Such variations in structure have made the functioning of plant PEBP, including its mode-of-action and functional determinants, a mystery. Nevertheless, thanks to the recent effort in solving how two of the representative members of plant PEBP, that are the floral promoting FT and its antagonist TFL1, can share the same structural scaffold but are totally opposite in activity, we start to get some clues on the functional determinants of plant PEBP.

2.2.3 Previous Studies on Plant PEBP

2.2.3.1 Swapping of Single Amino Acid between FT and TFL1

Based on the crystal structure of CENTRORADIALIS (CEN), a member of plant PEBP isolated from *Antirrhinum* (snapdragon) (Banfield and Brady, 2000), residues potentially important to the FT and TFL1 activity were identified. Then, three anion binding pockets residues (Y85, N110, and V120 in numbering of FT; H88, L113, and F123 in numbering of TFL1) showing contrasting charge and structural differences were chosen as their target of study (Hanzawa et al., 2005). After swapping these residues between FT and TFL1, the mutated forms were first expressed in wild-type (WT) background.

In case of *Arabidopsis*, WT plants pass through four main developmental phases, reflecting a sequence of identities in the shoot apical meristem. Following the first germination phase (G), the meristem has a vegetative (V) identity and produces leaf primordia on its flanks to form a rosette. On receipt of favorable signals, reproductive development is initiated and the apical meristem acquires an inflorescence identity (I), which itself has two distinct phases. During the first inflorescence phase (I1), 2-3 cauline leaf primordia are produced that subtend axillary inflorescence meristems. This is followed by a

second inflorescence phase (I2), during which determinate floral meristems are made on the periphery of the apex. Finally, floral phase (F) is reached where apex itself becomes a flower. However, for plants overexpressing *TFL1*, I1 phase is greatly extended, it is typically followed by an interim developmental phase known as I1*, where shoots lacking a subtending cauline leaf are produced (Ratcliffe et al., 1998). Whilst for plants overexpressing *FT*, the duration of V and I phase is greatly reduced and has mostly ended in the formation of a single terminal flower (Kardailsky, 1999; Kobayashi, 1999). In contrast, transformants of 35S::*mTFL1ΔH88Y* in their study showed a clear shift to early flowering, while plants overexpressing 35S::*mFTΔY85H* showed greatly extended V and I phases closely resembling the phenotype of 35S::*TFL1* plants (Hanzawa et al., 2005), suggesting that FT and TFL1 identity can be swapped via a single amino acid change in the WT background. However, to rule out the possibility that any of these phenotypes were caused by cosuppression, the mutated forms were then tested in the *tfl1;ft* double mutant background, where overexpressors of *FT* and *TFL1* showing phenotypes were consistent with that of the WT (Hanzawa et al., 2005).

In context of *tfl1;ft*, plants transformed with 35S::*mTFL1ΔH88Y* flowered consistently early and produced terminal flower similar to that of the FT overexpressor. On the contrary, although transformants of 35S::*mFTΔY85H* could prevent formation of terminal flower as seen in the *TFL1* overexpressors (Hanzawa et al., 2005), in terms of their capability to delay flowering time and to trigger the unique I1* phase, mFTΔY85H can at most be considered as a weakened floral inducer, but not a repressor like TFL1.

Altogether, these results suggest that swapping of a single pocket residue is sufficient to convert TFL1 into FT. However, such conversion is unidirectional as similar mutation cannot convert FT into TFL1, or even into a floral repressing molecule.

2.2.3.2 Swapping of Exons between *FT* and *TFL1*

Taking the advantages of having conserved exon-intron boundaries between *FT* and *TFL1*, in another study, individual exons were swapped between the genes. Then, the resulting chimeras were driven to express in the mutant background *tfl1;ft*. *In vivo* activities of these chimeras were evaluated by counting the number of rosette leaves (Ahn et al., 2006).

Perhaps not too surprisingly, given that there are over 90% of similarities between exon 2 and 3 of *TFL1* and *FT*, no significant effect can be observed in their swaps. Surprisingly, for exon 1 that encodes more than 40% of the molecule but has the lowest percentage of sequence conserved between the proteins, similar results were obtained and the swapping just seemed to have a very slight effect on rendering their activities. Nevertheless, a striking change in activity was observed in the case of swapping their exon 4, in which the exon 4-replaced *FT* just acted like its functional opposite *TFL1*. This implies that exon 4 contains the element critical for each of their activities.

To further pinpoint these critical elements, the exon 4 of *FT* and *TFL1* was subdivided into four pieces in accordance with their structural topology, and named from segment 4A through 4D. Swapping

experiment between these segments was performed similarly. The scientists found that in backbone of *TFL1*, almost all of the transformants with the swapped exons continued late flowering. Only for two of them holding both segment 4B and 4C show *FT*-like activity. On the contrary, in the framework of *FT*, either segment 4B or 4C of *TFL1* can switch FT into a floral repressing molecule. Therefore, based on these findings, the authors concluded that either segment 4B or 4C alone is sufficient to confer at least some *TFL1*-like activity, but segment 4B and 4C together are required for the activity of *FT* (Ahn et al., 2006).

2.2.3.3 Swapping of Exons between *FT* Paralogs

In sugar beet, regulation of flowering time is controlled by interplay of two paralogs of *FT*, namely *BvFT1* and *BvFT2*. BvFT1 acts like the TFL1 and represses flowering, while BvFT2 acts like the FT and promotes flowering. To investigate the cause for the opposite function of BvFT1 and BvFT2, the exonic swapping approach was adopted in a previous study (Pin et al., 2010). However, based on the findings of *Arabidopsis*, only swapping of the exon 4B of *BvFT1* and *BvFT2* were performed and the chimeras resulted were overexpressed in *Arabidopsis* from the constitutive 35S promoter. The authors demonstrated that, similar to the findings of *FT* and *TFL1* (Ahn et al., 2006), determinants of the antagonistic function of *BvFT1* and *BvFT2* were mapped to their exon 4B. As shown by sequence alignment, the protein encoded by exon 4B of *BvFT1* and *BvFT2* only differ by 3 amino acids; the authors then deduced that residues at three positions (N138, Q141, and Q142 in BvFT1 scaffold; Y134, G137, and W138 in BvFT2 scaffold) are the cause of the antagonistic function of BvFT1 and BvFT2.

However, as shown by their findings, transformants overexpressing *BvFT2221* (a chimera formed by replacing the exon 4 of *BvFT2* with that of the *BvFT1*), on average, flowered 27 leaves earlier than the native *BvFT1* under LD conditions. While instead of showing aberrant shoots corresponding to the featured I1* phase of the *TFL1* overexpressors (Ratcliffe et al., 1998), only 3 out of 15 transformants exhibited developmental aberrations with flowers lacking petals (Pin et al., 2010), suggesting that the TFL1 identity of BvFT2221 is doubtful. Therefore, from the findings, one can only conclude that introducing mutations N138Y, Q141G, and Q142W together can convert BvFT1 (TFL1-like) into BvFT2 (FT-like). Whether introducing the corresponding set of mutations, Y134N, G137Q, and W138Q, to the BvFT2 (FT-like) scaffold can render the molecule into a fully functional BvFT1 (TFL1-like) remains elusive. Further, whether all of these positions have to be mutated simultaneously in order to achieve the switching from BvFT1 to BvFT2 (or *vice versa*) is also unclear.

2.3 OBJECTIVES

Some reasons for explaining why FT and TFL1 can drive the flowering time to different extremes were found. However, exon-intron boundaries are not necessarily the divisions of structural domains. Therefore, exonic swapping has the limitation that it may lead to truncation of the domains. Also, for most of the exons of *FT* and *TFL1* (such as exon 2 and 3), their sequences share a high degree of similarity. Therefore, critical functional determinants may potentially be covered up if simply relying on exonic swapping. Further, having said that residue Y85 as well as the motif encoded by exon 4B and 4C showed to have a critical role in FT, how exactly they facilitate the FT floral promoting function is still unclear.

In this chapter, I present my study targeted at pinpointing the functional determinants of FT florigenic identity, and showing how these determinants can mediate floral inducing activities of FT protein.

2.4 METHODOLOGY

To prevent potential domain truncation, while ensuring the effect of the highest possible number of amino acid residues that could be tested, rather than relying on exonic swapping, in this study I chose to adopt PCR-mediated random mutagenesis to introduce point mutations into *FT* sequence (Figure 3A). In this way, domain integrity can be preserved while *FT* sequences can be mutated in an unbiased manner. Together with the C-terminal fusion of yellow fluorescent protein tag (mCitrine) allowed for confirmation of robust expression of full-length protein in the case of loss-of-function mutants, expression of thousands of mutated versions of *FT* were driven by the constitutive 35S promoter and transformed in pools in the WT Col-0 background. The resulting transformants were classified by the following logic (Figure 3B):

Firstly, in order to observe the effect of the mutations *per se*, plants were grown under SD conditions, where expression of the native *FT* is repressed. If a functionally unimportant residue is mutated, just like overexpressing a non-mutated copy of *FT*, its flowering time should be early. On the contrary, if a functionally important residue is mutated, FT function should be weakened and a slower acceleration of flowering observed. Then, in order to check if there is any mutual interaction between the native and mutated FT (mFT), the late flowering batch from the SD screen was propagated in LD conditions to see if there was any late flowering transformant caused by dominant negative effect. Together with any gain-of-function phenotypes, a comprehensive functional map for a plant PEBP was generated. Depending on their strength of effect, clones were selected for further structural and genetics studies.

By the unbiased and comprehensive “touching” of the amino acid residues of FT, I anticipated that the yet-to-be-known determinants critical to the FT function could be uncovered.

A

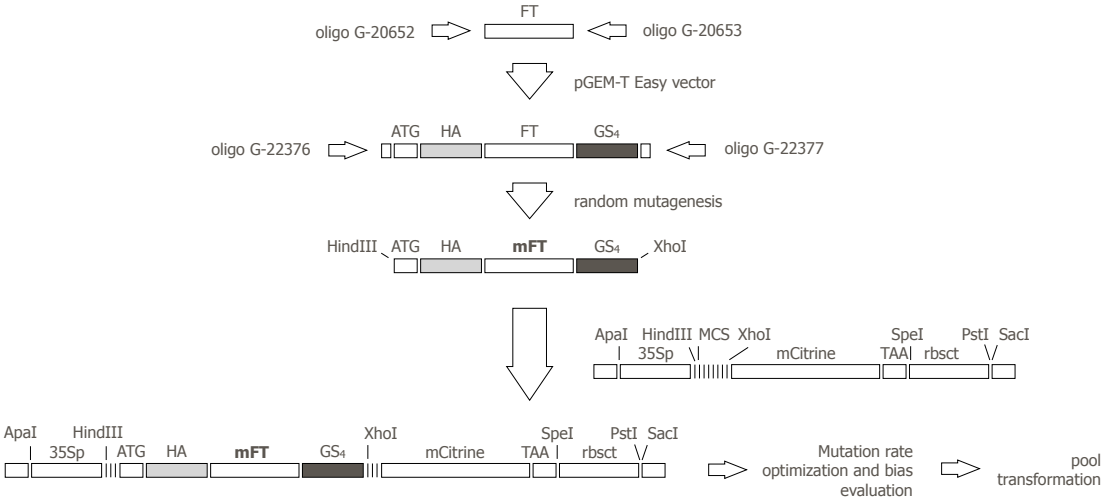

B

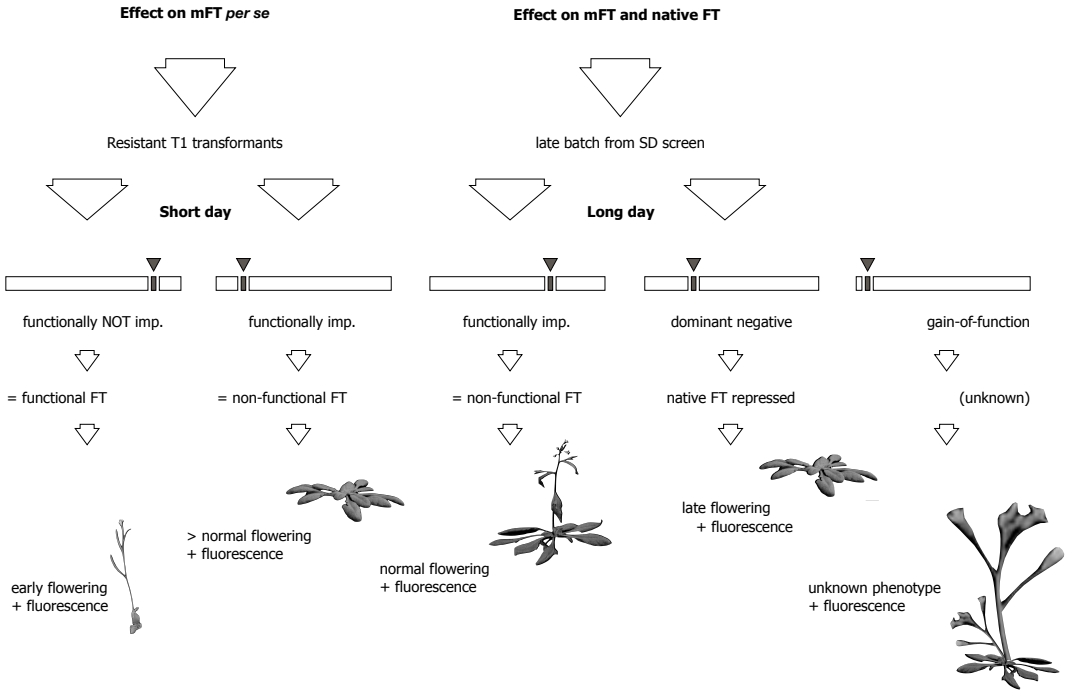

Figure 3. Chimera construction and screening logic. **(A)** Schematic diagram showing the construction of the fusion of site-directed mutagenized FT and mCitrine, flanked by human influenza hemagglutinin (HA) tag and flexible (Glycine-Serine)$_4$ or GS$_4$ linker. Oligo G-20652 = oligo specific to the 5' coding sequence of the start-codon-removed FT, preceded by ATG and coding sequence of HA tag; oligo G-20653 = oligo specific to the 3' coding sequence of the stop-codon-removed FT, followed by coding sequence of the flexible GS$_4$ linker; oligo G-22376 = oligo specific to ATG:HA preceded by a HindIII restriction site; oligo G-22377 = oligo specific to GS$_4$ followed by XhoI site. **(B)** Relationships between the phenotypes expected and the casual type of mutations when screening under SD and LD conditions. imp, important.

2.6 RESULTS

2.6.1 Mutation Rate Optimization and Bias Evaluation

Random mutagenesis is an effective and unbiased approach for probing residues critical to protein function. However, one limitation of the approach is that there is a trade-off between maximizing clones carrying a mutation and having as few multiple mutants as possible. To facilitate the subsequent data interpretation, mutation rate optimization is the prerequisite. To this end, nine different mutation libraries were constructed using different amounts of DNA templates, while 100 clones from each library were sequenced. On the basis of having the minimal amount of non-mutated clones but the highest number of *mFT* with a single mutation, 1 out of 9 mutation libraries (template amount: 0.15ug) was selected (Figure 4A). Then, by means of conventional cloning, about 36,000 mutated versions of *FT* in fusion with sequences encoded for fluorescence tags were generated. Prior to the actual experiment, 1241 clones were randomly sampled from the mutation pool. Randomness of mutation distribution and transition-to-transversion ratio were confirmed to fall into an acceptable range before proceeding to the next stage (Figure 4B).

2.6.2 Assessment of the Functional Retainment of mFT

To assess the function of the mutated population of *FT*, flower and flowering time phenotypes of 3320 T1 transformants growing under SD conditions were evaluated (Figure 5A). With reference to the leaf-count data of the non-mutated *FT* and the empty vector clones obtained in parallel to each of the sample sets, cutoff was determined and transformants were classified as early and late flowering. The late flowering batch with yellow fluorescence (level 1-4 in Figure 5C) was then subject to the LD screen to distinguish between lines with loss-of-function (normal flowering) and dominant negative activity (late flowering). On the whole, 2882 T2 segregating lines were individually assessed (Figure 5B). For those falling into the interesting ranges of flowering time while showing a strong level of yellow fluorescence indicative of robust expression of full-length protein (level 1 and 2 in Figure 5C), lines were selected for genotyping.

A

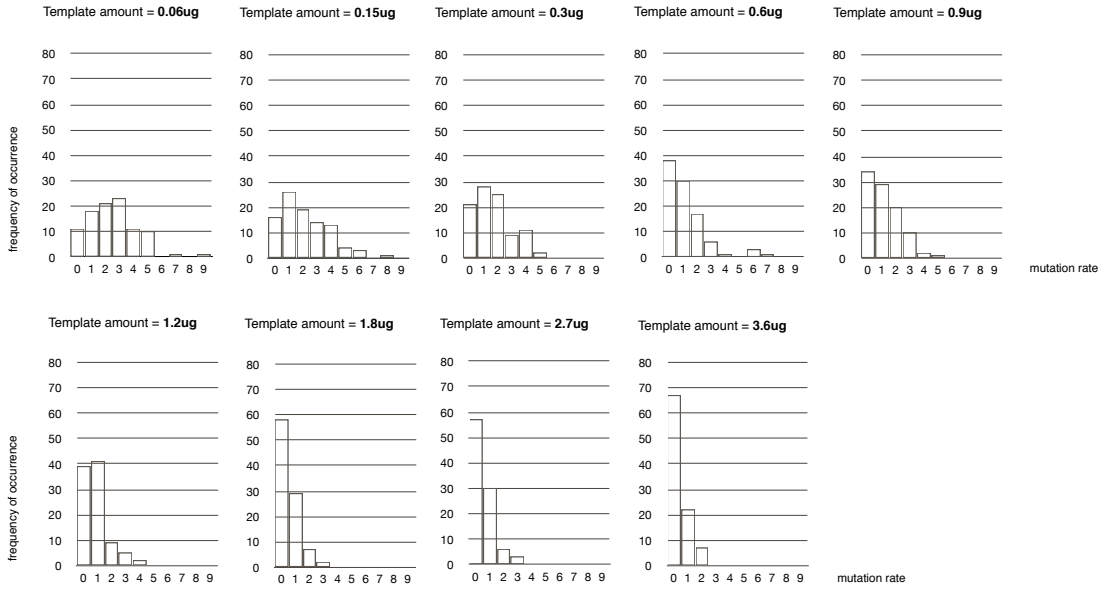

B

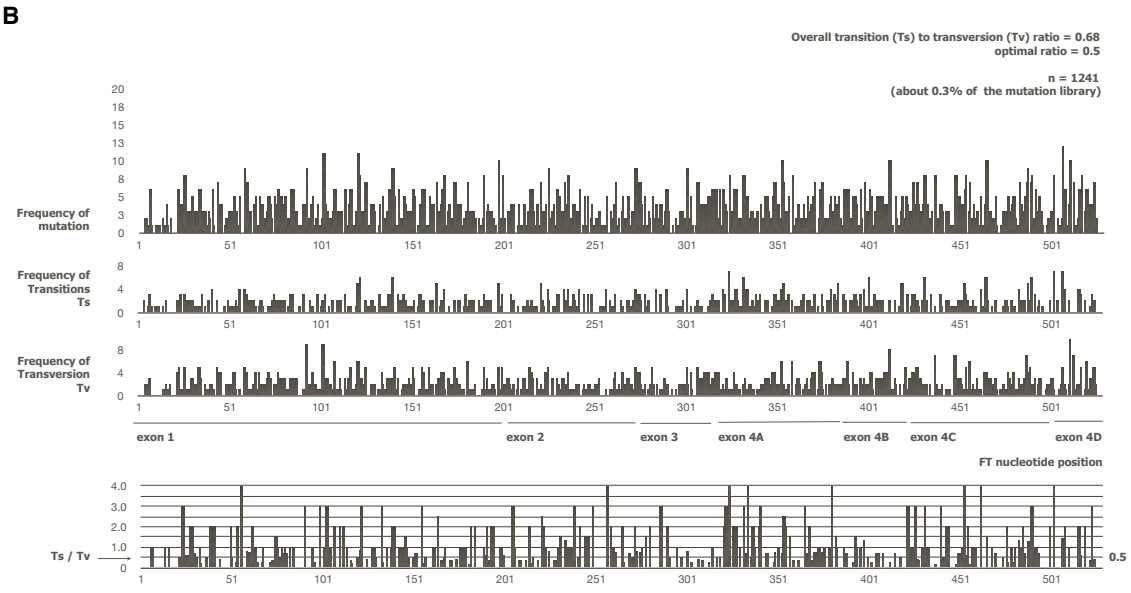

Figure 4. Mutation rate optimization and bias evaluation. **(A)** Selection of 1 out of 9 mutation libraries with the optimal rate of mutation of FT generated by means of random mutagenesis using increasing amount of DNA templates (from 0.06ug to 3.6ug). Library built up from template amount of 0.15ug was chosen due to its highest possession of singly mutated FT but minimal number of non-mutated copy among the candidates. **(B)** Mutation distribution and bias evaluation of the selected mutation libraries of FT.

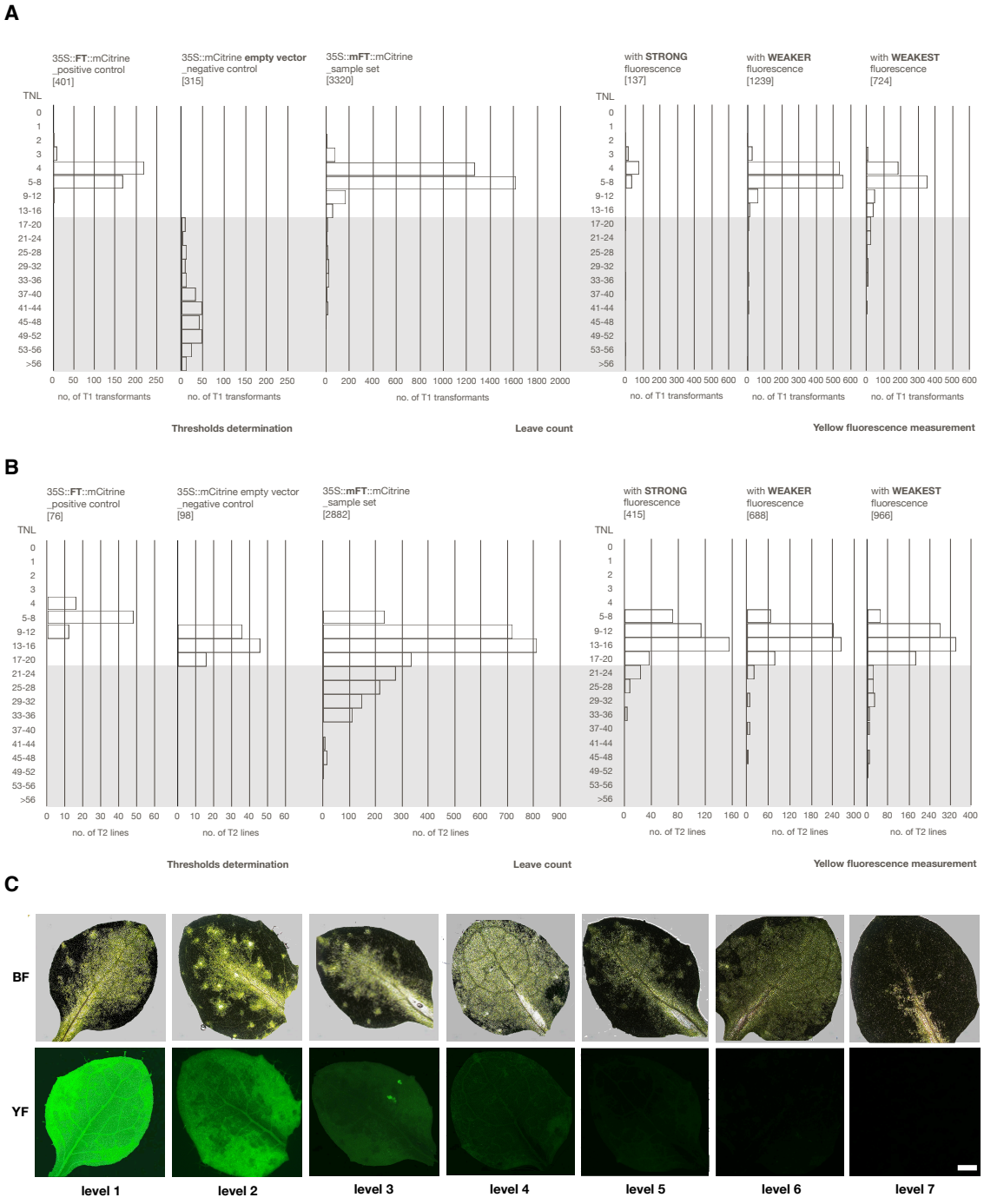

Figure 5. Functional retainment assessment of mFT pool and yellow fluorescence measurement. Overview of the flowering time phenotype and yellow fluorescence of 3320 T1 transformants and 2882 T2 segregating lines under **(A)** SD and **(B)** LD conditions respectively. With reference to each of their controls, cutoff of late flowering transformants for SD and LD screens are ≥17 and ≥21 leaves respectively. Total number of leaves (TNL) corresponding to the late flowering class in each screen are shaded. **(C)** Transformants showing differing level of yellow fluorescence. In this study, only level 1 and 2 fluorescence were classified as STRONG, level 3-4 were classified as WEAKER and level 5-6 were classified as the WEAKEST. Flowering time data of 1220 T1 transformants in SD screen and 813 T2 segregating lines in LD screen with no observable fluorescence (level 7) were not included in plots of **(A)** and **(B)**. BF, bright field; YF, Yellow fluorescence. Scale bar: 2.5mm.

2.6.3 Floral Promoter to Repressor via a Single Amino Acid Change

In my SD screen, apart from consistently obtaining the tyrosine-to-histidine mutation, 84 out of 87 of the ultraconserved residues of FT were "touched" with 478 ways of substitutions generated in my random mutagenesis studies. Among them, 77 of the mutations weakened the floral promoting and terminal flower forming ability of FT, while 40 of them switched FT into loss-of-function or almost loss-of-function molecules (Figure 6).

Further, even under the LD photoinductive conditions in which the native floral inducing FT is strongly expressed, 10 sets of the single or double mutations could override the effect of the endogenous FT and reproducibly delay the flowering time from 20 to more than 40 leaves (Figure 7 and Table 1). As some of these plants flower even later than *ft-10* (a null mutant of *FT*) while their positive transgene expression can be proven by the strong expression of the fluorescent tag, I conclude that the mutated FT resulted are not loss-of-function, but are acting as floral repressors and exert dominant negative effect to interfere with the work of the native FT. What could be the explanation for such behavior?

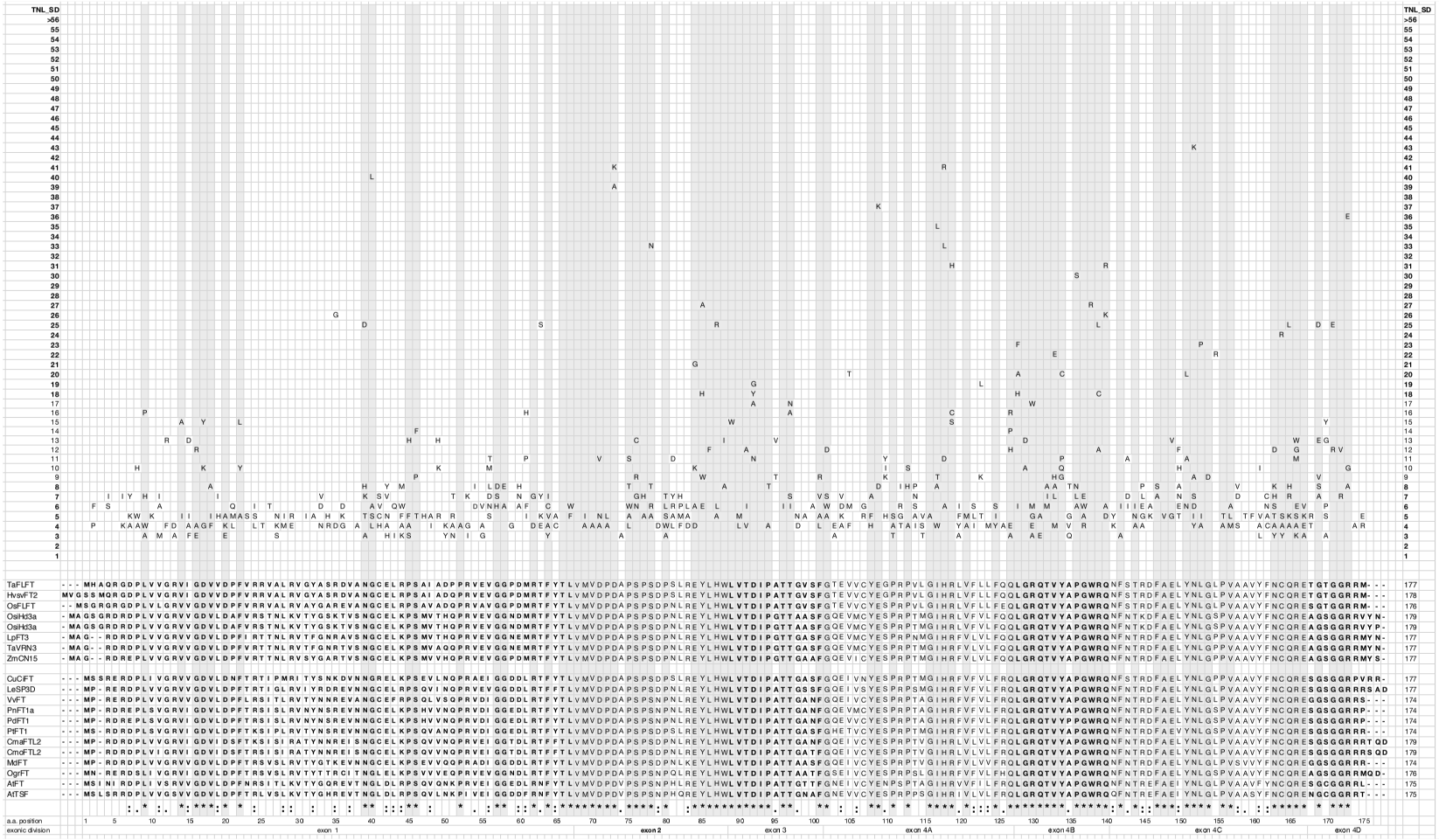

Figure 6. Random-mutagenesis-based preliminary functional map of FT showing the effect of point mutations on FT floral promoting and terminal flower forming ability under SD conditions. Flowering time of each T1 transformant was quantified by counting the total number of leaves (TNL) formed during the vegetative and first inflorescence phases. Flowering time of only the singly mutated or mutations with effect interpretable by comparison between lines shared the same mutation, while showing the STRONG level of yellow fluorescence were used in this plot. Residues ultraconserved in both monocots (upper panel of the alignment) and dicots (lower panel of the alignment) are highlighted in grey.

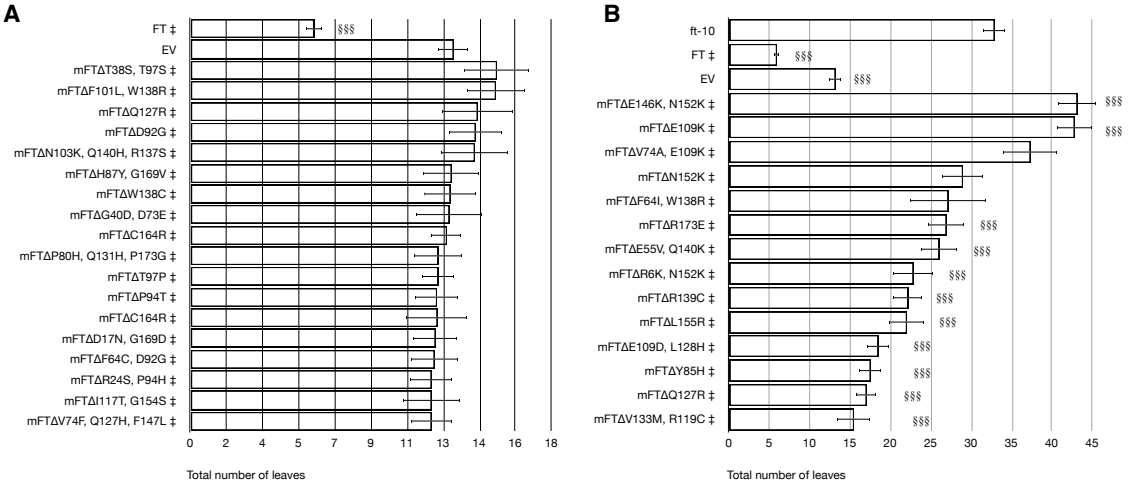

Figure 7. Effect of point mutations on the floral inducing or repressing ability of FT. Flowering time of part of the T2 segregating lines overexpressing the randomly point-mutated *FT* showing **(A)** normal and **(B)** late flowering phenotype (with four normal flowering lines shown for comparison) respectively under LD conditions. Numerical, statistical and abbreviation details of the plots and flowering time phenotype of their corresponding T1 parental lines grown under SD conditions are shown in **Table 1**.

Genotype *	No. of rosette leaves †	No. of cauline leaves †	Total no. of leaves †	*n*	No. of rosette leaves †	No. of cauline leaves †	Total no. of leaves †	*n*
	Experiment 1, LDs				*Experiment 3*, SDs ‖			
FT ‡	3.9 ± 0.7 (3-5)	2.3 ± 0.6 (1-3)	6.2 ± 0.8 (5-8) §§§	20	2.4 ± 0.6 (2-3)	1.9 ± 0.4 (1-2)	4.3 ± 0.5 (4-5)	20
EV	9.1 ± 1.3 (7-12)	4.0 ± 1.1 (2-6)	13.1 ± 1.5 (9-15)	20	43.1 ± 6.2 (25-54)	8.3 ± 1.7 (5-12)	49.3 ± 7.5 (41-59)	20
mFTΔT38S, T97S ‡	12.5 ± 4.2 (8-17)	3.3 ± 1.1 (2-5)	15.3 ± 3.2 (10-22)	19	12	3	15	1
mFTΔF101L, W138R ‡	12.9 ± 2.4 (9-19)	2.3 ± 0.8 (1-4)	15.2 ± 2.9 (10-21)	19	11	3	14	1
mFTΔQ127R ‡	12.1 ± 2.8 (7-17)	2.3 ± 1.0 (1-5)	14.3 ± 3.5 (8-21)	20	11	4	15	1
mFTΔD92G ‡	11.6 ± 1.9 (9-16)	2.6 ± 1.1 (1-6)	14.2 ± 2.6 (11-22)	15	11	3	14	1
mFTΔN103K, Q140H, R137S ‡	11.1 ± 2.8 (7-17)	3.1 ± 0.9 (2-5)	14.2 ± 3.3 (10-21)	19	12	3	15	1
mFTΔH87Y, G169V ‡	10.8 ± 2.5 (7-16)	2.3 ± 0.7 (1-4)	13.0 ± 2.9 (9-19)	20	10	3	13	1
mFTΔW138C ‡	10.8 ± 2.3 (8-16)	2.2 ± 0.6 (1-3)	12.9 ± 2.6 (9-19)	17	10	3	13	1
mFTΔG40D, D73E ‡	10.7 ± 2.6 (5-15)	2.2 ± 0.9 (1-4)	12.9 ± 3.3 (6-18)	18	11	2	13	1
mFTΔC164R ‡	11.0 ± 1.5 (9-13)	1.8 ± 0.6 (1-3)	12.8 ± 1.5 (11-15)	13	10	2	12	1
mFTΔP80H, Q131H, P173G ‡	10.6 ± 1.7 (8-15)	1.8 ± 0.8 (1-3)	12.3 ± 2.4 (9-18)	18	10	2	12	1
mFTΔT97P ‡	10.3 ± 1.4 (8-13)	2.1 ± 0.8 (1-3)	12.3 ± 1.6 (10-15)	18	9	3	12	1
mFTΔP94T ‡	9.3 ± 1.7 (6-12)	3.0 ± 0.9 (2-5)	12.3 ± 2.2 (9-16)	18	10	2	12	1
mFTΔC164R ‡	10.4 ± 2.8 (7-16)	1.9 ± 0.6 (1-3)	12.3 ± 3.1 (8-18)	17	10	2	12	1
mFTΔD17N, G169D ‡	9.9 ± 1.6 (7-12)	2.3 ± 0.7 (1-3)	12.2 ± 2.2 (8-15)	15	8	2	10	1
mFTΔF64C, D92G ‡	10.2 ± 2.2 (7-15)	2.0 ± 0.9 (1-4)	12.2 ± 2.4 (8-18)	20	9	3	12	1
mFTΔR24S, P94H ‡	10.2 ± 1.8 (7-14)	1.8 ± 0.6 (1-3)	12.0 ± 2.1 (9-16)	19	10	2	12	1
mFTΔI117T, G154S ‡	10.1 ± 2.1 (7-14)	1.9 ± 0.8 (1-3)	12.0 ± 2.8 (8-17)	14	10	2	12	1
mFTΔV74F, Q127H, F147L ‡	8.9 ± 2.1 (4-12)	3.1 ± 0.7 (2-4)	12.0 ± 2.0 (8-15)	20	7	2	9	1
	Experiment 2, LDs							
ft-10	2.7 ± 2.8 (20-33)	5.2 ± 1.5 (3-8)	32.9 ± 2.9 (27-39)	20	36.4 ± 6.9 (26-51)	13.0 ± 2.6 (9-17)	49.4 ± 6.8 (42-60)	20
FT ‡	3.8 ± 0.7 (3-5)	2.2 ± 0.6 (1-3)	5.9 ± 0.8 (4-6) §§§	20	-	-	-	-
EV	9.1 ± 1.0 (7-11)	4.1 ± 1.1 (2-6)	13.2 ± 1.6 (9-16) §§§	20	-	-	-	-
mFTΔE146K, N152K ‡	34.5 ± 3.2 (28-40)	8.6 ± 3.0 (4-14)	43.1 ± 4.7 (32-51) §§§	19	24	7	31	1
mFTΔE109K ‡	34.6 ± 3.8 (27-41)	8.2 ± 1.1 (7-10)	42.8 ± 4.4 (34-50) §§§	17	26	6	32	1
mFTΔV74A, E109K ‡	31.4 ± 5.3 (19-40)	5.9 ± (2-11)	37.3 ± 6.8 (21-51)	17	22	7	29	1
mFTΔN152K ‡	23.2 ± 5.1 (14-31)	5.8 ± 2.1 (2-10)	28.9 ± 5.1 (20-38)	17	25	5	30	1
mFTΔF64I, W138R ‡	23.0 ± 8.0 (14-40)	4.1 ± 1.7 (2-8)	27.1 ± 9.4 (16-48)	17	24	4	28	1
mFTΔR173E ‡	20.4 ± 4.5 (13-28)	6.4 ± 1.1 (5-8)	26.9 ± 4.6 (18-35) §§§	18	21	6	27	1
mFTΔE55V, Q140K ‡	21.7 ± 4.0 (14-29)	4.4 ± 1.5 (2-8)	26.0 ± 4.5 (16-33) §§§	20	21	5	26	1
mFTΔR6K, N152K ‡	19.7 ± 4.0 (14-28)	3.2 ± 1.5 (2-7)	22.8 ± 5.1 (17-33) §§§	20	19	4	23	1
mFTΔR139C ‡	18.1 ± 3.1 (13-24)	4.1 ± 1.3 (2-8)	22.2 ± 3.7 (17-28) §§§	20	18	4	22	1
mFTΔL155R ‡	18.5 ± 3.5 (14-25)	3.6 ± 1.6 (1-6)	22.0 ± 4.3 (16-31) §§§	20	13	5	18	1
mFTΔE109D, L128H ‡	15.7 ± 2.3 (12-20)	2.8 ± 0.9 (2-5)	18.5 ± 2.7 (14-24) §§§	20	16	3	19	1
mFTΔY85H ‡	13.8 ± 2.4 (11-18)	3.8 ± 1.0 (2-6)	17.5 ± 2.9 (13-23) §§§	20	14	3	17	1
mFTΔQ127R ‡	14.6 ± 2.3 (11-19)	2.4 ± 0.8 (1-4)	17.0 ± 2.6 (12-22) §§§	18	13	4	17	1
mFTΔV133M, R119C ‡	12.6 ± 3.7 (8-22)	2.9 ± 1.2 (1-5)	15.5 ± 4.2 (10-25) §§§	20	13	3	16	1

Table 1. Flowering time of mutant and transgenic plants generated by means of random mutagenesis. ***** EV, empty vector control; mFT, mutated FT. Genetic background of all transgenic plants are in Col-0. **†** Indicators of flowering time and shown as average ± standard derivation (range). Plants in each experiment were grown under LDs and SDs as indicated. For the T2 segregating line used in *Experiment 1* and *2*, only plant showing a STRONG level of yellow fluorescence are kept and evaluated. **‡** Native or mutated forms of FT tagged with mCitrine at its C-terminal with its expression driven by 35S promoter. Symbol **§** indicates the statistical significance of differences in comparison with EV (in *Experiment 1*) and *ft-10* (in *Experiment 2*) respectively using two-tailed multiple Student's *t*-test with Bonferroni correction. Single, double and triple symbols represent $P < 0.05$, $P < 0.01$, and $P < 0.001$ respectively. No symbol means that there was no statistically significant difference among indicated genotypes in each experiment (Student's *t*-test, $P \geq 0.05$). Statistical tests were done on the total number of leaves. **‖** *Experiment 3* indicates flowering time of the T1 parental lines corresponding to each of the T2 segregating lines used in *Experiment 1* and *2* under SD conditions.

2.6.4 Determining the Structural Determinants of the Florigenic Identity of FT

Except for two of these mutations were located at other sides of the molecule, mostly, all of these mutations were found at or close to the one side of the surface formed by the canonical anion binding pocket and lobes encoded by segment exon 4B and 4C (Figure 8A). As indicated by Poisson-Boltzmann equation based electrostatic calculation, the surface is dominant by negative charge (Figure 8B). Consistently, among the 10 sets of mutation, seven of the substitution (E109K, Q127R, W138R, Q140K, N152K, L155R, and R173E) involved a significant weakening in the negativity of their amino acid side chain. This leads to the question of whether “charge” is a critical determinant for maintaining the florigenic identity of FT.

To address this question, with respect to the 170 out of 175 amino acid residues of the FT protein, systematic modelings of their mutants were performed and each of their surface charge change was simulated (Supplementary Figure 1). For those point mutations that can lead to a significant charge reversion or disturbance on the FT surface, clones were selected and mutations were decided upon taking into account results obtained from my random mutagenesis studies. Having considered that mutations of the terminal residues exerted profound effect on the FT function and to prevent potential binding interruption of ligand(s) critical to the FT function, instead of terminal tagging, each selected clone of *mFT* was expressed under the control of the 35S (constitutive), SUC2 (phloem companion cell-specific), and FD (SAM-specific) promoters. The possibility of cosuppression was then minimized by verifying the statistical consistency of flowering time data collected under three independent expression contexts. Altogether, 696 *mFT* in their native scaffold were generated and transformed in the wet lab to examine the electrostatic effect on each of their florigenic identities.

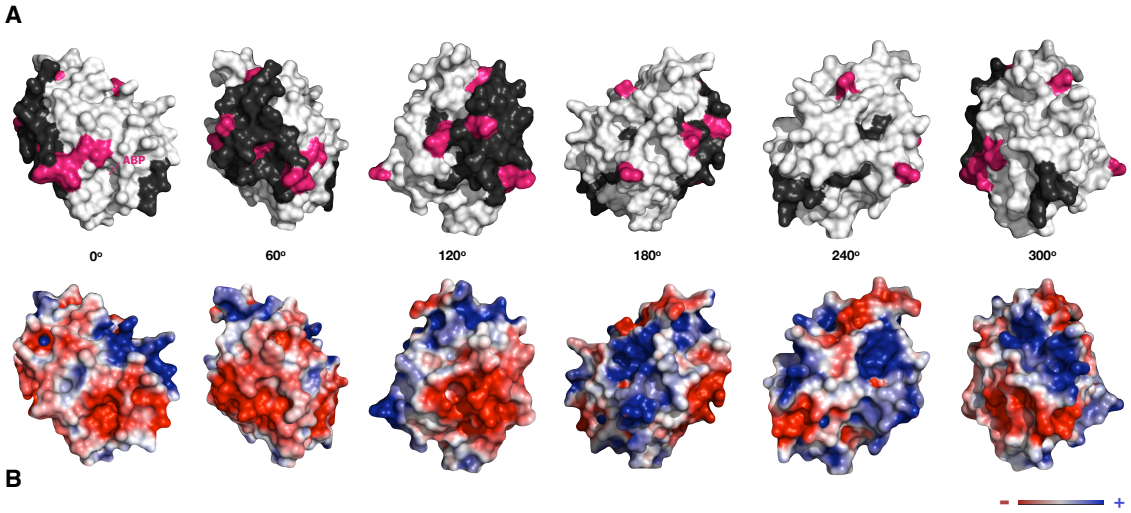

Figure 8. Distribution of 13 residues rendered floral promoting FT into repressing molecule. **(A)** An all-round view of FT. Rotation was done on y-axis with each time rotated by 60 degrees. Potential anion binding pocket was indicated as ABP. Color scheme: magenta, floral-repressor-rendering mutations; black, surface/lobes encoded by exon 4B and 4C (BCL) of FT. **(B)** Electrostatic potential of FT at the corresponding orientation. Negative and positive electrostatic potential is represented by red and blue color on the electrostatic map respectively. As shown by the electrostatic calculations, ABP and BCL are dominated by strongly negative charge.

2.6.6 Effect of Mutating the Canonical Residues on FT Function

Mostly due to the invariance among the PEBP family, previous studies suggested that several amino acid residues are critical to FT function (Hanzawa et al., 2005; Ahn et al., 2006; Lorenz et al., 2003; Pnueli et al., 2001; Taoka et al., 2011). Upon mutating any of these canonical residues, one would expect a profound impact on FT function. By means of the comprehensive site-directed mutagenesis on the FT sequence, 155 out of the 175 amino acid residues of FT were "touched" with 104 positions mutated more than once. Among the 232 mutations, point mutations at the canonical positions like P75 and R130 did not affect the floral promoting ability but terminal flower forming ability was reduced (Figure 9 and Table 2). Surprisingly, mutations at positions D71, P72, E146, R62, I150, and Y151 which are absolutely conserved in *Plantae* did not affect FT function at all and the floral promoting and terminal flower forming ability specific to the FT overexpressor were well-preserved. In contrast, single mutations at position D73 of the invariant DPDXP motif rendered FT into almost completely inactive, and no I1* could be observed in any of their transformants. In line with the previous findings, mutations at position Y85 could only weaken the FT floral promoting function, while merely 1-2 shoots corresponding to the I1* phase could occasionally be found in the Y85H transformants. Further, besides the canonical mutations, a range of mutations at the non-canonical but ultraconserved residues in *Plantae* were introduced. Surprisingly, most of them did not show significant effect on weakening the FT function, implying the high degree of tolerance of FT to substitution, while only a small group of residues are key to the FT functioning.

Figure 9

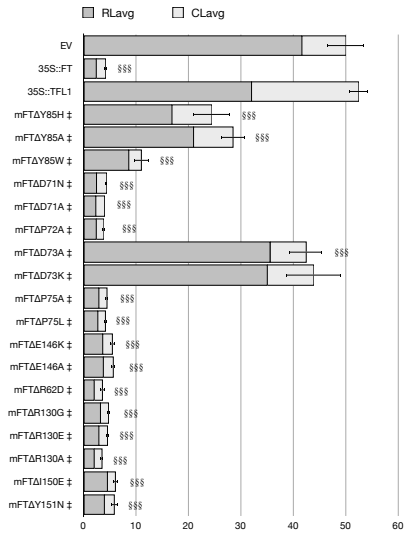

Table 2

Genotype *	No. of rosette leaves †	No. of cauline leaves †	Total no. of leaves †	I1*	TF †	*n*
	Experiment 1, SDs †					
EV	41.6 ± 6.3 (26-54)	8.4 ± 2.0 (5-12)	50.0 ± 7.2 (31-62)	N	N	20
35S::FT	2.4 ± 0.5 (2-3)	1.8 ± 0.4 (1-2)	4.2 ± 0.5 (3-5) §§§	N	Y	20
35S::TFL1	32.0 ± 3.3 (26-38)	20.5 ± 2.9 (15-29)	52.5 ± 3.7 (47-58)	Y	N	20
mFTΔY85H ‡	16.8 ± 4.0 (11-24)	7.6 ± 3.3 (4-13)	24.4 ± 7.0 (15-37) §§§	Y ¶	N	19
mFTΔY85A ‡	20.9 ± 3.4 (16-29)	7.5 ± 1.8 (5-11)	28.5 ± 4.7 (21-32) §§§	N	N	19
mFTΔY85W ‡	8.6 ± 2.4 (5-14)	2.4 ± 0.8 (1-4)	11.0 ± 2.9 (7-16) §§§	N	N	20
mFTΔD71N ‡	2.5 ± 0.5 (3-10)	2.0 ± 0.6 (1-3)	4.4 ± 0.5 (4-5) §§§	N	Y	20
mFTΔD71A ‡	2.3 ± 0.5 (2-3)	1.7 ± 0.5 (1-2)	4.0 ± 0.0 (4) §§§	N	Y	19
mFTΔP72A ‡	2.4 ± 0.5 (2-3)	1.5 ± 0.5 (1-2)	3.9 ± 0.6 (3-5) §§§	N	Y	20
mFTΔD73A ‡	35.5 ± 5.4 (24-43)	6.9 ± 1.9 (4-12)	42.4 ± 8.3 (28-51) §§§	N	N	20
mFTΔD73K ‡	35.0 ± 9.4 (21-47)	8.9 ± 1.7 (7-12)	43.9 ± 10.5 (29-57)	N	N	9
mFTΔP75A ‡	2.9 ± 0.7 (2-4)	1.6 ± 0.5 (1-2)	4.5 ± 0.6 (3-5) §§§	N	N	20
mFTΔP75L ‡	2.7 ± 0.6 (2-4)	1.5 ± 0.5 (1-2)	4.2 ± 0.6 (3-5) §§§	N	Y	20
mFTΔE146K ‡	3.6 ± 0.7 (3-5)	1.8 ± 0.6 (1-3)	5.5 ± 0.8 (4-7) §§§	N	Y	19
mFTΔE146A ‡	3.8 ± 0.9 (3-6)	1.9 ± 0.4 (1-3)	5.7 ± 0.8 (5-8) §§§	N	Y	20
mFTΔR62D ‡	2.6 ± 0.0 (2)	1.6 ± 0.5 (1-2)	3.6 ± 0.5 (3-4) §§§	N	Y	19
mFTΔR130G ‡	3.2 ± 0.4 (3-4)	1.6 ± 0.5 (1-2)	4.7 ± 0.7 (4-6) §§§	N	N	19
mFTΔR130E ‡	2.9 ± 0.6 (2-4)	1.7 ± 0.5 (1-2)	4.6 ± 0.5 (4-5) §§§	N	N	20
mFTΔR130A ‡	2.0 ± 0.0 (2)	1.5 ± 0.6 (0-2)	3.5 ± 0.6 (2-4) §§§	N	Y	20
mFTΔI150E ‡	4.5 ± 1.1 (3-7)	1.5 ± 0.5 (1-2)	6.1 ± 0.9 (4-8) §§§	N	Y	19
mFTΔY151N ‡	3.9 ± 1.1 (3-7)	1.9 ± 0.6 (1-3)	5.8 ± 1.4 (4-10) §§§	N	Y	19

Figure 9. Effect of point mutations at the canonical amino acid position of PEBP on the floral inducing or repressing ability of mFT. Numerical, statistical and abbreviation details of the plots are shown in **Table 2**.

Table 2. Flowering time of mutant and transgenic plants generated by mutating canonical residues of PEBP family. *EV, empty vector control; mFT, mutated FT. † Indicators of flowering time and shown as average ± standard derivation (range). Plants in each experiment were grown under SD as indicated. TF, terminal flower. ‡ Data of T1 transformants harboring transgenes driven by 35S promoter and expressed in Col-0 background were shown. Statistical consistence between the 35Spro, SUCpro and FDpro datasets were confirmed by Student *t*-test with Bonferroni correction **(Supplementary Table 1)**. Symbol § indicates the statistical significance of differences in comparison with 35S::*TFL1* using two-tailed multiple Student's *t*-test with Bonferroni correction. Single, double and triple symbols represent $P < 0.05$, $P < 0.01$ and $P < 0.001$ respectively. No symbol means that there was no statistically significant difference among indicated genotypes in each experiment (Student's *t*-test, $P \geq 0.05$). Statistical tests were done on the total number of leaves. ¶ Only 1-2 shoots corresponding to the I1* phase can be occasionally found in the Y85 mutated transformants.

2.6.6 Six Critical Amino Acid Residues as the FT Florigenic Determinants

After going through the flower and flowering time phenotypes of about 14000 T1 transformants, I decided to focus further analyses on six critical amino acid residues ultraconserved among FT homologs, with three of them (E109, W138, and Q140) sitting at the Binding Pocket Peripheral (BPP), while another three of them (L128, N152, and Y134) are found at the exon 4B and 4C encoded Lobe (BCL). For E109 (exon 4A) and Q140 (exon 4B), single amino acid changes (such as E109K and Q140K) were sufficient to revert the charge of the entrance of the ABP as shown by electrostatic calculation (Figure 10). Transformants of these mutated forms showed a floral delaying effect as strong as that of their native TFL1 (Figure 11 and Table 3). Though the charge reversion effect of mutations at N152 (exon 4C) and L128 (exon 4B) were less profound compared with that of E109 and Q140, mutations leading to localized positivity expansion at the BCL also render FT into a TFL1-like molecule. Interestingly, charge at regions corresponding to the BPP and BCL on TFL1 are strongly positive (Figure 10). For positions W138 (on BPP) and Y134 (on BCL), the effect seemed to be independent of the charge change (Supplementary Figure 2). While Y134K and Y134A could render FT into a TFL1-like molecule, position W138 did not tolerate any kind of mutation and a single substitution (such as W138E) could endow the FT backbone with the repressing power as potent as or even more potent than that of the native TFL1 (Figure 11 and Table 3).

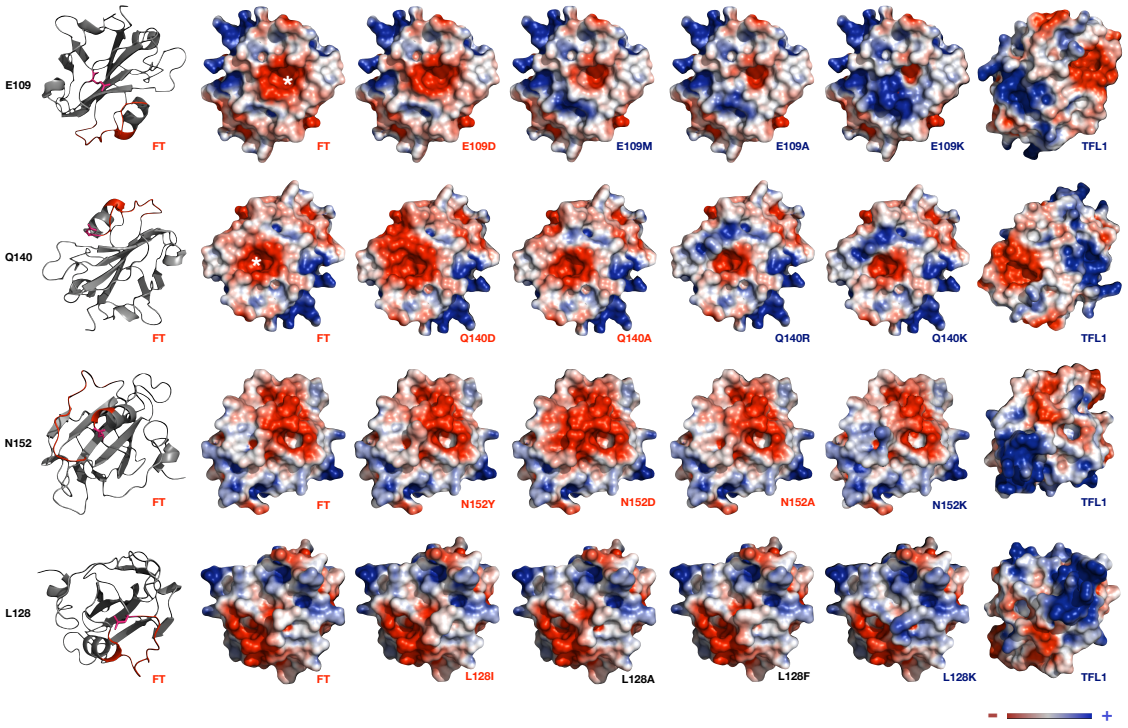

Figure 10. Effect of point mutations on the surface electrostatic potential of FT as determined by molecular modeling. Adaptive Poisson-Boltzmann Solver (APBS) plugin was used for calculating the electrostatic properties (Baker et al., 2001), while visualization was done by PyMOL. Positions of the residues concerned in each case are highlighted in pink, while the invariant loop and FT sequence signature respectively encoded by exon 4B and 4C are highlighted in red in the cartoon structure of FT. Negative and positive electrostatic potential are represented by red and blue color on the electrostatic map respectively. Electrostatic maps of TFL1 aligned in the same orientations in each case are shown for comparison. Labels of native and mutated FTs retain FT floral promoting and terminal flower forming ability are in red, while those showing floral repressing and I1* forming ability of TFL1 are in blue. Labels of loss-of-function or almost loss-of-function molecules are in black color. Position of the canonical ABP is marked by asterisk on the electrostatic maps at each orientation of native FT (if any).

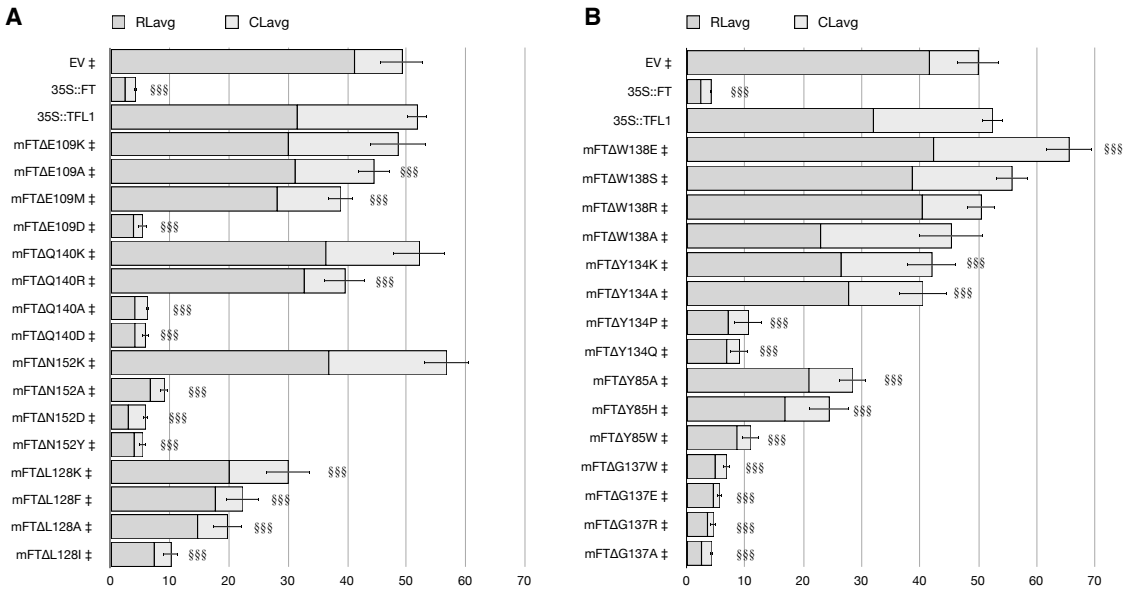

Figure 11. Effect of the amino acid side chain properties at six critical amino acid positions on the floral inducing or repressing ability of mFTs under SD conditions. **(A)** Charge-dependent positions. **(B)** Charge non-dependent positions. Mutations at G137 proposed to be capable of rendering FT into TFL1 (Pin et al., 2010) did not show effect on FT function in my study; flower and flowering time phenotypes of their transformants were listed for reference. Numerical, statistical and abbreviation details of the plots are shown in **Table 3**.

Genotype *	No. of rosette leaves †	No. of cauline leaves †	Total no. of leaves †	I1*	TF †	*n*
	Experiment 1, SDs †					
EV	41.2 ± 6.5 (24-52)	8.1 ± 1.8 (5-12)	49.3 ± 7.4 (29-60)	N	N	20
35S::FT	2.4 ± 0.5 (2-3)	1.8 ± 0.4 (1-2)	4.2 ± 0.5 (3-5) §§§	N	Y	20
35S::TFL1	31.5 ± 3.3 (26-37)	20.4 ± 3.0 (15-29)	51.9 ± 3.4 (47-58)	Y	N	20
mFTΔE109K ‡	30.0 ± 7.8 (14-46)	18.6 ± 6.2 (10-32)	48.6 ± 9.7 (32-70)	Y	N	20
mFTΔE109A ‡	31.2 ± 4.2 (19-37)	13.4 ± 2.4 (9-18)	44.5 ± 5.3 (33-53) §§§	Y	N	20
mFTΔE109M ‡	28.1 ± 3.6 (20-34)	10.8 ± 1.9 (8-15)	38.9 ± 4.5 (29-45) §§§	Y	N	19
mFTΔE109D ‡	3.8 ± 0.8 (3-5)	1.6 ± 0.8 (1-4)	5.4 ± 1.4 (4-9) §§§	N	Y	18
mFTΔQ140K ‡	38.4 ± 5.6 (28-45)	15.9 ± 6.4 (7-32)	52.2 ± 8.9 (35-75)	Y	N	20
mFTΔQ140R ‡	32.7 ± 6.5 (17-45)	6.9 ± 1.2 (5-10)	39.6 ± 7.0 (22-52) §§§	Y	N	16
mFTΔQ140A ‡	4.1 ± 0.6 (3-5)	2.2 ± 0.7 (1-4)	6.2 ± 0.7 (5-7) §§§	N	Y	17
mFTΔQ140D ‡	4.1 ± 1.2 (3-7)	1.8 ± 0.8 (1-3)	6.0 ± 1.3 (4-9) §§§	N	Y	14
mFTΔN152K ‡	36.8 ± 4.3 (29-44)	19.9 ± 6.3 (7-31)	56.8 ± 7.7 (41-70)	Y	N	19
mFTΔN152A ‡	6.7 ± 1.0 (5-8)	2.4 ± 0.9 (1-4)	9.1 ± 1.5 (7-11) §§§	N	Y	9
mFTΔN152D ‡	2.9 ± 0.7 (2-4)	2.9 ± 0.7 (2-4)	5.9 ± 1.0 (5-8) §§§	N	Y	19
mFTΔN152Y ‡	3.9 ± 1.2 (2-7)	1.5 ± 0.5 (1-2)	5.4 ± 1.3 (4-9) §§§	N	Y	16
mFTΔL128K ‡	20.0 ± 5.1 (13-30)	10.0 ± 2.9 (8-17)	30.0 ± 7.6 (21-47) §§§	Y	N	9
mFTΔL128F ‡	17.7 ± 4.8 (12-25)	4.7 ± 1.5 (2-7)	22.3 ± 5.7 (14-30) §§§	N	N	9
mFTΔL128A ‡	14.7 ± 3.7 (9-21)	5.1 ± 1.8 (2-8)	19.7 ± 4.9 (13-28) §§§	N	N	15
mFTΔL128I ‡	7.3 ± 2.2 (4-11)	2.9 ± 1.1 (2-5)	10.2 ± 2.7 (6-14) §§§	N	Y	9
	Experiment 2, SDs †					
EV ‡	41.6 ± 6.3 (26-54)	8.4 ± 2.0 (5-12)	50.0 ± 7.2 (31-62)	N	N	20
35S::FT	2.4 ± 0.5 (2-3)	1.8 ± 0.4 (1-2)	4.2 ± 0.5 (3-5) §§§	N	Y	20
35S::TFL1	32.0 ± 3.7 (26-38)	20.0 ± 2.9 (15-29)	52.5 ± 3.7 (47-58)	Y	N	20
mFTΔW138E ‡	42.3 ± 6.3 (32-56)	23.3 ± 5.5 (13-32)	65.6 ± 6.0 (49-78) §§§	Y	N	19
mFTΔW138S ‡	38.7 ± 4.0 (29-43)	17.1 ± 4.3 (11-23)	55.8 ± 5.4 (45-62)	Y	N	9
mFTΔW138R ‡	40.4 ± 4.3 (32-49)	10.2 ± 2.8 (5-18)	50.5 ± 4.9 (42-59)	Y	N	19
mFTΔW138A ‡	22.9 ± 6.4 (13-33)	22.4 ± 6.5 (13-36)	45.4 ± 11.1 (29-64)	Y	N	18
mFTΔY134K ‡	26.5 ± 8.6 (11-45)	15.6 ± 6.2 (7-29)	42.1 ± 8.5 (29-57) §§§	Y	N	20
mFTΔY134A ‡	27.8 ± 6.8 (14-39)	12.8 ± 2.2 (7-16)	40.5 ± 8.4 (27-55) §§§	Y	N	20
mFTΔY134P ‡	7.1 ± 3.2 (4-17)	3.5 ± 2.0 (1-9)	10.6 ± 4.8 (5-14) §§§	N	N	20
mFTΔY134Q ‡	6.8 ± 2.9 (3-14)	2.2 ± 0.9 (1-4)	9.1 ± 3.4 (5-18) §§§	N	N	19
mFTΔY85A ‡	20.9 ± 3.4 (16-29)	7.5 ± 1.8 (5-11)	28.5 ± 4.7 (21-37) §§§	N	N	19
mFTΔY85H ‡	16.8 ± 4.0 (11-24)	7.6 ± 3.3 (4-13)	24.4 ± 7.0 (15-37) §§§	Y ¶	N	18
mFTΔY85W ‡	8.6 ± 2.4 (5-14)	2.4 ± 0.8 (1-4)	11.0 ± 2.9 (7-17) §§§	N	N	20
mFTΔG137W ‡	4.9 ± 1.0 (3-6)	2.0 ± 0.9 (1-4)	6.9 ± 1.4 (5-10) §§§	N	Y	14
mFTΔG137E ‡	4.6 ± 0.8 (3-6)	1.1 ± 0.3 (1-2)	5.7 ± 0.8 (4-7) §§§	N	Y	18
mFTΔG137R ‡	3.6 ± 1.2 (2-7)	1.1 ± 0.4 (0-2)	4.7 ± 1.2 (3-8) §§§	N	Y	20
mFTΔG137A ‡	2.5 ± 0.7 (2-4)	1.8 ± 0.8 (0-3)	4.3 ± 0.7 (3-5) §§§	N	Y	19

Table 3. Flowering time of mutant and transgenic plants showing dependence (*Experiment 1*) or non-dependence (*Experiment 2*) on surface charge change of FT. *EV, empty vector control; mFT, mutated FT. **†** Indicators of flowering time and shown as average ± standard derivation (range). Plants in each experiment were grown under SD as indicated. TF, terminal flower. **‡** Data of T1 transformants harboring transgenes driven by 35S promoter and expressed in Col-0 background were shown. Statistical consistence between the 35Spro, SUCpro and FDpro datasets were confirmed by Student *t*-test with Bonferroni correction **(Supplementary Table 1)**. Symbol **§** indicates the statistical significance of differences in comparison with 35S::*TFL1* using two-tailed multiple Student's *t*-test with Bonferroni correction. Single, double and triple symbols represent $P < 0.05$, $P < 0.01$ and $P < 0.001$ respectively. No symbol means that there was no statistically significant difference among indicated genotypes in each experiment (Student's *t*-test, $P \geq 0.05$). Statistical tests were done on the total number of leaves. **¶** Only 1-2 shoots corresponding to the I1* phase can be occasionally found in the Y85 mutated transformants.

2.6.7 Floral Repressing Effect Is Not Caused by Cosuppression

As described earlier, specific mutations at any of the six positions that disrupt the nature of the determinants, such as an electrostatic reversion of BPP mediated by E109K, could render FT into a floral repressor as strong as the TFL1. However, in terms of the floral delaying effect, a double mutant of *FT* and *TSF*, like *ft-10 tsf-1* mimicking the cosuppressor of *FT* and *TSF*, is similarly late as the *TFL1* overexpressor under SD. The only apparent difference between them is the possession of the interim developmental phase known as I1*, that can only be found in the overexpressor of *TFL1*, but neither in *ft-10 tsf-1* double mutant nor in the cosuppressor of *FT* and *TSF*. To verify the TFL1 identity of these mutated forms of FT, while ruling out the possibility that the delaying effect was caused by the cosuppression of endogenous *FT* and *TSF*, developmental and morphological phenotypes with respect to the transformants overexpressing mutations at the six critical positions were carefully examined.

When the mutated *FT* were driven to express by the constitutive 35S promoter, similar to that of the *35S::TFL1*, the interim developmental phase I1* unique to the *TFL1* overexpressor and characterized by the formation of auxiliary shoots without subtending cauline leaf (Figure 12A) could clearly be observed in all of their transgenic lines (Table 3 and Figure 12D). Also, similar to the 35S:*TFL1*, floral aberrations, such as infertile floral organs surrounded by whorls of leaf-like petals that further characterize the progression of I1* phase (Figure 12B and C), could be identified in their transformants. Altogether, these findings support the conclusion that the floral repressing effect of these mutations is not caused by cosuppression, but rather via their TFL1 activity gained from the mutations.

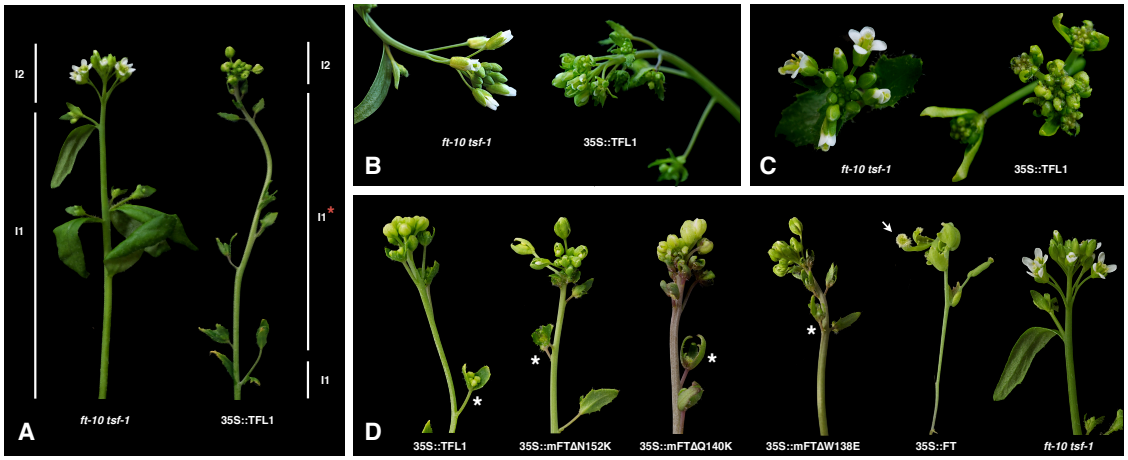

Figure 12. Phenotypic comparison of *FT* overexpressors mutated at the florigenic identity-determining positions in comparison to *TFL1* overexpressor and *ft-10 tsf-1* double mutant. **(A)** Node comparison between the *ft-10 tsf-1* double mutant and 35S::*TFL1*. The featured interim I1* can only be observed in 35S::*TFL1* but never in *ft-10 tsf-1* (a mimic of the *FT* and *TSF* cosuppressor). I1, inflorescence phase 1 where each shoot emerged is subtended by a cauline leaf; I1*, interim phase where shoots lacking a subtending cauline leaf are produced; I2, phase where normal flowers are produced. **(B, C)** Side- and top-view of the shoot apex of *ft-10 tsf-1* mutant and 35S::*TFL1*. Clusters of flowers surrounded by leaf-like organs arranged in a whorled phyllotaxy unique to the 35S::*TFL1* are shown. **(D)** Comparison of post-vegetative phase nodes between the 35S::*TFL1*, representative *FT* overexpressors mutated at the florigenic identity-determining positions at region BCL (N152K), region BPP (Q140K, charge-related) (W138E, charge-unrelated), 35S::*FT* and *ft-10 tsf-1* double mutant. Asterisks indicate shoots corresponding to I1* phase while arrow points out terminal flower, if any.

2.6.8 FT variants with single amino acid substitutions can fully mimic TFL1

To further confirm the TFL1-like activity of these mutated FT versions, complementation studies of *tfl1-1*, a severe knockdown allele of *TFL1*, were performed. Unlike FT, mutated FTs harbor the canonical tyrosine-to-histidine mutation and loss-of-function mutation (such as W88R), five of the FT variants with critical residues mutated (W138E, Y134K, Q140K, N152K, and E109K) expressed in the native *TFL1* genomic context could well complement the flowering time phenotype of *tfl1-1* (Figure 13 and Table 4). Also, these five mutated FT were sufficient to rescue both the plant architecture and the terminal flower phenotype of the *tfl1-1*, which again, could not be achieved by the non-mutated FT or any mutated FT without the TFL1 function (Figure 14). Based on these findings, I conclude that the determinant-mutated FT versions are able to fully mimic TFL1 function.

Figure 13

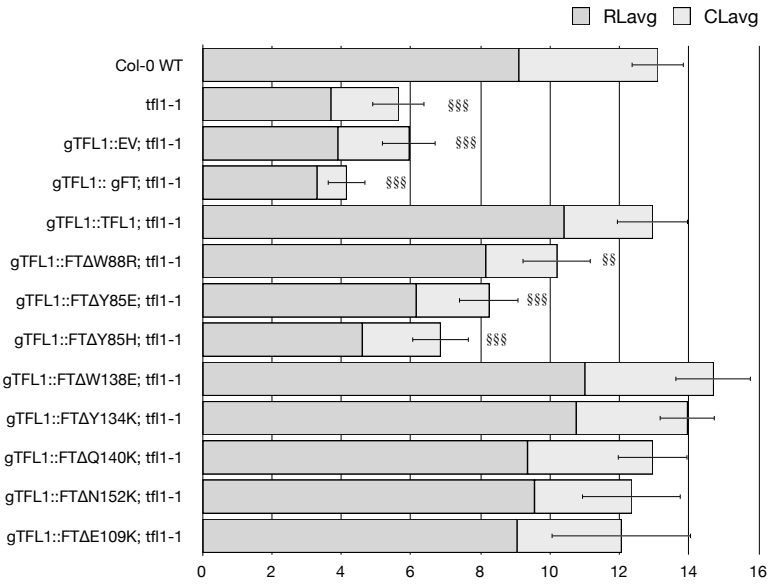

Figure 13. Flowering time comparison of *tfl1-1* transformed by *FT*, *TFL1* and five determinant-mutated *FT* driven by the genomic TFL1 sequence. Genomic fragment including 2.2kb upstream and 4.6kb downstream shown to have sufficient regulatory information for native *TFL1* expression (Sohn et al., 2007) was used as the expression backbone. Numerical, statistical and abbreviation details of the plots are shown in **Table 4.**

Table 4

Genotype *	No. of rosette leaves †	No. of cauline leaves †	Total no. of leaves †	*n*
	Experiment 1, LDs †			
Wild type (Col-0)	9.1 ± 1.3 (7-12)	4.0 ± 1.1 (2-6)	13.1 ± 1.5 (9-15)	20
tfl1-1	3.7 ± 1.3 (2-6)	2.0 ± 0.4 (1-3)	5.7 ± 1.5 (3-8) §§§	20
gTFL1::EV; *tfl1-1*	3.9 ± 1.3 (2-7)	2.1 ± 0.6 (1-3)	6.0 ± 1.6 (3-9) §§§	20
gTFL1::gFT; *tfl1-1*	3.3 ± 0.7 (2-4)	0.9 ± 0.7 (0-2)	4.2 ± 1.1 (2-6) §§§	20
gTFL1::TFL1; *tfl1-1*	10.4 ± 1.4 (8-13)	2.6 ± 0.8 (1-4)	13.0 ± 2.1 (9-17)	20
gTFL1::FTΔW88R; *tfl1-1*	8.2 ± 1.5 (6-11)	2.1 ± 0.6 (1-3)	10.2 ± 2.0 (7-14) §§	20
gTFL1::FTΔY85E; *tfl1-1*	6.2 ± 1.5 (4-10)	2.1 ± 0.4 (1-3)	8.3 ± 1.7 (6-12) §§§	20
gTFL1::FTΔY85H; *tfl1-1*	4.6 ± 1.3 (3-8)	2.3 ± 0.6 (2-4)	6.9 ± 1.6 (5-12) §§§	20
gTFL1::FTΔW138E; *tfl1-1*	11.0 ± 1.7 (8-14)	3.7 ± 0.7 (2-5)	14.7 ± 2.2 (10-18)	20
gTFL1::FTΔY134K; *tfl1-1*	10.8 ± 1.4 (8-13)	3.2 ± 0.8 (2-5)	14.0 ± 1.6 (11-16)	20
gTFL1::FTΔQ140K; *tfl1-1*	9.4 ± 1.4 (7-12)	3.6 ± 1.0 (2-6)	13.0 ± 2.0 (9-16)	20
gTFL1::FTΔN152K; *tfl1-1*	9.6 ± 2.1 (6-13)	2.8 ± 1.0 (1-5)	12.4 ± 2.9 (8-17)	20
gTFL1::FTΔE109K; *tfl1-1*	9.1 ± 3.2 (5-17)	3.0 ± 1.3 (1-6)	12.1 ± 4.0 (7-20)	20

Table 4. Flowering time of mutant and transgenic plants involved in the *tfl1-1* complementation test. *EV, empty vector control; mFT, mutated FT. † Indicators of flowering time and shown as average ± standard derivation (range). Plants in each experiment were grown under LD as indicated. Symbol **§** indicates the statistical significance of differences in comparison with gTFL1::*TFL1*; *tfl1-1* using two-tailed multiple Student's *t*-test with Bonferroni correction. Single, double and triple symbols represent $P < 0.05$, $P < 0.01$ and $P < 0.001$ respectively. No symbol means that there was no statistically significant difference among indicated genotypes in each experiment (Student's *t*-test, $P \geq 0.05$). Statistical tests were done on the total number of leaves.

Figure 14. Complementation of *tfl1-1* mutant. **(A)** Rescue of the plant architecture of *tfl1-1* and **(B)** their corresponding inflorescence phenotypes by one of the charge reverted mutation Q140K in comparison to FT, TFL1, a loss-of-function FT (W88R) and the canonical mFTΔY85H. Arrows indicate terminal flowers.

2.7 DISCUSSION

PEBPs form a ubiquitous protein family showing distinctive functionality. Amongst them, FT and TFL1 are two representative members of the *Plantae.* Though sharing the same origin and structural topology, FT and TFL1 are opposite in function, with FT promoting and TFL1 inhibiting flowering. To shed light on the critical determinants of their antagonistic function, in this study, I utilized unbiased "touching" via random and then site-directed mutagenesis to perform an in-depth investigation of the FT function. This way, I sought to overcome the limitation of the previous approaches, including exonic swapping that may grossly alter protein structure and obscure the function of individual residues. Then, by sorting the resulting transformants under SD and then LD conditions, classification of the flowering phenotype of thousands of mFT can be achieved at high resolution. After that, by combining the *in silico* structural analysis with genetic studies, I demonstrate that maintenance of charge and specific bondings for two localized surfaces, BPP and BCL, are critical for determining the florigenic identity of FT. Disturbance on either of these properties is good enough to render FT into a fully functional TFL1. My work identifies novel elements constituting the FT florigenic identity. Together with the additional information supplementing the previously identified determinants, I provide an integral point of view on factors determining FT florigenic identity and demonstrate these factors are preserved by sequence ultraconservancy.

2.7.1 Dominant-Negative Phenotype Is Not Caused by Mutations at Canonical Positions

Apart from repressing the flowering time, being an antagonist of FT (or so called an anti-florigen), TFL1 is also a key regulator of inflorescence development. So, upon overexpression, TFL1 could greatly delay the flowering time by extending the period of every single phase during the development of adult plant (Ratcliffe et al., 1998). In particular, TFL1 could prolong the transition from first (I1) to second (I2) inflorescence phase, resulting in a new interphase not found in wild-type and known as I1*. This property uniquely defines TFL1-like molecules.

Among the 232 mutations, the canonical positions such as the Tyr85 (Hanzawa et al., 2005), invariant DPDXP motif in LeSP3D (FT homolog in tomato) (Pnueli et al., 2001), typical phosphorylation site S153 (corresponding to E146 in FT) regulating hPEBP and Raf-1 binding (Lorenz et al., 2003) as well as residues constituting a salt bridge between FT and 14-3-3/GRF protein (R62 and R130) in HD3A (FT homolog in rice) (Taoka et al., 2011) were included. While most of the transformants remained a potent floral promoter (with only mFTΔP75A, R130G, and R130A having no terminal flower) among the site-directed mutagenesis batch, mutations at canonical position D73 showed one of the strongest floral delaying effects in SD among the canonical mutations (Figure 9). However, none of their transformants demonstrated the I1* transition (Table 2), suggesting they are simply loss-of-function, but cannot function like TFL1. For Y85H, though no terminal flowers could be found in any of the transformants, in contrast to the formation of around 15-39 auxiliary shoots lacking of cauline leaves in the 35S::*TFL1* transformants,

only 1-2 shoots corresponding to the I1* phase could be occasionally found in the Y85 mutated transformants under both SD and LD conditions. It indicates that Y85 mutations can only switch FT into a poorly functional TFL1. Altogether, my findings demonstrate that the canonical mutations cannot account for the dominant negative effect and there exists an alternative cause for switching FT from a florigen into the anti-florigenic TFL1.

It is also important to note is that a range of mutations at the non-canonical positions (Figure 7) are found to be capable of weakening the FT function significantly, suggesting that the approach adopted in this study can reveal residues critical to the FT functions that might have been missed by exon swapping and sequence/structural alignment used in previous work, which is potentially caused by domain truncation and selection bias respectively.

2.7.2 Factors Determining the FT Florigenic Identity

PEBP is a protein family found in almost every kingdom of species. Regardless of the origins of *Protista*, *Animalia* or *Plantae*, all members of this family share an invariant pocket encoded by the highly conserved residues of their exon 2 and 4B. Structural analysis showed either inorganic anions (acetate ions in Protein Data Bank entry 1A44; cacodylate ions in entry 1BEH) or organic anions (O-phosphotyrosine in Protein Data Bank entry 2QYQ; O-phosphorylethanolamine head group in entry 1B7A) could form a snug fit in the pocket of mammalian PEBP crystal structures (Banfield et al., 1998; Serre et al., 1998) (Figure 15).

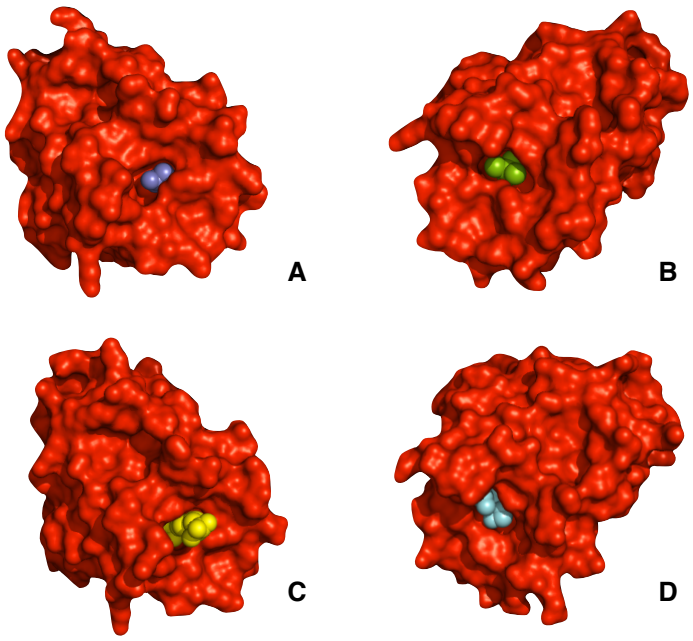

Figure 15. Mammalian PEBP crystal structures showing the formation of a snug-fit with either an organic or inorganic anion in their anion binding pocket. **(A)** PEBP from bovine brain with an acetate ion (purple) (PDB entry 1A44). **(B)** Human PEBP in complex with a cacodylate ion (green) (PDB entry 1BEH). **(C)** Human PEBP in complex with O-phosphotyrosine (yellow) (PDB entry 2QYQ). **(D)** PEBP from bovine brain with a O-phosphorylethanolamine head group (pale cyan) (PDB entry 1B7A).

Also, direct binding of phosphorylated peptide, Raf-1, to the same anion binding pocket in murine PEBP has recently been shown by a nuclear magnetic resonance (NMR) chemical shift study (Tavel et al., 2012). Altogether, the findings confirmed that this invariant pocket is a ligand binding site, and based on the nature consistency of its ligands, the site is called Anion Binding Pocket (ABP).

ABP is supposed to be positively charged and, intuitively, it should play a stabilizing role for accommodating the anionic groups of ligand. Surprisingly, irrespective of their positive or negative regulatory roles and their animal or plant origins, in all cases, my calculation shows that ABP of all identified PEBP carry a strongly negative electrostatic potential (Figure 16). In other words, both the pocket and their proven ligands have the same charge.

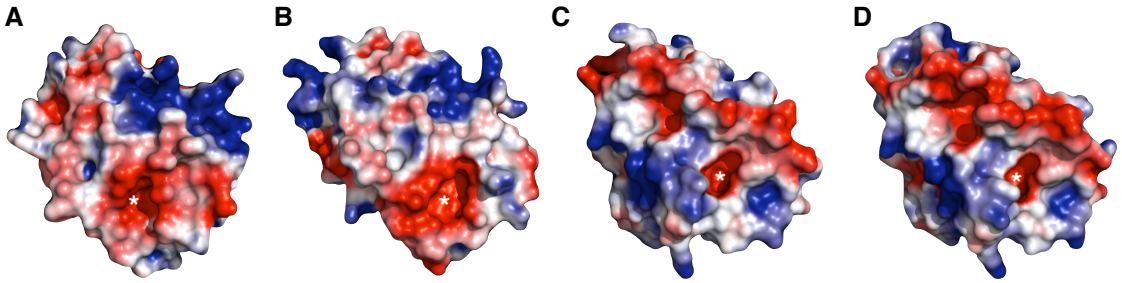

Figure 16. Electrostatic potential of plant and animal PEBPs. **(A)** FT of *Arabidopsis* (PDB entry 1WKP). **(B)** TFL1 of *Arabidopsis* (PDB entry 1WKO). **(C)** PEBP from bovine brain (PDB entry 1A44). **(D)** Human PEBP (PDB entry 1BEH). Negative and positive electrostatic potential are represented by red and blue color on the electrostatic map respectively. White asterisk indicates the position of the highly conserved anion binding pocket (ABP).

As direct association of a single anionic molecule with the ABP was proven to be functionally critical for the regulatory role of mammalian PEBP (Yeung et al., 1999), providing that the same is true in the plant system, it implies the presence of an attractive force exerted by the remaining binding interface in order to counter the repulsion at the ABP. What are those forces in the case of plant PEBP?

By carrying out random mutagenesis of FT, I obtained clues on charge as a critical determinant of FT as a florigen. Then, by means of the site directed mutagenesis, I show that, on the one hand, electrostatic reversion at position distal from the ABP, such as a cationic pocket centered at K29 and a cationic groove propagated from R44 to R53, had no significant effect on function or could at most render FT into a loss-of-function molecule respectively (Supplementary Table 2). On the other hand, I narrowed down and confirmed six residues capable of rendering the florigen FT into a fully functional TFL1, while verified Y85 is essential for FT function. In terms of their physical location on the 3D structure, the seven critical residues can be grouped into two separated but interconnected regions, namely Binding Pocket Peripheral (BPP) and exon 4B and 4C encoded Lobe (BCL).

2.7.2.1 Localized Positivity Avoidance at Binding Pocket Peripheral

Region Binding Pocket Peripheral **(**BPP) refers to the entrance or vicinity of the canonical anion binding pocket (ABP) (Banfield et al., 1998). Similar to the pocket itself, by nature, BPP is strongly negative in charge. My findings demonstrate that charge of the BPP is strongly affected by two residues, that are namely E109 (exon 4A) and Q140 (exon 4B).

For position E109, introduction of residues with a positive side chain (E109K) lead to a potent electrostatic reversion (Figure 10) and phenotypically, rendered FT act like a fully functional TFL1 (Table 3). Similarly, mutations to hydrophobic residues (E109A and E109M) diminished the negative charge of the region and lead to a localized expansion of positive charge mainly originated from residues R139 (exon 4B). While neutral and positive charged mutations at the position likewise led to the dominant negative phenotypes (Figure 11 and Table 3). The only tolerable mutation tested in my batch was E109D that could well preserve the native negative charge distribution of the BPP, while consistently maintaining the FT activity. This indicates that E109 is one of the critical residues determining the negativity of BPP. Governing of such negativity is essential for maintaining the FT florigenic identity.

Compared with E109, tolerance to mutation is relatively high at position Q140 (Figure 10). As apart from the negatively charged residue (Q140D), introduction of a residue with a neutral side chain (Q140A) could also nicely preserve both of the floral promoting and terminal flower forming ability of FT (Figure 11 and Table 3). However, similar to the position E109, mutations to residues with positive side chain (Q140K and Q140R) were absolutely not tolerated at Q140, or localized negativity was overridden by the positive charge developed rendering the molecule into a fully functional TFL1. Together with the fact that a potent localized positive charge can be observed at the BPP of the native TFL1, my findings illustrate the critical role of E109 and Q140 for maintaining the negativity of BPP. Avoidance of positive charge of the region has proven to be essential for preventing FT from switching to an anti-florigenic TFL1.

However, it is important to note that such avoidance was restricted to the pocket entrance of the ABP only. Charge reversion deep inside the pocket (such as D71N) could not convert FT into a TFL1 as shown by my data (Figure 9 and Table 2). Consistent with this finding, residues at the vicinity rather than within the pocket have recently been confirmed to be critical for the functioning of hPEBP (Tavel et al., 2012).

2.7.2.2 Localized Positivity Avoidance at Exon 4B and 4C Encoded Lobe

Region BCL refers to a lobe region built up from two invariant loops encoded by exon 4B and 4C. In terms of electrostatic potential, BCL of FT is mainly neutral in charge. In contrast to the drastic electrostatic disturbance observed when introducing mutations to BPP, single amino acid change at the region BCL could not lead to a widespread charge reversion effect. Having said so, region BCL and BPP share the same characteristic for not being tolerable to the positively charged mutation as demonstrated by my findings at two residues constituting the FT signature sequences, N152 (exon 4C) and L128 (exon 4B).

In the case of N152, similar to Q140, it is relatively flexible and can tolerate mutation to residues with negative (N152D), neutral (N152A), hydrophilic (N152S), or aromatic (N152Y) side chains. But in all cases, the neutral/very slightly negative property of the region were nicely preserved after each mutation (Figure 10). The only intolerable mutation among the batch was N152K that, as shown by electrostatic calculation, neutralize/revert the localized charge while introduced positivity to the point of mutation. Consistently, a phenocopy of the TFL1 overexpressor was observed when overexpressing mFTΔN152K (Figure 12D), suggesting the significance of avoiding positivity at the BCL region.

While for position L128, the only tolerated mutation is a substitution of the leucine by an isoleucine (L128I) with a comparable size and neutral in charge. In contrast, mutation to a relatively tiny (L128A) and bulky (L128F) size group renders FT into a loss-of-function molecule. While in the case of substitution to positively charged lysine (L128K; that is in same residue as K131 in TFL1), transformants show TFL1-like phenotypes (Figure 11 and Table 3). Although in terms of the I1* formation ability, the potency of mutations at L128 was relatively weak when compared to that of the other six critical positions (e.g. under LD, I1* = 24.4±12.5 in W138E; 3.4±3.5 in L128K); all of these positions share the same role for maintaining the localized negativity or neutrality of the regions. Notably, similar to the region BPP, BCL of TFL1 has a consistently strongly positive charge (Figure 10), implying that the positivity in the regions defines the anti-florigenic identity of TFL1, which in turn suggests the necessity of positivity avoidance in both region BPP and BCL for maintaining the FT florigenic identity.

Interestingly, besides sitting in close proximity to the complex interface between Hd3a (a rice homolog of FT) and GRF/14-3-3 protein (R62 and R130 in numbering of AtFT) (Taoka et al., 2011), BCL is adjacent to the canonical phosphorylation site S153 (E146 of AtFT) regulating hPEBP and Raf-1 binding (Yeung et al., 1999) (Figure 17A). In fact, evidence has shown that phosphorylation at S153 (adjacent to region BCL) of hPEBP could lead to the dissociation of its ligand, Raf-1, from ABP (surrounded by region BPP) implying that, there may be a regulatory connection between the two local areas via the invariant B loop (encoded by exon 4B). Therefore, it would be interesting to test for the structural dynamics between the two domains in future studies.

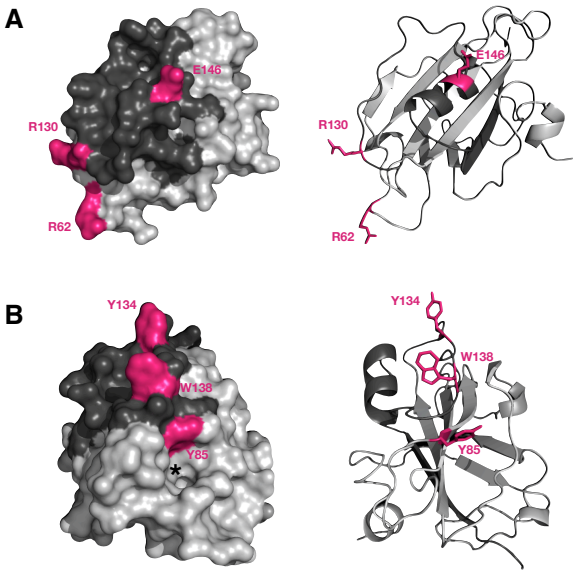

Figure 17. Surface and cartoon representation showing the positions of exon 4B and 4C encoded Lobe (BCL) relative to **(A)** E146, R130 and R62, and **(B)** Y85, Y134 and W138. Surface corresponding to the BCL is in dark grey, while the residues are in magenta. Black asterisk in (B) indicate the position of the canonical anion binding pocket of PEBP family.

2.7.2.3 Inter- and Intra-molecular Bondings Mediated by Tyr85

Next to the charge-effecting residues, in my study, W138 (region BPP) and Y134 (region BCL) were found to be critical determinants of FT florigenic identity, while Y85 is necessary for FT function. But unlike the residues at E109, Q140 (region BPP), and L128, N152 (region BCL), functional roles of the three residues are independent of the surface charge change (Figure 11 and Supplementary Figure 2). Their coherent possession of the aromatic side chain while sitting at close proximity in terms of their three-dimensional positions (Figure 17B) implies their consistent role in functioning of FT.

Y85 is one of the earliest identified residues determining the antagonistic function of FT and TFL1 (Hanzawa et al., 2005). As indicated by the latest crystal structure of hPEBP (PDB entry 2QYQ), O-phosphotyrosine could make a proper snug fit within the pocket bound by π-π stacking against W84 (corresponding to Y85 of AtFT) (L. Brady, personal communication), suggesting a role of Y85 in the docking of ligands.

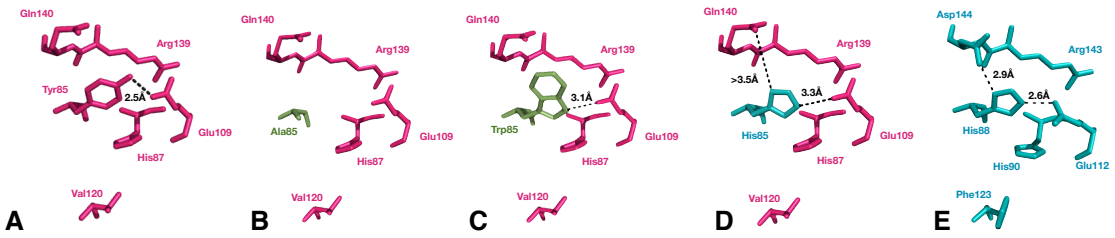

Figure 18. Intramolecular hydrogen bonding formation between residues constituting the canonical anion binding pocket (ABP) and effect of bonding(s) after mutation at position Y85. **(A)** FT. **(B)** mFTΔY85A. **(C)** mFTΔY85W. **(D)** mFTΔY85H. **(E)** TFL1. Hydrogen bonds, if any, are shown as dashed lines (distance in unit of Å). Hot pink indicates the residues of FT, teal cyan indicates from TFL1 residues, while smug green indicated other mutations.

Besides the role in mediating intermolecular interactions, Y85 residue is critical for intramolecular interactions. As in the case of TFL1, H88 (Y85 in numbering of FT) is responsible for the hydrogen bond formation with E122 (E109 in FT) and D144 (Q140 in FT) (Figure 18E). Although there was no detectable linkage between Y85 and Q140, hydrogen bond could be found between Y85 and E109 in the case of FT (Ahn et al., 2006) (Figure 18A) suggesting that Y85 plays an essential role in the intra-molecular binding as well as for maintaining molecular conformation. Interestingly, mutation Y85H could convert FT into a TFL1-like molecule (Hanzawa et al., 2005). Subsequent inspection of the crystal structures suggested the potential gaining of hydrogen bond between H85 and Q140 after Y85H mutation (Ahn et al., 2006). Similar to the tyrosyl group of tyrosine, the imidazole group of histidine also has the aromaticity required for the π-π stacking formation during the inter-molecular binding, implying that the TFL1-like ability of Y85H could be caused by the intra-molecular hydrogen bond formation with Q140.

To test this hypothesis, firstly, I mutated Y85 into an alanine. As a side group of alanine have no aromaticity and electronegativity for π-π stacking and hydrogen bond formation respectively, any inter- and intra-molecular bondings mediated by Y85 would be prevented (Figure 18B). As expected, upon

Y85A mutation, FT was converted to an almost loss-of-function molecule, with transformants producing up to 37 leaves before proceeding to the I2 phase in SD. Notably, no developmental feature corresponding to the I1* could be observed in any of *mFTΔY85A* transformants regardless of the constitutive ($35S_{pro}$), specific ($SUC2_{pro}$) or ectopic (FD_{pro}) expression (Supplementary Table 1). It suggests that the inter-molecular π-π stacking mediated by Y85, as well as the intra-molecular hydrogen bonding between Y85 and E109 are essential for the FT basal function. However, disruption of these bondings cannot account for the dominant negative phenotype. Secondly, I mutated Y85 into a tryptophan. Introduction of the tryptophan can restore the aromaticity, but NH of pyrrole ring on its indole side group is orientated in a way that only allow for the hydrogen bonding with E109 (Figure 18C). In contrast with Y85A, though no terminal flower could be observed, the FT floral promoting effect was significantly recovered in Y85W (Table 2). Provided that there was no alternative role/bonding found at position Y85, it suggests that hydrogen bond formation between Q140 and residues at position 85 can confer the FT scaffold with the TFL1-like ability. In agreement with this notion and compared with the native tyrosine, among all possible rotamers of histidine at position 85, the shortest and thus strongest possible hydrogen bond formed had a bond length of more than 3.5 Å (Figure 18D). If the bonding with Q140 bestows FT with the anti-florigenic ability, such weak linkage can hence explain why mFTΔY85H is only TFL1-like but cannot be classified as a fully functional TFL1 in terms of the I1* forming and floral delaying potency (Table 2).

2.7.2.4 Potential Intermolecular Bondings via Tyr134 and Trp138

In sugar beet, regulation of flowering time is controlled by interplay of two paralogs of FT, namely BvFT1 and BvFT2. BvFT1 acts like TFL1 and represses flowering, while BvFT2 acts like FT and promotes flowering (Pin et al., 2010). By means of swapping of their exon 4 and then 4B, a previous study demonstrated that, similar to the findings of *FT* and *TFL1* (Ahn et al., 2006), determinants of the antagonistic function of *BvFT1* and *BvFT2* were mapped to their exon 4B. Due to the fact that the peptide encoded by exon 4B of BvFT1 and BvFT2 only differ by three amino acids, they deduced that residues at the three positions (N138, Q141, and Q142 in BvFT1 scaffold; Y134, G137, and W138 in BvFT2 scaffold) are the cause of the antagonisms between BvFT1 and BvFT2.

However, transformants overexpressing *BvFT2221* (a chimera formed by replacing the exon 4 of *BvFT2* with that of the *BvFT1*) on average flowered 27 leaves earlier than transformants overexpressing the native *BvFT1* under LD conditions. While instead of showing aberrant shoots with an I1* phase, only 3 out of 15 transformants exhibited developmental aberrations with flowers lacking petals (Pin et al., 2010), making the anti-florigenic identity of the BvFT2221 doubtful. Therefore, from the findings one could only conclude that introducing mutations N138Y, Q141G, and Q142W together can convert BvFT1 into BvFT2. Whether corresponding mutations Y134N, G137Q, and W138Q in BvFT2 scaffold can convert into a fully functional BvFT1 remains elusive. Also, whether all of these positions have to be mutated simultaneously in order to achieve the switching from BvFT1 to BvFT2 is unclear.

In contrast, based on my mutagenesis studies, I could reveal critical residues the function of which was obscured when larger segments were swapped. By these means, I demonstrate that, firstly, in all types of mutations involving a tiny (G137A), bulky (G137W), negative (G137E) or positive (G137R) side group, none of them could revert the FT function and both the floral promoting and terminal flower forming ability of FT could be preserved nicely in all their transformants (Figure 11 and table 3). It suggests that the residue at position G137 is not the cause of the antagonistic function of FT and TFL. Secondly, rather than a weak floral repressor, as previously suggested, I show that mutation at either position 134 (Y134A, Y134K) or 138 (W138E, W138S, and W138A) could convert FT into a potent floral repressor that delays the flowering time comparable to that of the native TFL1, while I1* could clearly be observed in all transformants (Figure 11B and Table 3). Also, either W138E or Y134K could well complement the *tfl1-1* phenotypes (Figure 12 and Table 4). Therefore, my findings demonstrate the critical role of residues at position 134 and 138 for determining the FT florigenic identity, and touching either one of them is good enough to convert FT into a fully functional TFL1. Indeed, similar to Y85 in exon 2, Y134 (region BCL) and W138 (region BPP) are encoded by exon 4B, which is invariant among any homolog of FT (Figure 19) implying their necessity in the FT function. Together with the fact that mutation, such as in W138E, could lead to the strongest TFL1 phenotype among the six critical residues, it indicates that the invariance of these residues is the prerequisite for preventing FT to switch from a florigen into a potent anti-florigen.

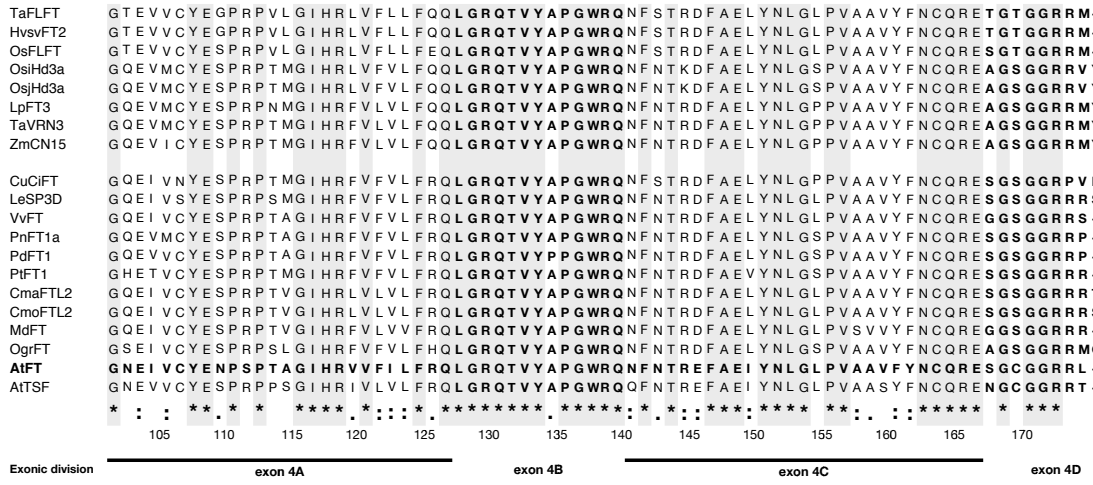

Figure 19. Sequence alignment of exon 4 of FT homologs. Sequences from monocot are in upper panel while sequence from either dicots or woody plants are in lower panel. Invariant residues are shaded.

However, unlike Y85 embedded in the pocket entrance, side groups of both Y134 and W138 are protruding and easily accessible (Figure 17B), implying that Y134 and W138 are quite likely to be involved in the inter-molecular bonding with ligand bound via the BPP and BCL surfaces.

2.7.2.5 The Repulsive-Lock Model of Floral Transition

Both Ahn et al. (2006) and Hanano and Goto (2011) suggested that FT and TFL1 recruit coactivators and corepressors. Providing that there is only a single coactivator and corepressor involved in the binding, based on the properties of the BPP and BCL surfaces observed, it can be summed up as two repulsive-lock models for explaining how the control of floral transition can be mediated by FT and TFL1 (Figure 20).

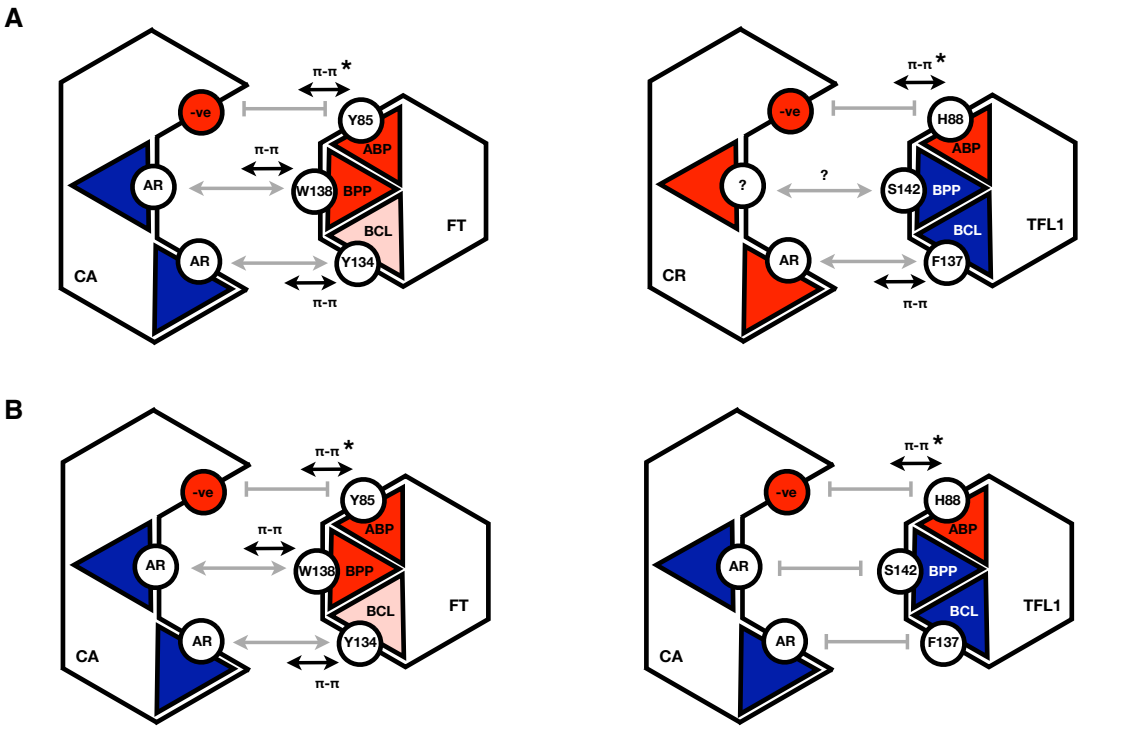

Figure 20. The Repulsive-Lock Models. **(A)** Model 1, which both of the FT-specific coactivator and TFL1-specific corepressor exist. **(B)** Model 2, which only FT-specific coactivator exists. Blue color represents a positively charged region; while red and pink color represent negatively charged and slightly negatively charged regions respectively. Grey double arrows indicate electrostatic attraction; grey double perpendicular lines indicate electrostatic repulsion. π-π represent the π-π stacking between aromatic groups that occur only when two molecules can be brought close enough together by the compatible surface charge. Hence, due to the intrinsic repulsion exerted by the negatively charged ABP, for the Y85 (in FT) or H88 (in TFL1), they cannot form π-π* with any anion unless the remaining parts of the ligand have got compatible charge and groups for bonding on their BPP and BCL. Only in this way, the repulsion can be overcome, while well-position the anion in close proximity to the Y85 (in FT) or H88 (in TFL1) for the π-π stacking formation. CA, coactivator; CR, corepressor; -ve, anion (e.g. phosphotyrosine); AR, aromatic side chain of amino acid residue; ABP, Anion Binding Pocket; BPP, Binding Pocket Peripheral; BCL, Exon 4B and 4C encoded Lobe.

In contrast to the strongly positively charged BPP and BCL surfaces of TFL1, due to the negativity of region BPP (maintained by E109 and Q140) and neutrality of BCL (maintained by L128 and N152), these endow FT with a general binding specificity for ligand with positive charge at its binding interfaces (Figure 20A). So, FT can bring in the positively charged coactivator in close proximity, but not the corepressor. On the contrary, due to the potent negativity of the corepressor at positions corresponding to the BPP and BCL surfaces, the corepressor can only approach and associate with

TFL1, but not with FT. Then, with aid of the two aromatic residues (Y134 and W138) found only on the FT surface, fine selectivity can be achieved, and only in case of coactivator possessing the two corresponding aromatic side-groups, π-π stacking can be formed with the FT. With these specific linkings, accurate positioning of the phosphorylated group of the coactivator at the ABP of FT can be accomplished, that in turn helps countering the repulsive force exerted by the ABP, and facilitates the snug fit formation between the phosphate and the ABP mediated via the specific in-pocket bindings, in particular by Y85. In this way, floral activating complex is completed. My model thus makes very explicit predictions about the molecular details of FT and TFL1 interacting with so far unknown coactivators or corepressors.

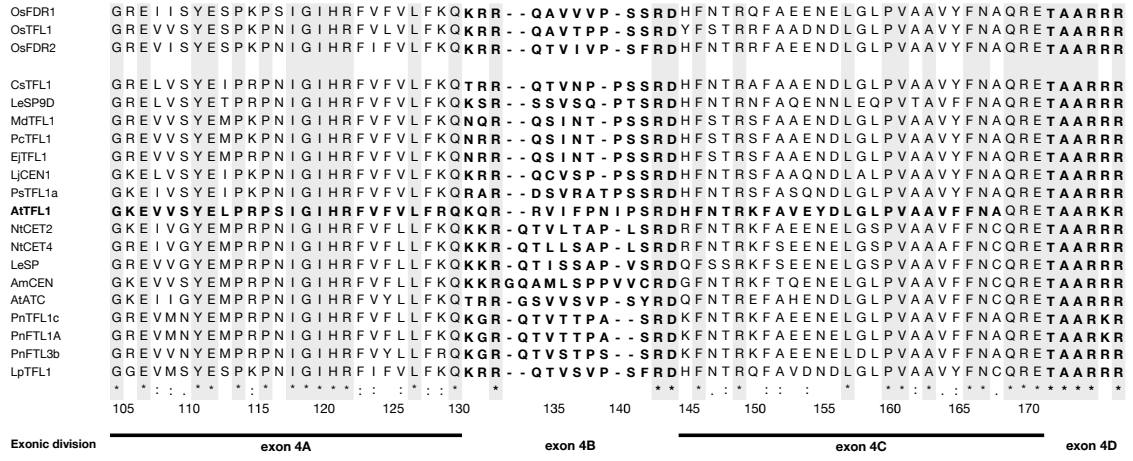

Figure 21. Sequence alignment of exon 4 of TFL1 homologs. Sequences from monocot are in upper panel while sequence from either dicots or woody plants are in lower panel. Invariant residues are shaded.

However, B loop encoded by the exon 4B is highly divergent among the TFL1 homologs (Ahn et al., 2006). For instance, at position F137 of AtTFL1 (corresponding to Y134 in all FT homologs), it can be a serine (LpTFL1, GenBank accession: AF316419), arginine (PsTFL1a, AY340579), asparagine (CsTFL1, AY344245), threonine (PnTFL1c, AB104629), isoleucine (OsFDR2, AF159882), valine (OsFDR1, AF159882), or lysine (NtCET1, AF145259). While for position S142 of AtTFL1 (corresponding to W138 in all FT homologs), it can be a cystine (AmCEN, S81193), phenylalanine (LpTFL1), or threonine (NtCET1) among the homologs of TFL1 (Figure 21). So, it implies that, unlike the invariant B loop of FT, residues on loop of TFL1, such as F137 and S142, may lack the selectivity to bring in a specific corepressor. This leads to an alternative model that, only a coactivator exists during the floral transition. Also, due to the incompatibility of charge and bonding of the BPP and BCL surface of TFL1, the coactivator can only bind with FT, but not with TFL1 (Figure 20B). However, TFL1 does not possess any canonical transcriptional repressor domain *per se* (Ahn et al., 2006), implying the existence of an atypical repressing domain in the TFL1 scaffold or of an alternative binding site of corepressor. Further investigation is required for testing the validity of this model.

During the suppression of MAP kinase signaling in human, hPEBP plays a inhibitory role by binding with Raf-1 kinase via its ABP that in turn prevents Raf-1 from being phosphorylated and so activated by a Src kinase (Yeung et al., 1999). This example suggested the potential selectivity conferred by the ABP. Therefore, it could lead to a third model that the contrasting differences in charge and bondings between the BPP and BCL surfaces of FT and TFL1 can provide binding specificity, and only if the ligand is non-phosphorylated/dephosphorylated at the position corresponding to the ABP site, it can bind with FT or TFL1. However, a recent NMR chemical shift study showed that hPEBP could bind with both of the non-phosphorylated or tri-phosphorylated Raf-1 kinase (Tavel et al., 2012), suggesting that the negativity of ABP is not responsible for selectively bind with a non-phosphorylated ligand. Moreover, as illustrated by the latest crystal structure of hPEBP (PDB entry 2QYQ), O-phosphotyrosine could make a proper snug fit within the pocket, bound by π-π stacking against W84, and a range of hydrogen bonds via H86, D70 and Y120 of hPEBP (L. Brady, personal communication). Thereby, it confirms the credibility and capability of the ABP to bind with a phosphorylated ligand and thus excludes the existence of the third potential model.

To sum up, the specific charge of region BPP and BCL governed by E109, Q140, N152, and L128 could be responsible for the coarse attraction of ligands to the binding site, while binding such as π-π stacking mediated via the aromatic side chains of Y134 and W138 could lead to the fine positioning of the ligand, that in turn facilitate the snug fit of phosphoryl group of the ligand at the ABP via Y85. Although the Repulsive-Lock Model may not be in line with our sense of the “Opposites Attract” in first instance, circumstantial evidence for binding and repulsion does exist, and such arrangement requires an increased charge- and bonding-specificity at BPP and BCL. Indeed, a charged surface can be formed with ease, but a charged surface with a specific bonding requirement can add one more layer of selectivity to the ligand binding, thereby increasing the stringency of control for this crucial developmental switch.

Chapter 3

Potential Floral Coactivators of FT

3.1 CONTRIBUTIONS

Unless otherwise specified, I performed all experiments presented in this chapter with the help of Pauline Ip for plant work.

Detlef Weigel[1], Friedrich Schoeffl[2], Jiawei Wang[3] and Rebecca Schwab[1] provided critical advices for defining the direction of my research. I designed the experiments with help from Detlef Weigel.

[1]Max Planck Institute for Developmental Biology, Tuebingen, Germany

[2]Center for Plant Molecular Biology (ZMBP), Eberhard-Karls University, Tuebingen, Germany.

[3]National Key Laboratory of Plant Genetics, Institute of Plant Physiology and Ecology, Shanghai Institutes for Biological Sciences, Shanghai, China

3.2 INTRODUCTION

3.2.1 Model 1 - Floral Activator and Repressor

Over the past two decades, beginning with the identification of TFL1, and then FT and FD (Shannon and Meeks-Wagner, 1991; Kardailsky, 1999; Kobayashi, 1999; Wigge et al., 2005; Abe, 2005), many models have been proposed to explain how these molecules affect flower initiation. Among all of the models proposed, the most popular seemed to be that the DNA binding FD is safeguarded by the floral repressor TFL1 at the shoot apical meristem (SAM). But once optimal conditions are reached, FT replaces the repressor TFL1, combines with FD before serving as the activator “by itself” for triggering the developmental shift (Figure 22A). However, this well-known model has recently challenged (Hanano and Goto, 2011).

3.2.2 Model 2 - Floral Activator nor Repressor

In study of Hanano and Goto, they showed that when TFL1 is fused with a transcriptional repressor domain named SDRX, it delayed flowering similar to that of the native TFL1. On the contrary, when TFL1 is linked to a transcriptional activator domain called VP16, plants flowered early and had a terminal flower similar to that of the overexpressor of FT. Notably, the activity of FT could be enhanced by a similar strategy, and *FT:VP16* overexpressing plants flower extremely early (Wigge et al., 2005). The absence of typical activator or repressor domains in TFL1 and FT (Ahn et al., 2006) together with these other findings indicate that, rather than being an activator or repressor by itself, FT and TFL1 are only transcriptional mediators or adaptor molecules that can specifically bring in a coactivator or cosupressor. The interplay with these additional molecules can determine the final role of the whole complex, either switching ON or OFF the floral patterning genes downstream (Figure 22B).

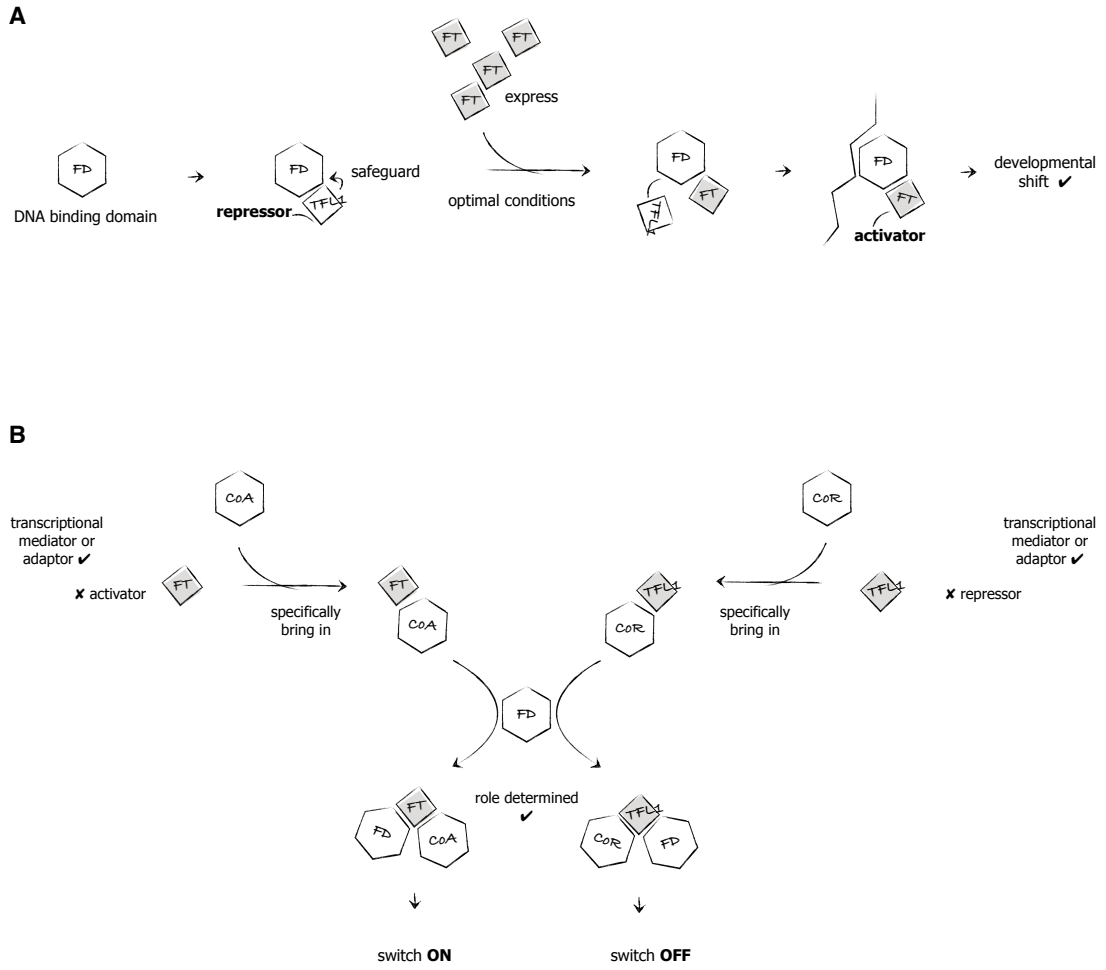

Figure 22. Hypothetical models of floral transition modulated by FT and TFL1 via FD. **(A)** A model in which FT serves as a floral activator to compete with an antagonistic floral repressor TFL1 for a DNA binding transcription factor FD during the developmental shift. **(B)** A model in which FT and TFL1 is only a transcriptional mediator that can specifically bring in a coactivator and corepressor respectively and bind with FD, so that the specific resulting complex triggers the developmental transition. CoA, coactivator; CoR, corepressor.

3.3 OBJECTIVES

So far, only model 2 can appropriately explain the floral transition modulated by FT and TFL1. However, if this scenario is true, what can the coactivator and corepressor be? In this chapter, I present a study targeted at determining the mystic identity of the coactivator of FT, to serve as the first step for validating the most up-to-dated model explaining the plant developmental shift.

3.4 METHODOLOGY

By means of mutagenesis, I generated mutations covering almost the whole FT molecule, from which I have successfully identified mutations located at one side of the molecule that can interestingly switch FT into a fully functionally TFL1, and this change could be reverted by restoring the surface charge via a single amino acid change. So, if the coactivating model is true, it is possible that the dominant negative effect resulted is caused by the binding interruption of the coactivator. In other words, the identified surface formed by those mutations could be the binding site of the coactivator of FT. In line with this thought, I decided to make use of the identified surface to start a systematic interaction analysis with all of the FT interactors available at that time (till 2010). By manipulating the charge change of the surface identified in part 1 of my study, one should be able to validate and so identify candidates of the mystic ligands. After confirming their relatedness to the flowering time control, the candidates could then be subject to genetic analysis to verify their genetic dependence on FT and its coactivating ability.

3.5 RESULTS

3.5.1 TCPs but Not GRF-FD Bind with Surface Defining FT Florigenic Identity

To gain clues on the identity of the elusive coactivator of FT, firstly, coding sequences (CDS) of each of the previously identified FT interactors including 14-3-3/GRF1-15 (Taoka et al., 2011), TCP (TEOSINTE BRANCHED1, CYCLOIDEA, PCF) 1-24 (Mimida et al., 2011), and FD (Abe, 2005; Wigge et al., 2005) were fused with the activation domain of the yeast transcriptional activator protein GAL4 (AD). While CDS fusions of the DNA binding domain of GAL4 (DBD) with FT, BPP-charge-reverted FT (ΔQ140K), BPP-charge-restored FT (ΔQ140D) and TFL1 were made individually. After cotransforming different combinations of the AD- and DBD-fused constructs in yeast, two yeast-2-hybrid based assays, including yeast growth and ortho-Nitrophenyl-β-galactoside (ONPG) enzymatic assays, were utilized to test for the effect of BPP charge reversion on their respective bindings.

In the qualitative growth assay, the known amount of transformed yeast cells was serially diluted and individually plated on the Leucine/Tryptophan/Histidine (-LTH) triple dropout media. So, only if the proteins in test interact, can they bring the AD (+L) and DBD (+T) in close proximity, triggering the production of histidine essential for the survival of the corresponding yeast line. From the assay, I found that consistent with a recent BiFC data (Hanano and Goto, 2011), both FT and TFL1 showed to have clear interaction with FD, and so do the bridging molecule GRF proteins (Figure 23). In contrast to members of the TCP family, surprisingly, the interaction between FT and FD/GRF persisted regardless of introducing the BPP charge reverting mutation. To verify this finding, the quantitative ONPG enzymatic assay measuring the β-galactosidase production resulting from the protein-protein interactions was utilized. Results of the quantitative assays showed that, no matter which interactor was used, activity of the β-galactosidase was not statistically different (Figure 24 and Table 5), suggesting that the identified surface constituted by the mutation is not for the binding of FD or GRF proteins.

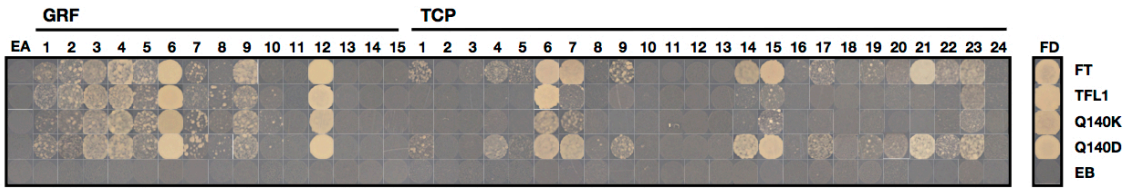

Figure 23. Quantitative β-galactosidase assay in yeast. FT, TFL1, mFTΔQ140K, mFTΔQ140D and empty DNA binding domain vector (EB) served as the baits. Empty activation domain vector (EA), GRF1-15, TCP1-24 and FD served at the preys. Auxotrophic selections were done on triple dropout (-LTH) synthetic defined medium with 75mM 3-AT at 25°C for 5 days. Triplicate for each combination were tested for ensuring consistence.

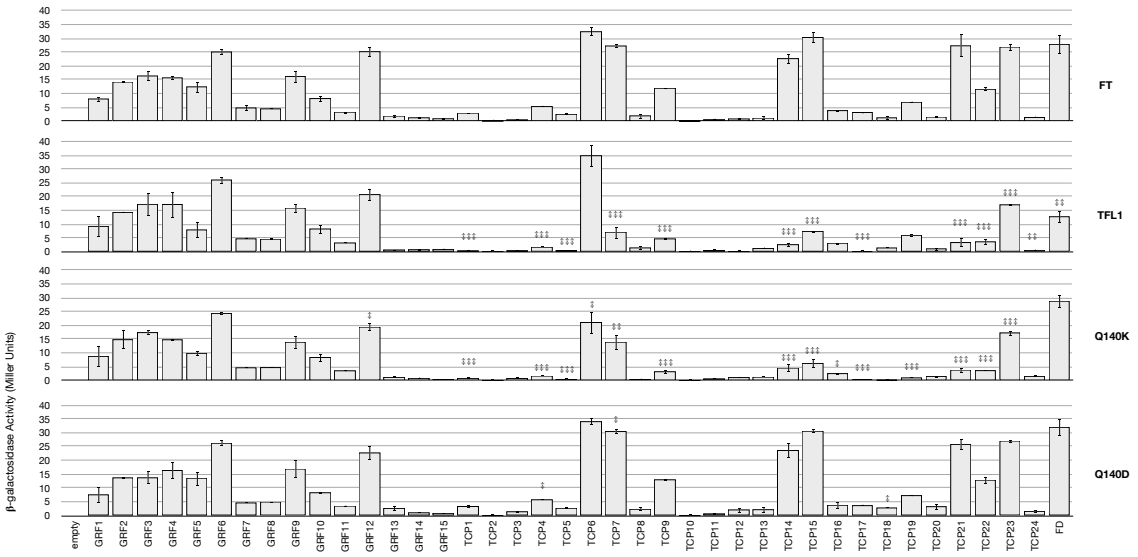

Figure 24. Quantitative Yeast-Two Hybrid assay testing the interaction of FT, mFTΔQ140K, mFTΔQ140D, TFL1 with GRF1-15, TCP1-24, FD. Numerical, statistical and abbreviation details of the plots are shown in Table 5.

β-galactosidase Activity (Miller Units) measured by quantitative ONPG enzyme activity assay

	GAL4 DBD:**FT**	GAL4 DBD:**TFL1**	GAL4 DBD:**mFTΔQ140K**	GAL4 DBD:**mFTΔQ140D**
GAL4 AD: **EV**	0.00 ± 0.00	0.00 ± 0.00	0.00 ± 0.00	0.00 ± 0.00
GAL4 AD:**GRF1**	8.01 ± 1.86 (6.30-10.33)	9.19 ± 7.28 (4.19-18.59)	8.71 ± 7.79 (3.11-18.75)	7.50 ± 6.05 (0.69-14.21)
GAL4 AD:**GRF2**	14.16 ± 0.81 (13.12-14.84)	14.25 ± 0.34 (13.91-14.76)	14.77 ± 6.68 (6.85-21.69)	13.64 ± 0.82 (12.13-14.25)
GAL4 AD:**GRF3**	16.35 ± 3.70 (13.89-21.12)	17.17 ± 8.58 (10.71-28.19)	17.33 ± 1.71 (15.32-20.24)	13.66 ± 4.66 (4.29-16.68)
GAL4 AD:**GRF4**	15.67 ± 1.57 (14.14-17.59)	17.11 ± 9.59 (9.04-29.27)	14.73 ± 0.83 (13.19-15.47)	16.30 ± 6.00 (10.33-26.99)
GAL4 AD:**GRF5**	12.41 ± 4.20 (8.92-17.74)	7.90 ± 5.63 (2.86-14.97)	9.81 ± 1.93 (7.62-13.32)	13.51 ± 5.25 (10.05-23.83)
GAL4 AD:**GRF6**	25.03 ± 2.36 (23.32-28.07)	25.99 ± 2.46 (24.22-30.66)	24.28 ± 1.27 (22.69-25.42)	26.17 ± 2.00 (23.56-28.49)
GAL4 AD:**GRF7**	4.77 ± 2.34 (2.83-7.75)	4.68 ± 0.03 (4.66-4.71)	4.59 ± 0.27 (4.19-4.92)	4.56 ± 0.19 (4.34-4.85)
GAL4 AD:**GRF8**	4.44 ± 0.28 (4.12-4.76)	4.55 ± 0.18 (4.34-4.89)	4.66 ± 0.30 (4.29-4.96)	4.89 ± 0.63 (4.31-5.67)
GAL4 AD:**GRF9**	16.17 ± 4.60 (11.08-21.35)	15.81 ± 3.29 (13.36-20.04)	13.84 ± 4.44 (9.61-19.31)	16.83 ± 6.48 (12.82-29.64)
GAL4 AD:**GRF10**	8.16 ± 2.18 (5.91-10.75)	8.24 ± 3.48 (5.61-12.71)	8.31 ± 2.94 (4.94-11.51)	8.25 ± 0.94 (6.36-8.77)
GAL4 AD:**GRF11**	3.25 ± 0.99 (2.38-4.50)	3.18 ± 0.06 (3.10-3.24)	3.49 ± 0.37 (3.05-3.93)	3.42 ± 0.38 (3.05-3.99)
GAL4 AD:**GRF12**	25.15 ± 3.80 (20.51-28.87)	20.70 ± 4.38 (12.08-24.32)	19.31 ± 2.72 (15.55-23.89) ‡	22.67 ± 5.17 (17.36-30.16)
GAL4 AD:**GRF13**	1.82 ± 1.20 (0.42-3.09)	0.64 ± 0.62 (0.14-1.87)	1.10 ± 0.06 (1.02-1.16)	2.58 ± 1.70 (0.67-4.47)
GAL4 AD:**GRF14**	1.21 ± 0.95 (0.44-2.41)	0.74 ± 0.96 (0.08-1.97)	0.75 ± 0.15 (0.54-0.93)	0.98 ± 0.10 (0.89-1.11)
GAL4 AD:**GRF15**	0.85 ± 0.95 (0.08-2.07)	0.78 ± 0.07 (0.69-0.88)	0.47 ± 0.63 (0.02-1.28)	0.79 ± 0.44 (0.09-1.23)
GAL4 AD:**TCP1**	2.90 ± 0.64 (2.10-3.49)	0.29 ± 0.08 (0.16-0.36) ‡‡‡	0.74 ± 0.04 (0.69-0.78) ‡‡‡	3.26 ± 1.15 (1.78-4.02)
GAL4 AD:**TCP2**	0.16 ± 0.07 (0.07-0.22)	0.19 ± 0.07 (0.07-0.25)	0.13 ± 0.08 (0.04-0.26)	0.18 ± 0.17 (0.15-0.24)
GAL4 AD:**TCP3**	0.47 ± 0.20 (0.30-0.64)	0.33 ± 0.15 (0.03-0.44)	0.72 ± 0.08 (0.64-0.79)	1.36 ± 0.91 (0.32-2.34)
GAL4 AD:**TCP4**	5.26 ± 0.16 (5.01-5.49)	1.64 ± 0.07 (1.55-1.71) ‡‡‡	1.59 ± 0.10 (1.49-1.72) ‡‡‡	5.70 ± 0.27 (5.26-5.99) ‡
GAL4 AD:**TCP5**	2.47 ± 0.16 (2.32-2.68)	0.40 ± 0.24 (0.14-0.76) ‡‡‡	0.47 ± 0.05 (0.41-0.52) ‡‡‡	2.62 ± 0.13 (2.48-2.80)
GAL4 AD:**TCP6**	32.38 ± 2.98 (28.60-34.87)	34.78 ± 7.75 (28.32-44.63)	20.98 ± 8.24 (13.73-31.35) ‡	34.00 ± 2.65 (31.36-37.21)
GAL4 AD:**TCP7**	27.21 ± 1.60 (25.16-28.37)	7.08 ± 4.63 (2.86-12.85) ‡‡‡	13.86 ± 5.89 (6.41-18.89) ‡‡	30.42 ± 1.99 (28.43-32.82) ‡
GAL4 AD:**TCP8**	1.90 ± 1.83 (0.70-4.26)	1.39 ± 1.35 (0.22-2.55)	0.34 ± 0.14 (0.16-0.56)	2.26 ± 1.36 (0.64-3.61)
GAL4 AD:**TCP9**	11.90 ± 0.61 (11.11-12.32)	4.66 ± 0.92 (3.27-5.69) ‡‡‡	3.15 ± 1.50 (1.49-4.84) ‡‡‡	12.94 ± 0.86 (11.93-13.95)
GAL4 AD:**TCP10**	0.06 ± 0.05 (0.02-0.12)	0.07 ± 0.03 (0.03-0.11)	0.10 ± 0.05 (0.01-0.16)	0.12 ± 0.09 (0.03-0.26)
GAL4 AD:**TCP11**	0.52 ± 0.04 (0.48-0.57)	0.50 ± 0.02 (0.47-0.53)	0.56 ± 0.11 (0.45-0.70)	0.60 ± 0.40 (0.12-0.99)
GAL4 AD:**TCP12**	0.79 ± 0.79 (0.19-1.80)	0.17 ± 0.13 (0.04-0.37)	1.03 ± 0.26 (0.73-1.30)	2.02 ± 1.92 (0.55-4.49)
GAL4 AD:**TCP13**	1.08 ± 1.42 (0.05-2.91)	1.16 ± 0.05 (1.08-1.21)	1.19 ± 0.13 (1.08-1.36)	2.11 ± 2.50 (0.23-5.32)
GAL4 AD:**TCP14**	22.63 ± 3.92 (19.42-29.83)	2.56 ± 1.48 (1.14-4.38) ‡‡‡	4.49 ± 3.05 (2.36-8.42) ‡‡‡	23.55 ± 5.54 (19.45-30.68)
GAL4 AD:**TCP15**	30.28 ± 3.71 (26.97-36.99)	7.36 ± 0.80 (6.16-8.27) ‡‡‡	6.16 ± 3.53 (3.19-10.64) ‡‡‡	30.53 ± 1.47 (28.80-32.04)
GAL4 AD:**TCP16**	3.81 ± 0.55 (3.17-4.45)	3.09 ± 0.94 (2.28-3.90)	2.48 ± 0.60 (1.79-3.12) ‡	3.72 ± 2.32 (0.88-5.94)
GAL4 AD:**TCP17**	3.12 ± 0.61 (2.08-3.82)	0.20 ± 0.09 (0.08-0.30) ‡‡‡	0.19 ± 0.06 (0.11-0.25) ‡‡‡	3.58 ± 0.08 (3.48-3.69)
GAL4 AD:**TCP18**	1.19 ± 1.33 (0.06-2.88)	1.37 ± 0.27 (1.13-1.70)	0.16 ± 0.02 (0.12-0.17)	2.74 ± 0.13 (2.61-2.96) ‡
GAL4 AD:**TCP19**	6.83 ± 0.33 (6.33-7.12)	5.95 ± 1.17 (4.46-6.91)	0.92 ± 0.07 (0.83-0.98) ‡‡‡	7.21 ± 0.34 (6.75-7.63)
GAL4 AD:**TCP20**	1.47 ± 0.72 (0.78-2.35)	1.05 ± 1.23 (0.09-2.63)	1.46 ± 0.96 (0.38-2.52)	3.21 ± 2.08 (0.74-5.33)
GAL4 AD:**TCP21**	27.28 ± 8.35 (21.29-38.03)	3.33 ± 3.09 (1.01-7.31) ‡‡‡	3.75 ± 1.72 (1.86-6.19) ‡‡‡	25.75 ± 4.02 (21.96-29.94)
GAL4 AD:**TCP22**	11.53 ± 1.42 (9.74-12.94)	3.60 ± 2.35 (1.84-6.62) ‡‡‡	3.55 ± 0.23 (3.24-3.93) ‡‡‡	12.81 ± 2.83 (9.80-16.09)
GAL4 AD:**TCP23**	26.88 ± 2.00 (23.78-29.89)	17.00 ± 0.40 (16.23-17.36) ‡‡‡	17.21 ± 1.87 (15.35-19.94) ‡‡‡	26.98 ± 1.17 (25.93-28.45)
GAL4 AD:**TCP24**	1.30 ± 0.09 (1.19-1.40)	0.56 ± 0.32 (0.13-0.91) ‡‡	1.46 ± 0.12 (1.32-1.68)	1.49 ± 1.19 (0.16-2.83)
GAL4 AD:**FD**	27.80 ± 7.02 (17.03-35.60)	12.68 ± 4.35 (8.92-18.18) ‡‡	28.69 ± 4.71 (20.92-32.42)	31.93 ± 6.38 (23.72-36.60)

Table 5. *In vitro* quantitative Y2H-based ONPG enzyme activity assay. MU = Miller units = β-galactosidase units. 1 unit of β-galactosidase = amount of β-galactosidase required for hydrolyzing 1 μmol of ONPG to o-nitrophenol and D-galactose per min per cell. Each set of assay is repeated for six times for ensuring accuracy and consistency. AD, activation domain; DBD, DNA binding domain. Symbol ‡ indicates the statistical significance of differences in comparison with dataset of FT using two-tailed multiple Student's *t*-test with Bonferroni correction. Single, double and triple symbols represent $P < 0.05$, $P < 0.01$ and $P < 0.001$ respectively. No symbol means that there was no statistically significant difference among indicated genotypes in each experiment (Student's *t*-test, $P \geq 0.05$).

Next, I tested the possibility for the antagonistic behavior of FT and TFL1 to link up with the last sets of candidates, the TCP (TEOSINTE BRANCHED1, CYCLOIDEA, PCF) transcription factor family. Among the 24 TCP proteins, at least 10 of them (such as TCP 4, 5, 7, 9, 14, 15, 17, 21, 22, and 23) were shown to have strong or clear interactions with FT (Figure 24 and Table 5), but when the charged-reverting mutation was introduced to BPP of FT (ΔQ140K), similar to that of the TFL1, these interactions were either significantly weakened or even diminished. But as long as the native charge was restored in BPP (ΔQ140D), their binding ability with the TCPs could be restored correspondingly.

To further examine the interactions, qualitative *in planta* split luciferase assay (Chen et al., 2007) was adopted. Before the assay, CDS of *GRF1-15*, *TCP1-24*, and *FD* were individually fused with the C-terminal of the firefly luciferase gene (*LUCc*), while CDS of the N-terminal of luciferase (*LUCn*) was fused with *FT*, *TFL1*, and mutated *FT*s. Constructs under the control of 35S promoter were transformed into *Agrobacterium tumefaciens* that were then mixed in desired combinations and infiltrated to epidermal cells of *Nicotiana benthamiana* leaves (Voinnet et al., 2003). Any interaction between the proteins tested can bring LUCn and LUCc in close proximity and produce luminescence. In the assay, while luminescence was not detected in either FT/mFT/TFL1:LUCn+LUCc or LUCc-GRF/TCP/FD+LUCn infiltrated leaves, both FT and TFL1 could consistently bind with GRF1-13 and FD *in planta*, with this binding pattern being independent of the charge change of the BPP (Figure 25A). In contrast, bindings between FT and 10 TCP members, including TCP4, 7, 9, 13, 14, 15, 17, 21, 22, and 23 were interrupted by the BPP-charge-reverted mutation, but not by the BPP-charge-restored version of FT (Figure 25B). Therefore, all of these findings suggest that, rather than the canonical GRF-FD, TCP family members interact with the surface defining FT florigenic identity.

Figure 25. Qualitative split luciferase assay of FT, TFL1, BPP charge-reverting FT (Q140K) and charge-restoring FT (Q140D) with **(A)** GRF1-13, **(B)** 13 TCP candidates and FD in *Nicotiana benthamiana*. Young but fully expanded 4-week-old leaves were strictly chosen for infiltration. At least triplicate experiments were performed for each set to ensure result accuracy and consistence.

3.5.2 Individual TCP-Clades May Act Redundantly in Flowering Time Control

For the 10 TCP family members that show differential FT interaction depending on the BPP charge (including TCP4, 7, 9, 13, 14, 15, 17, 21, 22, and 23), all except for TCP4, 13, and 17 are class I TCPs (Figure 26). This suggests that they may share the same functionality and interact redundantly with FT. Having said that TCP is a protein family that is more commonly known to relate to the development of leaves (Palatnik et al., 2003), is there any possibility its role for the control of flowering time has been overlooked?

To test this hypothesis, I attempted to obtain homozygous lines for 55 T-DNA insertions in different TCPs. I found that single knockdowns or knockouts of TCP members by T-DNA insertion, for instance *tcp5,* did not produce a significant flowering time phenotype (Figure 27 and Table 6). However, in the case of *tcp5;tcp13;tcp17* triple mutant where all members of TCP5-clade were disrupted by T-DNA insertion, flowering time was significantly delayed, suggesting that individual clade members of TCP may act redundantly on flowering time control. Notably, in the case of TCP4 (one of the few class II TCPs that bound with BPP of FT), flowering time was significantly delayed in the *tcp4* single mutant. An additive delaying effect was, however, observed in *tcp2;tcp4;tcp10* triple mutant where members from more than one genetic clade were T-DNA inserted, implying that role redundancy may only be limited to members of an individual clade, while different clades of TCP may work independently in flowering time control.

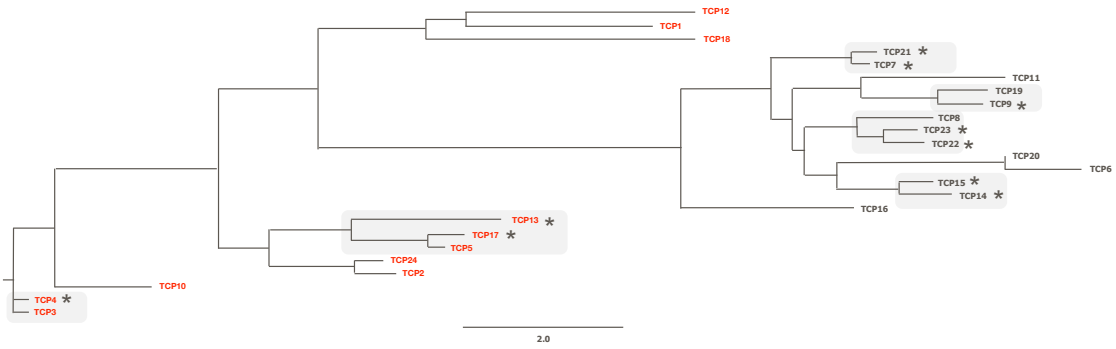

Figure 26. Phylogeny of TCPs. 24 full-length TCP proteins sequences were aligned using ClustalW with output format as PHYLIP. The alignments were then filtered with Gblocks using default settings to remove divergent regions and potentially poorly aligned positions. Phylogenies were reconstructed by maximum likelihood using Phyml 3.0. Final tree was visualized by FigTree. Name of class II TCP are in red color. TCP bound with FT via region BPP were labeled with asterisks, while individual genetic clades are shaded.

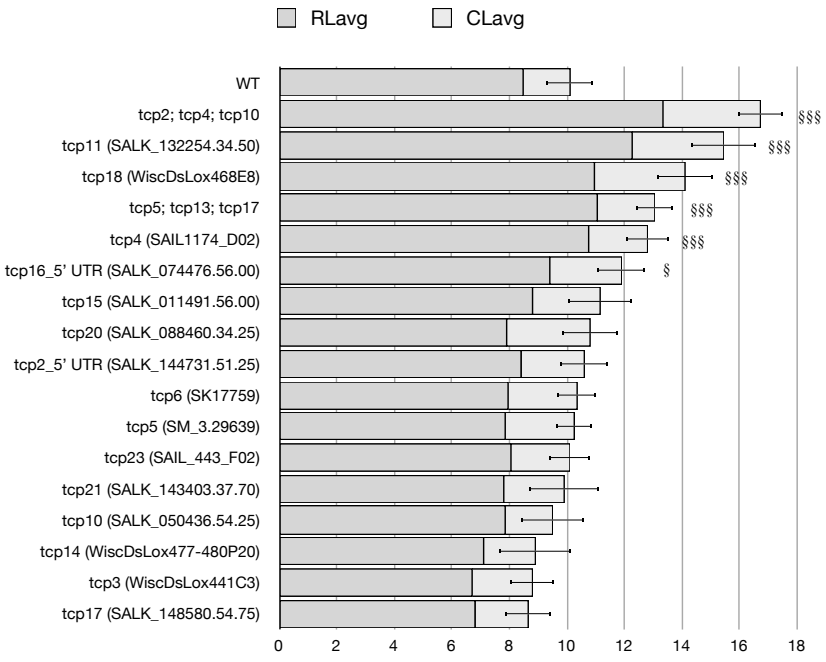

Figure 27. Flowering time of first and third order mutants or T-DNA insertion lines of *TCP*. ABRC code for each T-DNA line was blanketed. Numerical and statistical details are shown in **Table 6.**

Genotype *	No. of rosette leaves †	No. of cauline leaves †	Total no. of leaves †	*n*
	Experiment 1, LDs †			
WT	8.5 ± 1.2 (6-11)	1.6 ± 0.8 (1-3)	10.1 ± 1.6 (7-13)	19
tcp2; tcp4; tcp10	13.3 ± 1.7 (11-17)	3.4 ± 0.7 (2-5)	16.7 ± 1.6 (14-20) §§§	18
tcp11 (SALK_132254.34.50)	11.3 ± 1.8 (9-16)	3.0 ± 0.6 (2-4)	14.3 ± 2.1 (11-20) §§§	20
tcp18 (WiscDsLox468E8)	11.0 ± 1.7 (7-15)	3.2 ± 0.7 (2-5)	14.1 ± 1.9 (9-17) §§§	20
tcp5; tcp13; tcp17	11.1 ± 1.1 (10-14)	2.0 ± 0.9 (1-4)	13.1 ± 1.3 (11-16) §§§	20
tcp4 (SAIL1174_D02)	10.8 ± 1.6 (7-14)	2.1 ± 0.5 (1-3)	12.8 ± 1.5 (9-16) §§§	20
tcp16_5' UTR (SALK_074476.56.00)	9.4 ± 1.4 (7-12)	2.5 ± 0.6 (2-4)	11.9 ± 1.7 (9-15) §	20
tcp15 (SALK_011491.56.00)	8.8 ± 1.9 (6-12)	2.4 ± 0.5 (2-3)	11.2 ± 2.2 (8-15)	20
tcp20 (SALK_088460.34.25)	7.9 ± 1.8 (5-11)	2.9 ± 0.4 (2-4)	10.6 ± 1.9 (7-14)	19
tcp2_5' UTR (SALK_144731.51.25)	8.4 ± 1.5 (6-12)	2.2 ± 0.5 (1-3)	10.6 ± 1.7 (9-14)	20
tcp6 (SK17759)	8.0 ± 1.3 (5-10)	2.4 ± 0.6 (1-3)	10.4 ± 1.3 (7-12)	20
tcp5 (SM_3.29639)	7.9 ± 1.1 (6-10)	2.4 ± 0.6 (1-3)	10.3 ± 1.2 (8-12)	20
tcp23 (SAIL_443_F02)	8.1 ± 1.2 (6-10)	2.1 ± 0.4 (1-3)	10.1 ± 1.4 (8-12)	20
tcp21 (SALK_143403.37.70)	7.8 ± 2.0 (4-11)	2.1 ± 0.7 (1-3)	9.9 ± 2.4 (5-14)	20
tcp10 (SALK_050436.54.25)	7.9 ± 1.8 (5-12)	1.7 ± 0.7 (1-3)	9.5 ± 2.2 (7-14)	20
tcp14 (WiscDsLox477-480P20)	7.1 ± 2.5 (5-14)	1.8 ± 0.7 (1-4)	8.9 ± 2.5 (8-15)	20
tcp3 (WiscDsLox441C3)	6.7 ± 1.1 (5-9)	2.1 ± 0.7 (1-3)	8.8 ± 1.5 (7-11) §	20
tcp17 (SALK_148580.54.75)	6.8 ± 1.2 (5-10)	1.9 ± 0.7 (1-3)	8.7 ± 1.6 (6-12) §§	20

Table 6. Flowering time of *tcp2;tcp4;tcp10, tcp5;tcp13;tcp17* triple mutants and first order T-DNA insertion mutants of *TCP* family transcription factor family. *****WT, Col-0 WT. **†** Indicators of flowering time and shown as average ± standard derivation (range). Plants in each experiment were grown under LDs as indicated. Symbol **§** indicates the statistical significance of differences in comparison with WT of Col-0 using two-tailed multiple Student's *t*-test with Bonferroni correction. Single, double, and triple symbols represent $P < 0.05$, $P < 0.01$ and $P < 0.001$ respectively. No symbol means that there was no statistically significant difference among indicated genotypes in each experiment (Student's *t*-test, $P \geq 0.05$). Statistical tests were done on the total number of leaves.

3.5.3 Involvement of specific TCPs and TCP Clades in Modulating Flowering Time

Because of the limited flowering time phenotypes in single knockout plants, combinations of knockdown targets were determined and 26 amiRNAs were designed to systematically knockdown the TCP clades of interest (Table 7).

In comparison with the normal flowering phenotype of single TCP mutants like *tcp5* or *tcp23*, simultaneous knockdown of TCP5 clades members (including TCP5, 13, and 17) or TCP8 clades (in combination like TCP22+23 or TCP8+23) led to a significant delay in flowering time, further supporting the functional redundancy among the TCP clade members (Figure 28 and Table 8). Notably, these TCPs are ones, in which interaction with FT was significantly affected by charge reversion of BPP as described in the assays (Figure 24 and 25). Similarly, simultaneous knockdown of expression of TCP3, 4, and the phylogenetically closely related TCP10 also resulted as a delaying phenotype. However, the repressing effect was not significantly enhanced when compared to that of the *tcp4* standalone mutant, suggesting TCP4 may act independent of its clade members in the FT-mediated flowering time control. Last but not least, flowering time of the TCP candidates, like TCP14 and 15 (where interaction with FT was profoundly affected upon charge reversion on BPP), was surprisingly not affected by their knockdown in expression. Providing that the amiRNAs functioned as expected, it implies that binding of TCP to the FT function-defining surface may not necessarily play a role in the control of flowering.

amiR ID	Sequence	**Target(s)**	Potential Off-Target(s)
TKB1	TGGATTTATGACCTCGCTCAC	**TCP8, 14, 15**	transposable elements
TKB2	TTTATGACCTAGCTCTCGCGG	**TCP8, 14, 22**	-
TKB3	TTATGATAGAAGGCTCAGCTT	**TCP7, 21**	-
TKB4	TTGTCCGAAATCCGGCGTCGC	**TCP7, 21**	-
TKB5	TGCTAGGCTGACTCGGCCCTA	**TCP5, 17**	-
TKB6	TCTTGAAGGTCGTAGAGTTGA	**TCP5, 13, 17**	-
TKB7	TACTGAAGGGTCCCCCTGCTA	**TCP2, TCP24**	-
TKB8	TACTGAAGGGTCCCCTTGCTA	**TCP2, TCP24**	-
TKB9	TGATAAGCCAATCAGCGGCAT	**TCP3, TCP4, TCP10**	-
TKB10	TACTGGACTGAAGGGGCCCAC	**TCP3, TCP4, TCP10**	-
TKB11	TCTTAATTCAAGTCCAGGCGG	**TCP6**	-
TKB12	TGTAACCTAACTCTACGACCA	**TCP6**	-
TKB13	TGGATTTATGACCTAGCGCTC	**TCP5, 8, 17**	TCP14, 22
TKB14	TGAAAAACTCTAGCCGCGCAC	**TCP5, 8, 17**	TCP9, 21
TKB15	TGTGTCTATCTTTGCCTCCAA	**TCP2, 24, 5, 17**	TCP13
TKB16	TTAATCGATCTTGAGGGTCCT	**TCP2, 5, 17**	-
TKB17	TCTTTGCCACCGAATGCTCGT	**TCP2, 24**	TCP17
TKB18	TGTGTCTATCTTTGCCTCCAA	**TCP2, 24, 14, 15, 22**	TCP5, 17
TKB19	TTAATCGATCTTGAGGGTCCT	**TCP2, 14, 22**	TCP5, 17
TKB20	TAGTTCCGTTAACCGATACTG	**TCP9, 19**	-
TKB21	TCCGAATCGTTTCGCCGTCGG	**TCP9, 19**	-
TKB22	TGCGATGATAGCTGGCTGCGC	**TCP22, 23**	-
TKB23	TCCTAGCTGTTGACCTCCCAG	**TCP22, 23**	-
TKB24	TAAAGTAGAGAAGTTCGCCGC	**TCP8, 23**	-
TKB25	TAAAGTAGAGAAGTTCGCCGG	**TCP8, 23**	TCP14, 15
TKB26	TGCATACGAATTCGCCGTCCC	**TCP8, 22**	-

Table 7. 26 Artificial microRNAs (amiRNA) used for knocking down the expression of different combinations of *TCPs*. Specific amiRNAs were designed by WMD3 - Web MicroRNA Designer (Ossowski et al., 2008). amiRNA ranked with the best specificity and minimal unfavorable properties such as minor off-targets or weak hybridization to their target sites were chosen. Potential off-target(s) were predicted by the "Target-Search" function of WMD3.

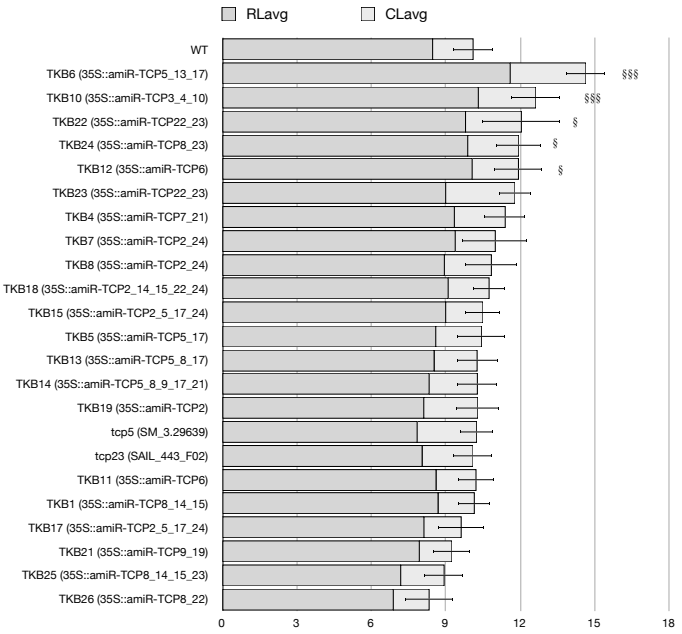

Figure 28. Flowering time of high order T-DNA insertion mutants of *TCP* and plants with *TCP* expression knockdown by artificial mircoRNAs. Numerical and statistical details are shown in **Table 8.**

Genotype *	No. of rosette leaves †	No. of cauline leaves †	Total no. of leaves †	*n*
	Experiment 1, LDs †			
WT	8.5 ± 1.2 (6-11)	1.6 ± 0.8 (1-3)	10.1 ± 1.6 (7-13)	19
TKB6 (35S::amiR-TCP5_13_17)	11.6 ± 1.8 (8-15)	3.1 ± 1.1 (1-6)	14.7 ± 2.0 (11-19) §§§	20
tcp4 (SAIL1174_D02)	10.8 ± 1.6 (7-14)	2.1 ± 0.5 (1-3)	12.8 ± 1.5 (9-16) §§§	20
TKB10 (35S::amiR-TCP3_4_10)	10.3 ± 2.3 (8-15)	2.3 ± 1.5 (1-7)	12.6 ± 3.1 (9-22) §	19
TKB22 (35S::amiR-TCP22_23)	9.8 ± 1.1 (8-12)	2.3 ± 1.0 (1-4)	12.1 ± 1.8 (9-15) §	20
TKB24 (35S::amiR-TCP8_23)	9.9 ± 1.5 (7-12)	2.1 ± 0.6 (1-3)	11.9 ± 1.9 (9-15) §	18
TKB12 (35S::amiR-TCP6)	10.1 ± 1.0 (9-12)	1.9 ± 0.5 (1-3)	11.9 ± 1.3 (10-14) §	15
TKB23 (35S::amiR-TCP22_23)	9.0 ± 1.2 (7-11)	2.8 ± 1.1 (1-5)	11.8 ± 1.7 (8-16)	19
TKB4 (35S::amiR-TCP7_21)	9.4 ± 1.1 (7-11)	2.1 ± 2.3 (0-3)	10.9 ± 1.4 (8-13)	20
TKB9 (35S::amiR-TCP3_4_10)	9.4 ± 1.6 (7-13)	2.1 ± 1.2 (0-4)	11.4 ± 2.1 (9-17)	16
TKB16 (35S::amiR-TCP2_5_17)	9.5 ± 1.2 (7-12)	1.5 ± 0.5 (1-2)	11.0 ± 1.3 (8-13)	18
TKB7 (35S::amiR-TCP2_24)	9.4 ± 1.0 (8-11)	1.6 ± 0.7 (1-3)	11.0 ± 1.5 (9-14)	13
TKB8 (35S::amiR-TCP2_24)	8.9 ± 1.7 (7-13)	1.9 ± 0.6 (1-3)	10.8 ± 2.0 (8-16)	19
TKB18 (35S::amiR-TCP2_14_15_22_24)	9.1 ± 1.7 (7-13)	1.7 ± 0.7 (1-4)	10.8 ± 1.7 (9-15)	20
TKB15 (35S::amiR-TCP2_5_17_24)	9.0 ± 1.4 (7-12)	1.5 ± 0.6 (1-3)	10.5 ± 1.6 (8-14)	20
TKB5 (35S::amiR-TCP5_17)	8.6 ± 1.5 (6-12)	1.9 ± 0.7 (1-3)	10.4 ± 1.7 (8-15)	19
TKB13 (35S::amiR-TCP5_8_17)	8.5 ± 1.2 (6-10)	1.7 ± 0.8 (0-3)	10.3 ± 1.3 (8-12)	15
TKB14 (35S::amiR-TCP5_8_9_17_21)	8.3 ± 1.3 (7-11)	1.9 ± 0.6 (1-3)	10.3 ± 1.6 (8-14)	18
TKB19 (35S::amiR-TCP2)	8.1 ± 1.2 (6-11)	2.2 ± 0.9 (1-4)	10.3 ± 1.4 (8-13)	17
tcp5 (SM_3.29639)	7.9 ± 1.1 (6-10)	2.4 ± 0.6 (1-3)	10.3 ± 1.2 (8-12)	20
tcp23 (SAIL_443_F02)	8.1 ± 1.2 (6-10)	2.1 ± 0.4 (1-3)	10.1 ± 1.4 (8-12)	20
TKB11 (35S::amiR-TCP6)	8.6 ± 1.2 (6-11)	1.6 ± 0.7 (1-3)	10.2 ± 1.3 (9-13)	17
TKB1 (35S::amiR-TCP8_14_15)	8.7 ± 1.8 (5-11)	1.5 ± 0.5 (1-2)	10.2 ± 1.9 (7-13)	13
TKB17 (35S::amiR-TCP2_5_17_24)	8.1 ± 1.4 (7-11)	1.5 ± 0.5 (1-2)	9.6 ± 1.6 (8-13)	8
TKB21 (35S::amiR-TCP9_19)	7.9 ± 1.7 (8-11)	1.3 ± 0.5 (1-2)	9.3 ± 1.9 (7-13)	16
TKB25 (35S::amiR-TCP8_14_15_23)	7.2 ± 1.3 (5-9)	1.8 ± 0.9 (1-4)	8.9 ± 1.6 (6-13) §	16
TKB26 (35S::amiR-TCP8_22)	6.9 ± 1.2 (5-9)	1.4 ± 0.5 (1-2)	8.3 ± 1.3 (7-11) §§	9

Table 8. Flowering time of *tcp2;tcp4;tcp10* triple mutants and transgenic plants overexpressing artificial microRNAs targeting different clades of *TCP* family members. *WT, Col-0 WT; TKB1-26, label conversion of the 26 amiRNAs used in this study. Details of each amiRNA gene cassette was blanketed † Indicators of flowering time and shown as average ± standard derivation (range). Plants in each experiment were grown under LDs as indicated. Symbol **§** indicates the statistical significance of differences in comparison with WT of Col-0 using two-tailed multiple Student's *t*-test with Bonferroni correction. Single, double and triple symbols represent $P < 0.05$, $P < 0.01$ and $P < 0.001$ respectively. No symbol means that there was no statistically significant difference among indicated genotypes in each experiment (Student's *t*-test, $P \geq 0.05$). Statistical tests were done on the total number of leaves.

3.6 DISCUSSION

Rather than serving as a transcriptional activator and repressor respectively, it has been suggested that FT and TFL1 are only mediators of the transcriptional regulatory complex during the developmental shift (Hanano and Goto, 2011). So apart from interacting with FD, FT requires the binding of a coactivator in order to mediate the transcriptional activation of floral patterning genes. But up to now, identity of the FT coactivator remains elusive.

In the first part of my study, I demonstrated that charge of regions such as BPP determines FT florigenic identity. Introduction of electrostatic reversion to the region could switch FT into its functional opposite TFL1, thereby inferring the potential role of those regions for acting as a binding site for the coactivator of FT. To shed light on the coactivator identity, in this study, I made use of yeast growth, quantitative Y2H, and *in vivo* split luciferase assays to test for the interactions between the known FT interactors and mutated FT with charge manipulated at region BPP. Based on the variation of interaction patterns upon charge change, I could verify the coactivator identity. From my experiments I concluded that the ligand bound to the surface defining the FT florigenic identity is not GRF or FD, but TCP. As shown by the analysis of the first and third orders of T-DNA insertion lines of *TCP*, individual TCP-clades may act redundantly on flowering time control. Further, by means of systematic knockdown of *TCP* by artificial microRNA, I demonstrated the involvement of the TCP5 clade, specific members of the TCP8 clade and TCP4 alone in modulating flowering time, implying the potential of TCP for serving as a FT coactivator during the floral transition.

3.6.1 Dominant-Negative Is Not Caused by Binding Disruption of GRF-FD

In some but not all previous studies, Y2H assays showed that FD binds more strongly with FT than with TFL1 (Abe, 2005; Wigge et al., 2005; Hanano and Goto, 2011). This observation led some to claim that differential strength of FT/TFL1-FD interaction is the basis for the antagonism between FT and TFL1.

In this study, consistent with a recent finding that, opposite to a positive role of FT, TFL1 can serve as a negative regulator of the FD-dependent transcription (Hanano and Goto, 2011), my data demonstrates that both FT and TFL1 could clearly interact with the bridging molecule GRF, and so did FD in yeast (Figure 23) and *in planta* (Figure 25A). Upon mutation Q140K, which could lead to a significant charge reversion on region BPP, strength of the interactions between the mFT and GRF/FD was almost unchanged and comparable to that of native FT (Figure 24 and Table 5). Therefore, my findings suggest that the dominant negative phenotype of converting FT into TFL1 is not caused by the weakening of binding with the GRF-FD module. Further, provided that the arrangement of the floral activation complex (FAC) is highly conserved among the *Plantae* (so FD is linked with FT via GRF proteins), as shown by my mutagenesis studies, mutations on either residues R62 or R130 (R64 and R132 in numbering of HD3A, a ortholog of FT in rice) responsible for establishing the salt bridge linkage between HD3A and GRFs (Taoka et al., 2011) could only render FT into a loss-of-function molecule (Figure 9 and Table 2). It suggests that

binding disruption of GRF-FD can at most abolish the activation mediated by FT, but cannot render the FT molecule a fully function TFL1 mimic.

3.6.2 TCPs Serve as Potential FT Coactivator

TCPs make up a plant-specific transcription factor family sharing a highly conserved basic helix-loop-helix (bHLH) motif/TCP domain that allows for DNA and protein binding (Cubas et al., 1999; Kosugi and Ohashi, 1997). Based on the differences of their bHLH motifs, members of this family can be classified as class I and II TCP. While class I TCP is mainly constituted by PCF or PCF-like proteins, depending on the possession of specific domains flanking the bHLH motif (for instance, ECE motif (Howarth and Donoghue, 2006) and R domain (Cubas et al., 1999)), class II TCP can be subdivided into three genetic clades namely, TB1, CYC, and CIN. Since the identification of the first family member in 1999, TCP were shown to engage in a wide range of plant developmental processes. Especially, extensive data had shown the specific involvement of TCP in control of organ morphology and body symmetry (Doebley et al., 1997; Luo et al., 1996; Palatnik et al., 2003).

In my interaction studies, eight TCP proteins were shown to be the ligand for surface defining FT florigenic identity, in which seven of them are class I TCP (TCP 7, 9, 14, 15, 21, 22, and 23), while one of them belongs to class II TCP (TCP4). In general, class I TCP promotes while class II represses cell proliferation and plant growth (Martín-Trillo and Cubas, 2010). So, at first glance, binding with class II TCP may not be in line with the FT promoting role in flowering time control and floral development. However, floral transition is not only representing the initiation of the floral phase, but at the same time, it also indicates the termination of processes involved in the inflorescence and vegetative phases. Therefore, it is necessary for the florigen FT to possess the bilateral ability to activate and repress different genes promoting inflorescence and vegetative identity, respectively. To this end, switching by binding with either class I or class II TCP seems to be necessary. Also, recent findings indicated that either class of TCP actually includes both transcriptional activators and repressors (for instance, class I TCP20 enhances transcription of CYCB1;1 (Li et al., 2005), while class II TCP13 promotes PSBD transcription (Baba et al., 2001), suggesting that regulatory function of TCP could be independent of their class or type of TCP domain. Further, previous study on TCP20 suggested the possibility that some TCP proteins are even possible to function as activators or repressors depending on their partner of interaction (Herve et al., 2009). It implied that, upon binding, FT may have the ability to switch the role of a normally repressing class II TCP into a floral activator. In agreement with this notion, ABP of human PEBP was demonstrated to function via binding with a phosphorylated ligand that in turn modulates the ligand function (Yeung et al., 1999). Correspondingly, TCP also possesses stretches of phosphorylatable residues in their highly conserved amphipathic helices of their bHLH motifs (Cubas et al., 1999), raising the possibility that the TCP regulatory role maybe shaped upon binding with FT. Unfortunately, crystal structures of TCP and FT-TCP are not yet available, making structural dynamic studies impossible. Further advancement on the structural aspects of FT-TCP binding is required before the scenario proposed can be validated.

3.6.3 TCPs Serve as Potential Enhancer-Recruiter or Complex-Stabilizer

As shown by the search of consensus sequences, among the TCP candidates, the class II TCP, including TCP4, 13, 17, 22, and 23, does contain the 9-amino acid transactivation domain (9aaTAD) (Supplementary Table 3). Also, these candidates additionally showed delayed flowering phenotype when their expression was knocked down by amiRNA (Figure 28), suggesting their capability and the possibility that the TCP candidates serve as co-activating recruiter for the general transcription activators during the FT-mediated floral transition.

Nevertheless, in *Arabidopsis*, evidence showed that TCP binding sites could cooperate with other regulatory elements to promote target transcription (Herve et al., 2009; Li et al., 2005; Vandepoele et al., 2006). These findings indicated the potential of TCP for serving as a recruiter for the *cis*- or *trans*-regulatory sequences, while implying a special way of "coactivation" mediated by TCP. Notably, based on the latest crystal structure of FAC involving the FT-GRF-FD in rice (Taoka et al., 2011), region BPP (the ligand binding site for the potential FT coactivator) was shown to locate at the side opposite to the GRF-FD while sitting in close proximity with chromatin (Figure 29).

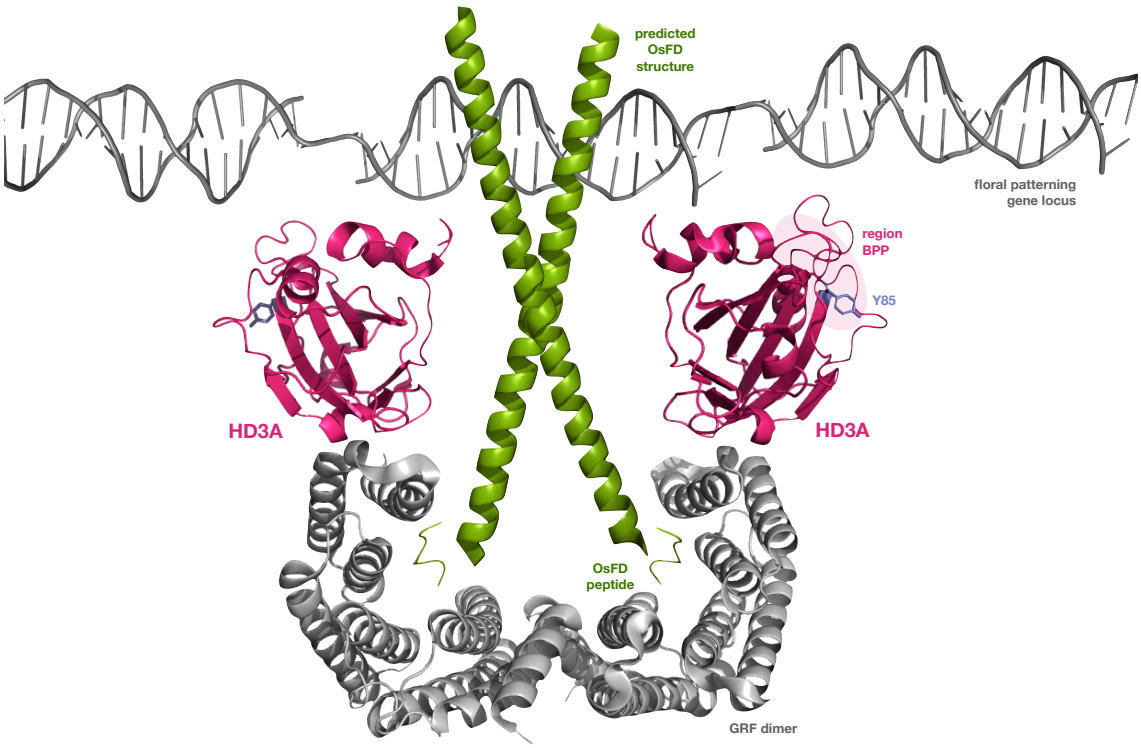

Figure 29. Position of region BPP on model of floral activation complex (FAC). HD3A, GRF dimer, OsFD peptide, OsFD predicted structure and DNA corresponding to a floral patterning gene locus are colored in magenta, light grey, green and dark grey respectively. Region BPP of one of the HD3A is shaded. The canonical Y85 highly conserved in region BPP of all FT homologs is colored in pale purple. Figure was generated based on Taoka et al., 2011.

On the one hand, such orientation of the region BPP provides additional evidence that binding of FT with GRF-FD is not the cause of the dominant negative phenotype. On the other hand, it suggests the unknown coactivator may bind DNA. In line with this thought, a transcription factor like TCP that is capable of binding with both DNA and FT protein can fulfill such requirement, and one of the possible scenarios is:

FT, together with GRF-FD, forms part of the floral activating complex at a floral patterning gene locus. However, in order to make the developmental transition happen, TCP has to bind with FT, where it serves as a recruiter to specifically bring in the necessary enhancer sequence close to the FAC, making expression of the patterning gene strong enough to overcome the activation barrier (Figure 30A).

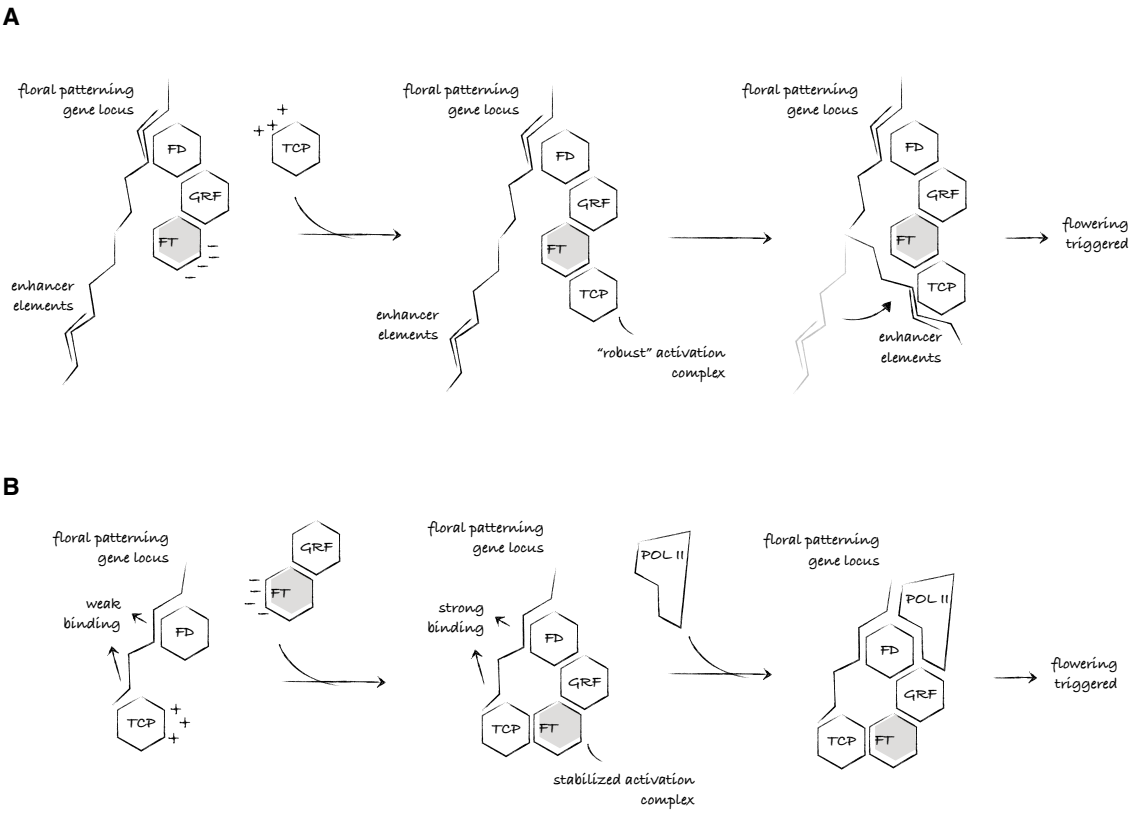

Figure 30. Models of TCP co-acting role during floral transition. **(A)** TCP serves as an enhancer recruiter. Based on the highly stringent charge and bonding arrangements of surface defining FT florigenic identity, such as BPP, specific TCP protein is recruited to the floral activation complex. Then, with aid of the specific DNA binding specificity, the TCP protein recruits the proximal *cis*- or distal *trans*-regulatory elements, such as enhancer sequence to the floral patterning gene locus. In this way, transcription of the gene and so flowering can be triggered. GRF, GENERAL REGULATORY FACTOR; FT, FLOWERING LOCUS T; TCP, TEOSINTE BRANCHED1, CYCLOIDEA, PCF. **(B)** TCP serves as a floral activation complex stabilizer. Both FT-FD and TCP bind independently to the same floral patterning gene loci, but only very weakly. Protein-protein interaction between TCP and FT-FD via region BPP can help stabilize the FAC to recruit POL II transcription-initiation complex necessary for the expression of the patterning gene. POL II, POL II transcription-initiation complex.

Alternatively, FD and TCP independently bind to the floral patterning gene loci, but only weakly. Protein-protein interaction between TCP and FT-FD via BPP can facilitate their recruitment to DNA and stabilize their formation of FAC, which can then recruit the POL II transcription-initiation complex necessary for the transcription and, thereby, for the initiation of floral transition (Figure 30B). However, further genetic studies are essential for validating the mutual genetic dependence between FT, FD, and TCPs, while expression analysis and chromatin immunoprecipitation (ChIP) with respect to the target loci, such as *AP1*, are required before these models can be verified.

Chapter 4 Conclusion

Despite the diversified seasonal patterns of flowering in different plant species, exogenous and endogenous clues lead to the expression of small groups of floral integrators that trigger this important developmental shift. In *Arabidopsis*, most pathways control expression of the florigen *FT*. In contrast to the rich literature on the transcriptional control of *FT* expression, much less is known about how FT, with its partners GRF, FD, and TCP, affects downstream gene expression. Previous studies identified several regions important for FT protein function, including Y85 as well as the motif encoded by exon 4B and 4C. However, whether additional residues are involved in their action and how exactly the canonical mutations and motifs can mediate the floral inducing function of FT remained unclear. Further, recent findings suggested the existence of a coactivator of FT. Therefore, the identity of this ligand still remains a mystery.

In my study, I showed that the residues ultraconserved in *Plantae* are not necessarily essential for full FT activity, while canonical positions do not determine the florigenic or antiflorigenic activity of FT and TFL1. Instead, I identify six residues essential for the maintenance of a specific charge and bondings of two localized surfaces. Disturbance of either of these properties is sufficient to convert FT into a complete TFL1 mimic. Further, I demonstrate that the dominant negative phenotype is not caused by interrupting the interaction with previously identified FT complex components GRFs or FD. Instead, specific members of a transcription factor family named TCPs are likely to play a key role in differentiating between FT and TFL1 action. Altogether, my work reveals novel and surprising insights into both FT evolution and function.

Chapter 5 Material and Methods

5.1 General Material and Methods

Standard techniques and buffers. The preparation of buffer and media, and standard molecular techniques, were performed according to Sambrook and Russell (Sambrook and Russell, 2001). All chemicals, unless otherwise specified, were purchased from Sigma (Munich, Germany), Roth (Karlsruhe, Germany), Merck (Darmstadt, Germany) and Roche (Mannheim, Germany). Restriction endonucleases were purchased from Fermentas (Burlington, Canada). DNA Polymerases (Phusion and Taq), T4 DNA ligase and S1 nuclease were purchased from Fermentas (Burlington, Canada). Oligonucleotides were ordered from MWG (Ebersberg, Germany).

Plant material and growth conditions. *Arabidopsis* accessions were obtained from the European Arabidopsis Stock Center (NASC). *Arabidopsis* plants were cultivated in growth room under a 1:2 mixture of cool white (F36W/840 Cool White De Luxe, Sylvania, Danvers, MA, USA) and warm fluorescent (Luxline Plus F36W/830 Warm White De Luxe, Sylvania) light or in growth chambers (Percival Scientific, Perry, IA, USA) illuminated with F17T8/TL741 bulbs (Philips Electronics, Eindhoven, Netherlands). Plants were grown at 65% humidity under long (16 hours of light) or short days (8 hours of light) at 23°C, unless otherwise specified.

Genomic DNA extraction. Plant tissue was freshly collected and immediately frozen in liquid nitrogen. After grounding to fine powder, 200 µl of a CTAB solution (1.4M NaCl, 0.1M Tris pH 8.0, 20 mM EDTA, 2% CTAB, 1% polyvinylpyrrolidone, 1µg/µl RNAse A) were added to the tube and incubated for one hour at 65°C. 200 µl of a chloroform:isoamylacohol 24:1 solution were then added. After vigorous mixing by vortex, the tubes were centrifuged for 15 minutes at 14.000 g. The supernatant was transferred to new tubes and mixed with 150 µl of isopropanol. After 15 minutes of centrifugation at 14.000 g, the supernatant was discarded and the pellet washed with 200 µl of 75% ethanol. After centrifugation at 14.000 g for five minutes, the pellet was dried for 30 minutes at 37°C and then resuspended in 50 µl of deionized water. As template for PCR, 2µl of a 1:10 dilution of this DNA were used.

For DNA extraction in 96-well plates, a modified protocol was adopted. Samples were collected directly in 96-well plates. A metal bead was added to each well, the samples were frozen at -80°C and then ground using a Retsch MM 300 homogenizer (Retsch GmbH, Haan, Germany). The ground tissue was then resuspended in 500 µl of a modified CTAB solution (1.42M NaCl, 0.1M Tris pH 8.0, 20 mM EDTA, 2% CTAB, 0.2% *beta*-mercaptoethanol, 1µg/µl RNAse A) pre-heated at 65°C and incubated at 65°C for one hour. After addition of 500 µl of chloroform:isoamylacohol 24:1, samples were centrifuged at

4.000 g for 20 minutes. 200 µl of the supernatant were transferred to new plates, and 0.7 volumes of isopropanol were added and mixed by pipetting. The samples were incubated at -20°C for at least 30 minutes and then centrifuged for 15 minute at 4000 g. The pellet was washed with 100 µl of 75% ethanol, air dried, and resuspended in 250 µl of deionized water. 1µl of the DNA solution was directly used as PCR template.

RNA extraction and cDNA synthesis. RNA was extracted using either TRIzol reagent (Invitrogen Corporation, Carlsbad, CA, USA) or RNeasy Plant Mini Kit (Qiagen Corperation, Venlo, Netherlands) following manufacturer instructions, unless otherwise specified. For cDNA synthesis, the SuperScript II cDNA Synthesis Kit (Invitrogen Corporation, Carlsbad, CA, USA) was used according to manufacturer instruction. 2 µg of total RNA treated with DNAse (Fermentas) were used as template.

Plant transformation. Transgenes were introduced in *Arabidopsis thaliana* plants using *Agrobacterium tumefaciens* mediated floral dip transformation (Weigel and Glazebrook, 2002). All binary vectors used for *Arabidopsis* transformation are based on the pGREEN vector (Hellens et al., 2000).

Measurement of flowering time in *Arabidopsis*. The timing of *A. thaliana* flowering was carefully measured by counting the number of leaves (including rosette and cauline leaves) formed before the initiation of flowering. This developmental measure allows for the identification of mutants impaired in gene encoding regulators of flowering time rather than those involved in more general processes, such as controlling growth rate (Koornneef et al., 1991).

5.2 Material and Methods for Chapter 2

Construction of chimeras for random mutagenesis. For construction of an expression vector, cauliflower mosaic virus (CaMV) 35S promoter was amplified by oligos G-20760 and G-20761 to flank it with a 5'-ApaI and a 3'-SacII sites using FK209 as template (Oligo List 1). PCR products and vector FK202 were digested with ApaI and SacII and ligated (WH27). Ribulose-1,5-bisphosphate carboxylase oxygenase (RuBisCO/rbcs) terminator was amplified by oligos G-20762 and G-20763 to flank it with 5'-SpeI and 3'-PstI using FK139 as template. PCR products and WH27 were digested with ApaI and SacII and ligated (WH28). Coding sequence (CDS) of the modified yellow fluorescent citrine (mCitrine/YFP) was amplified by oligos G-22312 and G-22313 to equip it with a multiple cloning site (MCS; EcoRI-HindIII-XbaI-NotI-SmaI-XhoI) at its 5'-end and a SpeI site to its 3'-end. PCR products and WH28 were digested with EcoRI and SpeI and ligated (WH31).

For construction of a *FT* mutation library, FT CDS was amplified by oligos G-20652 and G-20653 using plasmid JM13 as PCR template. By the amplification, start and stop codons of *FT* CDS were removed, while the CDS was equipped with HindIII restriction site, ATG and *Human influenza hemagglutinin* (*HA*) tag at its 5'-end, and XhoI restriction site, *(Glycine-Serine)$_4$* (*GS$_4$*) linker at its 3'-end. After cloning the resulted fragment into pGEM-T Easy vector (Promega Corporation, Wisconsin, USA) (WH25), oligos G-22376 and G-22377 specific only to the flanking sequences of the harbored FT (i.e. the CDS of HA tag and GS_4 linker respectively) were used for performing the PCR-mediated random mutagenesis using GeneMorph II Random Mutagenesis Kit (Clontech Laboratories Inc., Mountain View, CA, USA). Procedures were done according to the manufacturer instructions and recommended conditions with nine varied amount of WH25 (i.e. 0.06ug, 0.15ug, 0.3ug, 0.6ug, 0.9ug, 1.2ug 1.8ug, 2.7ug and 3.6ug) as templates, while number of PCR cycles was fixed at 30. PCR products were digested and ligated with WH31 linearized by HindIII and XhoI (WH32). Around 120-130 clones were picked from each of the nine mutation libraries to check for the randomness and mutation bias (transition-to-transversion ratio) by DNA sequencing using oligos G-22376 and G-22377 as sequencing primers. Library with the maximal amount of singly mutated *FT* but minimal number of non-mutated copies (i.e. template amount = 0.15ug) was selected.

For positive control, oligos G-22376 and G-22377 were used for amplifying non-mutated copy of tagged FT (ATG:HA:FT:GS_4) using WH25 as PCR template. PCR products and WH31 were digested with HindIII and XhoI and ligated (WH33). WH31 was used as a negative control. WH32 was pool transformation to Col-0 wild-type, while positive and negative controls were individually transformed via floral dip method.

Yellow fluorescence measurement. At four- to six-leaves stage, transgenic plants were examined for the expression of mCitrine using a Leica MZ FLIII microscope fitted with wide- and band-pass YFP filters and a AxioCam HRc (Zeiss) digital camera with AxioVison software (version 3.1). Before each time of measurement, the microscope was calibrated using leaves of WH33 (positive control) and WH31 (negative control) transformed plants to define the uppermost fluorescence flux that lead to any background fluorescence in case of WH31, while contrasting yellow fluorescence from leaves of WH33. During the measurement, rosette leaves from each plant were freshly excised in dim light. Level of yellow fluorescence were determined by evaluating the visibility of yellow fluorescence starting from the uppermost threshold, then lowering the flux at six intervals (resulting as level 1 to 7). At least three leaves from each plant were examined to ensure consistence of the level determined.

***In silico* FT mutagenesis and electrostatic potential calculation.** Three-dimensional structures of wild-type of FT (entry 1WKP) and TFL1 (entry 1WKO) were obtained from RCSB Protein Data Bank (PDB; www.rcsg.org). Chain A in each file was used for the visualization by a molecular graphics system known as PyMOL (Version 1.5.0.4 Schrödinger, LLC). During the *in silico* mutagenesis, first backbone dependent

rotamer representing the highest frequencies of occurrence in proteins was adopted in each case unless otherwise specified. During the electrostatic potential calculation, software for evaluating the electrostatic properties of nanoscale biomolecular systems known as Adaptive Poisson-Boltzmann Solver (APBS) plugin was applied (Baker et al., 2001). Before the calculation, any water and solvent molecules that disturb the native potential of proteins found in the visualization were removed. PDB2PQR and default grid settings were applied for the calculations unless otherwise specified. Calculated potential was visualized by color on solvent accessible surface with color space in CMYK, with +2 and -2 as the high and low thresholds respectively.

Construction of chimeras for site-directed mutagenesis. For generating site-directed mutated *FT* with mutations at the interim region of FT protein (i.e. 8th - 169th amino acid), *FT* CDS was firstly amplified by oligo G-25689 (annealing to 5'-end of *FT* CDS) and one of the MR oligos (MR1-MR262; each containing a different non-synonymous mutation of *FT* at the mid of the oligo sequence) in reaction A, while by one of the MF oligos (MF1-MF262; oligo reverse but complementary to the corresponding oligo MR with the same number) and G-25690 (oligo anneal to 3'-end of *FT* CDS) in reaction B using JM13 as template (Oligo List 2). Size of PCR products was checked by gel electrophoresis and excised. The gel purified products from both reaction A and B were used as templates in the 2nd round of PCR using G-25689 and G-25690 as primers for flanking the products with HindIII and XhoI sites. Resulting PCR products were gel purified, restricted with HindII and XhoI and ligated with pJLBlueF (pENTR1A:attL1:MCS:attL2) Gateway entry vector, which was linearized with the same pair of restriction enzymes. Then, Gateway LR cloning (Invitrogen Corporation, Carlsbad, CA, USA) was used for shuttling each of the mutated *FT* from the entry clone to three destination vectors including FF40 (pGREENIIS:35Spro:attR1-2:rbcst), FF29 (pGREENIIS:SUC2pro:attR1-2:ocst) and FF25 (pGREENIIS:FDpro:attR1-2:ocst) for plant expression.

For construction of site-directed mutated FT mutation at either terminal (i.e. 1st - 7th, and 170th - 175th amino acid), either EMF oligo (EMF49, 50) and G-25690, or oligo G-25689 and EMR oligo (EMR175-184, 221-224) were used for amplifying, thus flanking the resulting fragment with HindIII and XhoI sites while introducing non-synonymous mutation to the *FT* sequence. PCR products were gel purified, restricted with HindII and XhoI, and ligated with pJLBlueF entry vector that was linearized with the same pair of restriction enzymes. Gateway LR cloning was again utilized for shuttling each of the mutated *FT* from the entry clone to the FF40, FF29, and FF25 destination vectors for plant expression.

Construction of chimeras for *tfl1-1* complementation. To reconstruct the genomic regulatory context of TFL1 (Sohn et al., 2007), firstly, oligos AF61_2 and AR61 were used for amplifying while flanking the 2.2kb- upstream regulatory sequence of genomic *TFL1* (*gTFL1*) with XhoI and PstI sites using total genomic DNA of WT Col-0 as template. SUC promoter was released from FF29 via XhoI and PstI that were then used for ligating with the upstream sequence digested with the same pair of enzymes (WH1352). Secondly, oligo AF125 and AR125 were used to amplify while flanking the 4.6kb- downstream

of gTFL1 (proven to be critical for the regulation of *TFL1* expression (Kaufmann et al., 2010)) with SpeI and SacI sites using WT genomic DNA as template (Oligo List 3). Resulting PCR products and WH1352 were digested with SpeI and SacI and ligated (WH1353). Sequence fidelity of the 5'-upstream and 3'-downstream sequences were checked by DNA sequencing using oligos SF50-SF54, SR10 and oligos SF55-SF64, SR11 respectively. Thirdly, PstI and BamHI were used for releasing the stretch flanked by attR1-2 from WH1353 that were then replaced by an MCS (PstI-NotI-SmaI-SalI-NcoI-BamHI) generated by annealing oligo LF6 and LR6 (WH1354).

For inserts, genomic and CDS of *TFL1* were prepared by oligo AF149 and AR149 using total genomic DNA and total cDNA of WT Col-0 as the respective amplification template. Resulting clones and WH1354 were digested with PstI and SpeI, and then ligated. Genomic and CDS of *FT* were prepared by oligo AF154 and AR154 using total genomic DNA and cDNA of WT Col-0 as the respective amplification template. Resulting clones and WH1354 were digested with NotI and NcoI, and then ligated. Mutated *FT* including ΔY85H, ΔY85E, ΔW88R, ΔE109K, ΔY134K, ΔW138E, and ΔN152K were prepared by oligo AF154 and AR154 using the entry clones prepared from the site-directed mutagenesis (i.e. WH54, WH789, WH47, WH55, WH801, WH80 and WH58) as their respective PCR template. Resulting clones and WH1354 were digested with NotI and NcoI, and then ligated.

5.3 Material and Methods for Chapter 3

Construction of chimeras for yeast growth and quantitative ONPG enzyme activity assays. To facilitate the subsequent cloning, a pair of novel entry vectors, EN2F and EN2R, was made. Firstly, to remove the ApaI site, INT329 was digested with ApaI before the vector was self-ligated after S1 nuclease treatment (EN1). Oligos LF1 and LR1 were PCR amplified, so that the resulting MCS (EcoRI overhang-2bp-NotI-NcoI-KpnI-HindIII-SmaI-BglII-PstI-ApaI-SalI-SpeI-1bp-EcoRI overhang) served as the insert for direct ligation with EcoRI-digested EN1 (Oligo List 4). Depending on the forward or reverse orientation of MCS, the entry vectors were named EN2F (forward) and EN2R (reverse).

For the destination vector of bait, oligo AF14 and AR14 were used for amplifying while flanking the attR1-2 stretches from FF40 with NdeI and NotI sites. PCR products and pGBKT7 (Clontech Laboratories Inc., Mountain View, CA, USA) were digested with NdeI and NotI then ligated (WH1016). For the destination vector of prey, oligo AF55 and AR55 were used for amplifying while flanking the attR1-2 stretches from FF40 with NdeI and XhoI sites. PCR products and pGADT7 (Clontech Laboratories Inc., Mountain View, CA, USA) were digested with NdeI and XhoI then ligated (WH1017).

For the cloning of baits and preys of the assays, total RNA from WT Col-0 was extracted by RNeasy Plant Mini Kit (Qiagen Corperation, Venlo, Netherlands), while cDNA was synthesized using SuperScript II cDNA Synthesis Kit (Invitrogen Corporation, Carlsbad, CA, USA). For clonings of *GRF1-15*,

TCP1-24, *FD*, *FT* and its homologs including *ATC*, *BFT*, *MFT*, *TSF*, *TFL1*, forward oligos AF15-53, AF7, G-25689, AF56-59, AF10 and reverse oligos AR15-53, AR10_2, G-25690, AR56-59, and AR13 were used (Oligo List 4). For *GRF1-15* and *TCP1-24* (except *TCP9*, *11*, and *21*), their PCR products and EN2F were digested with NotI and XhoI and ligated (WH1069-1091, 1093, 1095-1103, and 1105-1107). For *TCP9*, *11*, *21*, and *ATC*, their PCR products and EN2F were digested with NotI and SpeI and ligated (WH1092, 1094, 1104, and 1060). For *BFT*, *MFT*, *TSF*, *FD* and *TFL1*, their PCR products and EN2F were digested with HindIII and XhoI and ligated (WH1061-1065). Entry clones of *GRF1-15*, *TCP1-24*, and *FD* were shuttled to WH1017 (having resulted as WH1231-1269, 1276), while *FT*, *ATC*, *BFT*, *MFT*, *TSF* and *TFL1* were shuttled to WH1016 (having resulted as WH1186-1191) by Gateway LR cloning. WH1231-1269, and 1276 were transformed to yeast strain AH109, while WH1186-1191 were transformed to yeast strain Y187 for mating according to the procedures described in CLONTECH Laboratories Yeast Protocols Handbook (protocol no. PT3024-1, version no. PR13103; Stratagene).

Quantitative ONPG enzyme activity assay in yeast. Yeast two-hybrid *beta*-galactosidase quantifications were carried out using ONPG assays as described in CLONTECH Laboratories Yeast Protocols Handbook. The yeast strains were grown overnight at 30°C with shaking in 5 mL of Trp/Leu dropout media (0.7% yeast nitrogen base without amino acids, 0.1% mix of all essential amino acids excluding Trp and Leu). Two mL of overnight culture were then transferred to 8 mL of yeast peptone dextrose (YPD; 1% bacto-yeast extract, 2% bacto-peptone, 2% dextrose) media and grown at 30°C with shaking for approximately 2 hrs (OD_{600} of 1 mL 5 0.5–1). Six replicates were separated from each culture. The yeast cells were pelleted by centrifugation and washed once with Z buffer (Na2HPO4, NaH2PO4, KCl, and MgSO4). The yeast cell pellets were then resuspended in Z buffer and were lysed using five sequential freeze thaw cycles involving transfers from liquid nitrogen to a 37°C water bath. A Z buffer/BME solution was added along with a Z buffer/ONPG solution. The samples were then incubated in a 30°C water bath and timed for rate of yellow coloration emergence. The ONPG reactions were quenched with Na_2CO_3, centrifuged at 20,800g for 10 mins, and the OD_{420} was measured. *beta*-galactosidase activity was measured in Miller units : *beta*-galactosidase units = 1000 x OD_{420}/(t x V x OD_{600}); t = elapsed time (min) of ONPG reaction incubation; V = 0.1 mL x concentration factor; OD_{600} = A_{600} of 1 mL of culture after the approximately 2hrs YPD grow up.

Yeast growth assay. Yeast cultures were grown as described above to yield OD_{600} of 1 mL equal to 0.5 to 1 in YPD media. A total of $1x10^8$ cells of each culture were extracted and placed into a sterile tube. The cells were pelleted by centrifugation and were washed twice with Leu/Trp/His (triple) dropout media. The final pellets were resuspended in 200 mL of triple dropout media. An aliquot of 5 mL of each culture was plated on triple dropout agar plates and growth was assessed after 6 days.

Construction of chimeras for *in planta* split luciferase assay. For destination vectors harboring the C-terminal of luciferase (*LUCc*), oligo AF129 and AR129 were used for amplifying while flanking the attR1-2 stretch from FF40 with KpnI and PstI sites (Oligo List 5). PCR products and JW772 were digested with KpnI and PstI then ligated (WH1353). For destination vectors harboring the N-terminal of luciferase (*LUCn*), oligo AF385 and AR387 were used for amplifying while flanking the attR1-2 stretch from FF40 with KpnI and SalI sites. PCR products and JW771 were digested with KpnI and SalI then ligated (WH1354).

For entry clones to be in fused with LUCc, including *GRF1-15*, *TCP1-24* and *FD*, entry clones used in the chimeric construction in Y2H assay were used (WH1069-1107, WH1066). For entry clones to be in fused with *LUCn*, including *FT*, *TFL1*, *mFTΔQ140K* and *mFTΔQ140D*, stop codons have to be removed from the sequences, therefore oligos AF261 and AR261 were used for amplifying while flanking *FT*, *mFTΔQ140K* and *mFTΔQ140D* with HindIII and XhoI sites, while AF260 and AR260 were used in the case of *TFL1*. PCR products resulted and EN2F were digested with HindIII and XhoI and then ligated (WH1354-1357). Gateway LR cloning was used for shuttling of the entry clones WH1069-1107, WH1066 into WH1353, while WH1354-1357 were shuttled to WH1354. Expression clones were transformed to Agrobacterium GV3101 for infiltration.

***In planta* split luciferase assay.** Single colony of the transformed *A.tumefaciens* was inoculated to 5mL of LB broth with antibiotics (including kanamycin, gentamicin and rifamycin, KGR) and incubated at 28°C with vigorous shaking. Two milliliter of overnight culture were subcultured to 50mL of LB medium with KGR and incubated for 16-20hrs at 28°C. Bacteria were then recovered by centrifugation at 2000g for 10 min at 4°C. Pellet was resuspended in a 30mL infiltration medium (10mM $MgCl_2$, 10mM MES pH5.7, and 150μm acetosyringone) and incubated for 16-20hrs at room temperature with gentle shaking. The volume of the culture with infiltration medium was adjusted to a final concentration of OD_{600} = 0.8. For each set of assay, sample in test and three controls were infiltrated with: (i) empty:*LUCn* + *LUCc*:empty (WH1354+WH1353), (ii) *FT*/*TFL1*/*mFT*:*LUCn* + *LUCc*:empty (WH1354-1357+WH1353), (iii) empty:*LUCn* + *LUCc:GRF*/*TCP*/*FD* (WH1354+ WH1069-1107,WH1066) and (iv) *FT*/*TFL1*/*mFT*:*LUCn* + *LUCc:GRF*/*TCP*/*FD* (WH1354-1357+ WH1069-1107,WH1066), into the same young but fully expanded leaf of *N. benthamiana* plant with 1mL syringe (without needle), while counter pressure was applied from the other side of the leaf by fingertip. The infiltrated leaves were marked with a small tag to the petiole. At least three replicates were performed on independent plants for each assay.

At three days after the inoculation, one millimolar of luciferin was infiltrated to the leaves and materials were kept in dark for 6 min to quench the fluorescence. Before the measurement, leaves only infiltrated with luciferin (negative control) and leaves infiltrated with 35S::*LUC* construct and luciferin (positive control) were used for calibrating the Orca 2-BT cooled CCD camera (Hamamatsu Photonics, Hamamatsu, Japan). Relative LUC activity was measured at exposure time fixed at 150 sec unless otherwise specified.

Genotyping of T-DNA insertion lines. Procedures and oligos for the genotyping was designed based on the T-DNA Design online resources available from SIGnAL (Salk Institute Genomic Analysis Laboratory; http://signal.salk.edu/tdnaprimers.2.html) (Oligo List 6).

Construction of chimeras for systematic knockdown of *TCP*/ *TCP* clades. Sets of oligos for generating stemloop-precursors to target the *TCP*/*TCP* clades were designed by Web MicroRNA Designer (WMD3) (Ossowski et al., 2008). amiRNA ranked best in specificity and minimal unfavorable properties such as minor off-targets or weak hybridization to their target sites and were, thus, chosen. Potential off-target(s) were predicted by the "Target-Search" function of WMD3.

In the first round of PCR, oligos mOA+1-26KD4, 1-26KD3+1-26KD2, 1-26KD1+mOB were used for setting up reactions a, b, and c (Oligo List 7) following the conditions described in an online protocol available at: http://wmd3.weigelworld.org/cgi-bin/webapp.cgi?page=Downloads;project=stdwmd. Size of PCR products was checked on gel. In the second round of PCR, gel purified PCR products from reaction a, b, and c were served as the PCR template using mOA and mOB as oligo. In this way, stemloop precursors targeting specific *TCP*/*TCP* clades flanked with HindIII and XhoI sites were generated. Gateway LR cloning was used for shuttling the entry clones into FK209 for plant expression.

References

Abe, M. (2005). FD, a bZIP Protein Mediating Signals from the Floral Pathway Integrator FT at the Shoot Apex. *Science* **309**, 1052–1056.

Ahn, J. H., Miller, D., Winter, V. J., Banfield, M. J., Lee, J. H., Yoo, S. Y., Henz, S. R., Brady, R. L. and Weigel, D. (2006). A divergent external loop confers antagonistic activity on floral regulators FT and TFL1. *EMBO J.* **25**, 605–614.

Aki, T., Shigyo, M., Nakano, R., Yoneyama, T. and Yanagisawa, S. (2008). Nano Scale Proteomics Revealed the Presence of Regulatory Proteins Including Three FT-Like proteins in Phloem and Xylem Saps from Rice. *Plant and Cell Physiology* **49**, 767–790.

An, H. (2004). CONSTANS acts in the phloem to regulate a systemic signal that induces photoperiodic flowering of Arabidopsis. *Development* **131**, 3615–3626.

Andres, F., Galbraith, D. W., Talon, M. and Domingo, C. (2009). Analysis of PHOTOPERIOD SENSITIVITY5 Sheds Light on the Role of Phytochromes in Photoperiodic Flowering in Rice. *PLANT PHYSIOLOGY* **151**, 681–690.

Andrés, F. and Coupland, G. (2012). The genetic basis of flowering responses to seasonal cues. *Nat. Rev. Genet.* **13**, 627–639.

Angel, A., Song, J., Dean, C. and Howard, M. (2011). A Polycomb-based switch underlying quantitative epigenetic memory. *Nature* **476**, 105–108.

Ausín, I., Alonso-Blanco, C., Jarillo, J. A., Ruiz-García, L. and Martínez-Zapater, J. M. (2004). Regulation of flowering time by FVE, a retinoblastoma-associated protein. *Nat Genet* **36**, 162–166.

Baba, K., Nakano, T., Yamagishi, K. and Yoshida, S. (2001). Involvement of a nuclear-encoded basic helix-loop-helix protein in transcription of the light-responsive promoter of psbD. *PLANT PHYSIOLOGY* **125**, 595–603.

Baker, N. A., Sept, D., Joseph, S., Holst, M. J. and McCammon, J. A. (2001). Electrostatics of nanosystems: application to microtubules and the ribosome. *Proc. Natl. Acad. Sci. U.S.A.* **98**, 10037–10041.

Banfield, M. J. and Brady, R. L. (2000). The structure of Antirrhinum centroradialis protein (CEN) suggests a role as a kinase regulator. *J. Mol. Biol.* **297**, 1159–1170.

Banfield, M. J., Barker, J. J., Perry, A. C. and Brady, R. L. (1998). Function from structure? The crystal structure of human phosphatidylethanolamine-binding protein suggests a role in membrane signal transduction. *Structure* **6**, 1245–1254.

Bäurle, I. and Dean, C. (2006). The Timing of Developmental Transitions in Plants. *Cell* **125**, 655–664.

Blackman, B. K., Strasburg, J. L., Raduski, A. R., Michaels, S. D. and Rieseberg, L. H. (2010). The Role of Recently Derived FT Paralogs in Sunflower Domestication. *Current Biology* **20**, 629–635.

Bollengier, F. and Mahler, A. (1988). Localization of the novel neuropolypeptide h3 in subsets of tissues from different species. *J. Neurochem.* **50**, 1210–1214.

Briggs, W. R. and Olney, M. A. (2001). Photoreceptors in plant photomorphogenesis to date. Five phytochromes, two cryptochromes, one phototropin, and one superchrome. *PLANT PHYSIOLOGY* **125**, 85–88.

Campoli, C., Drosse, B., Searle, I., Coupland, G. and Korff, von, M. (2012). Functional characterisation of HvCO1, the barley (Hordeum vulgare) flowering time ortholog of CONSTANS. *The Plant Journal* **69**, 868–880.

Chen, H., Zou, Y., Shang, Y., Lin, H., Wang, Y., Cai, R., Tang, X. and Zhou, J. M. (2007). Firefly Luciferase Complementation Imaging Assay for Protein-Protein Interactions in Plants. *PLANT PHYSIOLOGY* **146**, 368–376.

Corbesier, L. and Coupland, G. (2006). The quest for florigen: a review of recent progress. *Journal of Experimental Botany* **57**, 3395–3403.

Corbesier, L., Vincent, C., Jang, S., Fornara, F., Fan, Q., Searle, I., Giakountis, A., Farrona, S., Gissot, L., Turnbull, C., et al. (2007). FT Protein Movement Contributes to Long-Distance Signaling in Floral Induction of Arabidopsis. *Science* **316**, 1030–1033.

Cornwall, G. A., Tulsiani, D. R. and Orgebin-Crist, M. C. (1991). Inhibition of the mouse sperm surface alpha-D-mannosidase inhibits sperm-egg binding in vitro. *Biol. Reprod.* **44**, 913–921.

Cubas, P., Lauter, N., Doebley, J. and Coen, E. S. (1999). The TCP domain: a motif found in proteins regulating plant growth and development. *Plant J.* **18**, 215–222.

Davies, P. J. (2010). *Plant Hormones: Biosynthesis, Signal Transduction, Action!* Springer.

De Lucia, F., Crevillen, P., Jones, A. M. E., Greb, T. and Dean, C. (2008). A PHD-polycomb repressive complex 2 triggers the epigenetic silencing of FLC during vernalization. *Proceedings of the National Academy of Sciences* **105**, 16831–16836.

Doebley, J., Stec, A. and Hubbard, L. (1997). The evolution of apical dominance in maize. *Nature* **386**, 485–488.

Doi, K. (2004). Ehd1, a B-type response regulator in rice, confers short-day promotion of flowering and controls FT-like gene expression independently of Hd1. *Genes & Development* **18**, 926–936.

Dubcovsky, J., Loukoianov, A., Fu, D., Valarik, M., Sanchez, A. and Yan, L. (2006). Effect of Photoperiod on the Regulation of Wheat Vernalization Genes VRN1 and VRN2. *Plant Mol. Biol.* **60**, 469–480.

Efroni, I., Blum, E., Goldshmidt, A. and Eshed, Y. (2008). A Protracted and Dynamic Maturation Schedule Underlies Arabidopsis Leaf Development. *THE PLANT CELL ONLINE* **20**, 2293–2306.

Finnegan, E. J. and Dennis, E. S. (2007). Vernalization-Induced Trimethylation of Histone H3 Lysine 27 at FLC Is Not Maintained in Mitotically Quiescent Cells. *Current Biology* **17**, 1978–1983.

Fornara, F., de Montaigu, A. and Coupland, G. (2010). SnapShot: Control of Flowering in Arabidopsis. *Cell* **141**, 550–550.e2.

Fornara, F., Panigrahi, K. C. S., Gissot, L., Sauerbrunn, N., RUhl, M., Jarillo, J. A. and Coupland, G. (2009). Arabidopsis DOF Transcription Factors Act Redundantly to Reduce CONSTANS Expression and Are Essential for a Photoperiodic Flowering Response. *Developmental Cell* **17**, 75–86.

Fu, X. (2004). The Arabidopsis Mutant sleepy1gar2-1 Protein Promotes Plant Growth by Increasing the Affinity of the SCFSLY1 E3 Ubiquitin Ligase for DELLA Protein Substrates. *THE PLANT CELL ONLINE* **16**, 1406–1418.

Fujiwara, S., Oda, A., Yoshida, R., Niinuma, K., Miyata, K., Tomozoe, Y., Tajima, T., Nakagawa, M., Hayashi, K., Coupland, G., et al. (2008). Circadian Clock Proteins LHY and CCA1 Regulate SVP Protein Accumulation to Control Flowering in Arabidopsis. *THE PLANT CELL ONLINE* **20**, 2960–2971.

Galvao, V. C., Horrer, D., Kuttner, F. and Schmid, M. (2012). Spatial control of flowering by DELLA proteins in Arabidopsis thaliana. *Development* **139**, 4072–4082.

Gendall, A. R., Levy, Y. Y., Wilson, A. and Dean, C. (2001). The VERNALIZATION 2 gene mediates the epigenetic regulation of vernalization in Arabidopsis. *Cell* **107**, 525–535.

Goodrich, J., Puangsomlee, P., Martin, M., Long, D., Meyerowitz, E. M. and Coupland, G. (1997). A Polycomb-group gene regulates homeotic gene expression in Arabidopsis. *Nature* **386**, 44–51.

Griffiths, J., Murase, K., Rieu, I., Zentella, R., Zhang, Z. L., Powers, S. J., Gong, F., Phillips, A. L., Hedden, P., Sun, T. P., et al. (2006). Genetic Characterization and Functional Analysis of the GID1 Gibberellin Receptors in Arabidopsis. *THE PLANT CELL ONLINE* **18**, 3399–3414.

Hanano, S. and Goto, K. (2011). Arabidopsis TERMINAL FLOWER1 Is Involved in the Regulation of Flowering Time and Inflorescence Development through Transcriptional Repression. *THE PLANT CELL ONLINE*.

Hanzawa, Y., Money, T. and Bradley, D. (2005). A single amino acid converts a repressor to an activator of flowering. *Proc. Natl. Acad. Sci. U.S.A.* **102**, 7748–7753.

Harberd, N. P. (2003). Relieving DELLA Restraint. *Science* **299**, 1853–1854.

Hayama, R., Agashe, B., Luley, E., King, R. and Coupland, G. (2007). A Circadian Rhythm Set by Dusk Determines the Expression of FT Homologs and the Short-Day Photoperiodic Flowering Response in Pharbitis. *THE PLANT CELL ONLINE* **19**, 2988–3000.

Hayama, R., Yokoi, S., Tamaki, S., Yano, M. and Shimamoto, K. (2003). Adaptation of photoperiodic control pathways produces short-day flowering in rice. *Nature* **422**, 719–722.

He, Y. and Amasino, R. M. (2005). Role of chromatin modification in flowering-time control. *Trends in Plant Science* **10**, 30–35.

He, Y., Michaels, S. D. and Amasino, R. M. (2003). Regulation of flowering time by histone acetylation in Arabidopsis. *Science* **302**, 1751–1754.

Hellens, R. P., Edwards, E. A., Leyland, N. R., Bean, S. and Mullineaux, P. M. (2000). pGreen: a versatile and flexible binary Ti vector for Agrobacterium-mediated plant transformation. *Plant Mol. Biol.* **42**, 819–832.

Heo, J. B. and Sung, S. (2011). Vernalization-Mediated Epigenetic Silencing by a Long Intronic Noncoding RNA. *Science* **331**, 76–79.

Herve, C., Dabos, P., Bardet, C., Jauneau, A., Auriac, M. C., Ramboer, A., Lacout, F. and Tremousaygue, D. (2009). In Vivo Interference with AtTCP20 Function Induces Severe Plant Growth Alterations and Deregulates the Expression of Many Genes Important for Development. *PLANT PHYSIOLOGY* **149**, 1462–1477.

Howarth, D. G. and Donoghue, M. J. (2006). Phylogenetic analysis of the "ECE" (CYC/TB1) clade reveals duplications predating the core eudicots. *Proc. Natl. Acad. Sci. U.S.A.* **103**, 9101–9106.

Hsu, C.-Y., Adams, J. P., Kim, H., No, K., Ma, C., Strauss, S. H., Drnevich, J., Vandervelde, L., Ellis, J. D., Rice, B. M., et al. (2011). FLOWERING LOCUS T duplication coordinates reproductive and vegetative growth in perennial poplar. *Proceedings of the National Academy of Sciences* **108**, 10756–10761.

Itoh, H., Nonoue, Y., Yano, M. and Izawa, T. (2010). A pair of floral regulators sets critical day length for Hd3a florigen expression in rice. *Nat Genet* **42**, 635–638.

Jang, S., Marchal, V., Panigrahi, K. C. S., Wenkel, S., Soppe, W., Deng, X.-W., Valverde, F. and Coupland, G. (2008). Arabidopsis COP1 shapes the temporal pattern of CO accumulation conferring a photoperiodic flowering response. *EMBO J.* **27**, 1277–1288.

Jang, S., Torti, S. and Coupland, G. (2009). Genetic and spatial interactions between FT, TSFand SVP during the early stages of floral induction in Arabidopsis. *The Plant Journal* **60**, 614–625.

Johanson, U. (2000). Molecular Analysis of FRIGIDA, a Major Determinant of Natural Variation in Arabidopsis Flowering Time. *Science* **290**, 344–347.

Jung, J.-H., Ju, Y., Seo, P. J., Lee, J.-H. and Park, C.-M. (2011). The SOC1-SPL module integrates photoperiod and gibberellic acid signals to control flowering time in Arabidopsis. *The Plant Journal* **69**, 577–588.

Kardailsky, I. (1999). Activation Tagging of the Floral Inducer FT. *Science* **286**, 1962–1965.

Kaufmann, K., Wellmer, F., Muino, J. M., Ferrier, T., Wuest, S. E., Kumar, V., Serrano-Mislata, A., Madueño, F., Krajewski, P., Meyerowitz, E. M., et al. (2010). Orchestration of Floral Initiation by APETALA1. *Science* **328**, 85–89.

Kim, H.-J., Hyun, Y., Park, J.-Y., Park, M.-J., Park, M.-K., Kim, M. D., Kim, H.-J., Lee, M. H., Moon, J., Lee, I., et al. (2004). A genetic link between cold responses and flowering time through FVE in Arabidopsis thaliana. *Nat Genet* **36**, 167–171.

Kobayashi, Y. (1999). A Pair of Related Genes with Antagonistic Roles in Mediating Flowering Signals. *Science* **286**, 1960–1962.

Kobayashi, Y. and Weigel, D. (2007). Move on up, it's time for change mobile signals controlling photoperiod-dependent flowering. *Genes & Development* **21**, 2371–2384.

Koornneef, M., Hanhart, C. J. and van der Veen, J. H. (1991). A genetic and physiological analysis of late flowering mutants in Arabidopsis thaliana. *Mol. Gen. Genet.* **229**, 57–66.

Kosugi, S. and Ohashi, Y. (1997). PCF1 and PCF2 specifically bind to cis elements in the rice proliferating cell nuclear antigen gene. *Plant Cell* **9**, 1607–1619.

Lang, A. (1952). Physiology of flowering. *Annual Review of Plant Physiology* **3**, 265–306.

Laubinger, S., Marchal, V., Le Gourrierec, J., Gentilhomme, J., Wenkel, S., Adrian, J., Jang, S., Kulajta, C., Braun, H., Coupland, G., et al. (2006). Arabidopsis SPA proteins regulate photoperiodic flowering and interact with the floral inducer CONSTANS to regulate its stability. *Development* **133**, 3213–3222.

Lazaro, A., Valverde, F., Piñeiro, M. and Jarillo, J. A. (2012). The Arabidopsis E3 Ubiquitin Ligase HOS1 Negatively Regulates CONSTANS Abundance in the Photoperiodic Control of Flowering. *THE PLANT CELL ONLINE* **24**, 982–999.

Lee, I. I., Aukerman, M. J. M., Gore, S. L. S., Lohman, K. N. K., Michaels, S. D. S., Weaver, L. M. L., John, M. C. M., Feldmann, K. A. K. and Amasino, R. M. R. (1993). Isolation of LUMINIDEPENDENS: a gene involved in the control of flowering time in Arabidopsis. *Plant Cell* **6**, 75–83.

Lee, J. H., Yoo, S. J., Park, S. H., Hwang, I., Lee, J. S. and Ahn, J. H. (2007). Role of SVP in the control of flowering time by ambient temperature in Arabidopsis. *Genes & Development* **21**, 397–402.

Lee, J., Oh, M., Park, H. and Lee, I. (2008). SOC1 translocated to the nucleus by interaction with AGL24 directly regulates LEAFY. *The Plant Journal* **55**, 832–843.

Li, C., Potuschak, T., Colón-Carmona, A., Gutiérrez, R. A. and Doerner, P. (2005). Arabidopsis TCP20 links regulation of growth and cell division control pathways. *Proc. Natl. Acad. Sci. U.S.A.* **102**, 12978–12983.

Li, D., Liu, C., Shen, L., Wu, Y., Chen, H., Robertson, M., Helliwell, C. A., Ito, T., Meyerowitz, E. and Yu, H. (2008). A Repressor Complex Governs the Integration of Flowering Signals in Arabidopsis. *Developmental Cell* **15**, 110–120.

Liljegren, S. J., Gustafson-Brown, C., Pinyopich, A., Ditta, G. S. and Yanofsky, M. F. (1999). Interactions among APETALA1, LEAFY, and TERMINAL FLOWER1 specify meristem fate. *Plant Cell* **11**, 1007–1018.

Liu, H., Yu, X., Li, K., Klejnot, J., Yang, H., Lisiero, D. and Lin, C. (2008a). Photoexcited CRY2 interacts with CIB1 to regulate transcription and floral initiation in Arabidopsis. *Science* **322**, 1535–1539.

Liu, L. J., Zhang, Y. C., Li, Q. H., Sang, Y., Mao, J., Lian, H. L., Wang, L. and Yang, H. Q. (2008b). COP1-Mediated Ubiquitination of CONSTANS Is Implicated in Cryptochrome Regulation of Flowering in Arabidopsis. *THE PLANT CELL ONLINE* **20**, 292–306.

Liu, L., Liu, C., Hou, X., Xi, W., Shen, L., Tao, Z., Wang, Y. and Yu, H. (2012). FTIP1 is an essential regulator required for florigen transport. *PLoS Biol* **10**, e1001313.

Lorenz, K., Lohse, M. J. and Quitterer, U. (2003). Protein kinase C switches the Raf kinase inhibitor from Raf-1 to GRK-2. *Nature* **426**, 574–579.

Luo, D., Carpenter, R., Vincent, C., Copsey, L. and Coen, E. (1996). Origin of floral asymmetry in Antirrhinum. *Nature* **383**, 794–799.

Macknight, R. (2002). Functional Significance of the Alternative Transcript Processing of the Arabidopsis Floral Promoter FCA. *THE PLANT CELL ONLINE* **14**, 877–888.

Macknight, R., Bancroft, I., Page, T., Lister, C., Schmidt, R., Love, K., Westphal, L., Murphy, G., Sherson, S., Cobbett, C., et al. (1997). FCA, a gene controlling flowering time in Arabidopsis, encodes a protein containing RNA-binding domains. *Cell* **89**, 737–745.

Martín-Trillo, M. and Cubas, P. (2010). TCP genes: a family snapshot ten years later. *Trends in Plant Science* **15**, 31–39.

Mathieu, J., Warthmann, N., Küttner, F. and Schmid, M. (2007). Export of FT Protein from Phloem Companion Cells Is Sufficient for Floral Induction in Arabidopsis. *Current Biology* **17**, 1055–1060.

Mathieu, J., Yant, L. J., Mürdter, F., Küttner, F. and Schmid, M. (2009). Repression of flowering by the miR172 target SMZ. *PLoS Biol* **7**, e1000148.

Michaels, S. D. and Amasino, R. M. (1999). FLOWERING LOCUS C encodes a novel MADS domain protein that acts as a repressor of flowering. *Plant Cell* **11**, 949–956.

Michaels, S. D. and Amasino, R. M. (2001). Loss of FLOWERING LOCUS C activity eliminates the late-flowering phenotype of FRIGIDA and autonomous pathway mutations but not responsiveness to vernalization. *Plant Cell* **13**, 935–941.

Mimida, N., Kidou, S. I., Iwanami, H., Moriya, S., Abe, K., Voogd, C., Varkonyi-Gasic, E. and Kotoda, N. (2011). Apple FLOWERING LOCUS T proteins interact with transcription factors implicated in cell growth and organ development. *Tree Physiology*.

Navarro, C., Abelenda, J. A., Cruz-Oró, E., Cuéllar, C. A., Tamaki, S., Silva, J., Shimamoto, K. and Prat, S. (2011). Control of flowering and storage organ formation in potato by FLOWERING LOCUS T. *Nature* 1–5.

Ossowski, S., Schwab, R. and Weigel, D. (2008). Gene silencing in plants using artificial microRNAs and other small RNAs. *The Plant Journal* **53**, 674–690.

Palatnik, J. F., Allen, E., Wu, X., Schommer, C., Schwab, R., Carrington, J. C. and Weigel, D. (2003). Control of leaf morphogenesis by microRNAs. *Nature* **425**, 257–263.

Perry, A. C., Hall, L., Bell, A. E. and Jones, R. (1994). Sequence analysis of a mammalian phospholipid-binding protein from testis and epididymis and its distribution between spermatozoa and extracellular secretions. *Biochem. J.* **301 (Pt 1)**, 235–242.

Pin, P. A., Benlloch, R., Bonnet, D., Wremerth-Weich, E., Kraft, T., Gielen, J. J. L. and Nilsson, O. (2010). An Antagonistic Pair of FT Homologs Mediates the Control of Flowering Time in Sugar Beet. *Science* **330**, 1397–1400.

Pin, P. A., Zhang, W., Vogt, S. H., Dally, N., Büttner, B., Schulze-Buxloh, G., Jelly, N. S., Chia, T. Y. P., Mutasa-Göttgens, E. S., Dohm, J. C., et al. (2012). The Role of a Pseudo-Response Regulator Gene in Life Cycle Adaptation and Domestication of Beet. *Current Biology* **22**, 1095–1101.

Pnueli, L., Gutfinger, T., Hareven, D., Ben-Naim, O., Ron, N., Adir, N. and Lifschitz, E. (2001). Tomato SP-interacting proteins define a conserved signaling system that regulates shoot architecture and flowering. *Plant Cell* **13**, 2687–2702.

Piskacek, S., Gregor, M., Nemethova, M., Grabner, M., Kovarik, P. and Piskacek, M. (2007). Nine-amino-acid transactivation domain: Establishment and prediction utilities. Genomics 89, 756–768.

Purugganan, M. D. and Fuller, D. Q. (2009). The nature of selection during plant domestication. *Nature* **457**, 843–848.

Putterill, J., Robson, F., Lee, K., Simon, R. and Coupland, G. (1995). The CONSTANS gene of Arabidopsis promotes flowering and encodes a protein showing similarities to zinc finger transcription factors. *Cell* **80**, 847–857.

Quesada, V., Macknight, R., Dean, C. and Simpson, G. G. (2003). Autoregulation of FCA pre-mRNA processing controls Arabidopsis flowering time. *EMBO J.* **22**, 3142–3152.

Ratcliffe, O. J., Amaya, I., Vincent, C. A., Rothstein, S., Carpenter, R., Coen, E. S. and Bradley, D. J. (1998). A common mechanism controls the life cycle and architecture of plants. *Development* **125**, 1609–1615.

Ratcliffe, O. J., Bradley, D. J. and Coen, E. S. (1999). Separation of shoot and floral identity in Arabidopsis. *Development* **126**, 1109–1120.

Razem, F. A., El-Kereamy, A., Abrams, S. R. and Hill, R. D. (2006). The RNA-binding protein FCA is an abscisic acid receptor. *Nature* **439**, 290–294.

Sambrook, J. and Russell, D. W. D. W. (2001). *Molecular Cloning*. CSHL Press.

Sawa, M., Nusinow, D. A., Kay, S. A. and IMAIZUMI, T. (2007). FKF1 and GIGANTEA Complex Formation Is Required for Day-Length Measurement in Arabidopsis. *Science* **318**, 261–265.

Schoentgen, F., Saccoccio, F., Jollès, J., Bernier, I. and Jollès, P. (1987). Complete amino acid sequence of a basic 21-kDa protein from bovine brain cytosol. *Eur. J. Biochem.* **166**, 333–338.

Schomburg, F. M., Patton, D. A., Meinke, D. W. and Amasino, R. M. (2001). FPA, a gene involved in floral induction in Arabidopsis, encodes a protein containing RNA-recognition motifs. *Plant Cell* **13**, 1427–1436.

Schwechheimer, C. and Willige, B. C. (2009). Shedding light on gibberellic acid signalling. *Curr. Opin. Plant Biol.* **12**, 57–62.

Seddiqi, N., Bollengier, F., Alliel, P. M., Périn, J. P., Bonnet, F., Bucquoy, S., Jollès, P. and Schoentgen, F. (1994). Amino acid sequence of the Homo sapiens brain 21-23-kDa protein (neuropolypeptide h3), comparison with its counterparts from Rattus norvegicus and Bos taurus species, and expression of its mRNA in different tissues. *J. Mol. Evol.* **39**, 655–660.

Serre, L., Vallée, B., Bureaud, N., Schoentgen, F. and Zelwer, C. (1998). Crystal structure of the phosphatidylethanolamine-binding protein from bovine brain: a novel structural class of phospholipid-binding proteins. *Structure* **6**, 1255–1265.

Shannon, S. and Meeks-Wagner, D. R. (1991). A Mutation in the Arabidopsis TFL1 Gene Affects Inflorescence Meristem Development. *THE PLANT CELL ONLINE* **3**, 877–892.

Shannon, S. and Meeks-Wagner, D. R. (1993). Genetic Interactions That Regulate Inflorescence Development in Arabidopsis. *THE PLANT CELL ONLINE* **5**, 639–655.

Sheldon, C. C., Rouse, D. T., Finnegan, E. J., Peacock, W. J. and Dennis, E. S. (2000). The molecular basis of vernalization: the central role of FLOWERING LOCUS C (FLC). *Proc. Natl. Acad. Sci. U.S.A.* **97**, 3753–3758.

Simpson, G. G., Dijkwel, P. P., Quesada, V., Henderson, I. and Dean, C. (2003). FY is an RNA 3' end-processing factor that interacts with FCA to control the Arabidopsis floral transition. *Cell* **113**, 777–787.

Sohn, E. J., Rojas-Pierce, M., Pan, S., Carter, C., Serrano-Mislata, A., Madueño, F., Rojo, E., Surpin, M. and Raikhel, N. V. (2007). The shoot meristem identity gene TFL1 is involved in flower development and trafficking to the protein storage vacuole. *Proc. Natl. Acad. Sci. U.S.A.* **104**, 18801–18806.

Sung, S. and Amasino, R. M. (2004). Vernalization in Arabidopsis thaliana is mediated by the PHD finger protein VIN3. *Nature* **427**, 159–164.

Swiezewski, S., Liu, F., Magusin, A. and Dean, C. (2009). Cold-induced silencing by long antisense transcripts of an Arabidopsis Polycomb target. *Nature* **462**, 799–802.

Taoka, K.-I., Ohki, I., Tsuji, H., Furuita, K., Hayashi, K., Yanase, T., Yamaguchi, M., Nakashima, C., Purwestri, Y. A., Tamaki, S., et al. (2011). 14-3-3 proteins act as intracellular receptors for rice Hd3a florigen. *Nature* 1–7.

Tavel, L., Jaquillard, L., Karsisiotis, A. I., Saab, F., Jouvensal, L., Brans, A., Delmas, A. F., Schoentgen, F., Cadene, M. and Damblon, C. (2012). Ligand Binding Study of Human PEBP1/

RKIP: Interaction with Nucleotides and Raf-1 Peptides Evidenced by NMR and Mass Spectrometry. *PLoS ONE* **7**, e36187.

Turner, A. (2005). The Pseudo-Response Regulator Ppd-H1 Provides Adaptation to Photoperiod in Barley. *Science* **310**, 1031–1034.

Valverde, F. (2004). Photoreceptor Regulation of CONSTANS Protein in Photoperiodic Flowering. *Science* **303**, 1003–1006.

Vandepoele, K., Casneuf, T. and Van de Peer, Y. (2006). Identification of novel regulatory modules in dicotyledonous plants using expression data and comparative genomics. *Genome Biol.* **7**, R103.

Voinnet, O., Rivas, S., Mestre, P. and Baulcombe, D. (2003). An enhanced transient expression system in plants based on suppression of gene silencing by the p19 protein of tomato bushy stunt virus. *Plant J.* **33**, 949–956.

Wang, J.-W., Czech, B. and Weigel, D. (2009). miR156-Regulated SPL Transcription Factors Define an Endogenous Flowering Pathway in Arabidopsis thaliana. *Cell* **138**, 738–749.

Weigel, J. G. D. and Glazebrook, J. (2002). *Arabidopsis: A Laboratory Manual*. CSHL Press.

Wigge, P. A., Kim, M. C., Jaeger, K. E., Busch, W., Schmid, M., Lohmann, J. U. and Weigel, D. (2005). Integration of spatial and temporal information during floral induction in Arabidopsis. *Science* **309**, 1056–1059.

Xue, W., Xing, Y., Weng, X., Zhao, Y., Tang, W., Wang, L., Zhou, H., Yu, S., Xu, C., Li, X., et al. (2008). Natural variation in Ghd7 is an important regulator of heading date and yield potential in rice. *Nat Genet* **40**, 761–767.

Yamaguchi, A., Wu, M.-F., Yang, L., Wu, G., Poethig, R. S. and Wagner, D. (2009). The MicroRNA-Regulated SBP-Box Transcription Factor SPL3 Is a Direct Upstream Activator of LEAFY, FRUITFULL, and APETALA1. *Developmental Cell* **17**, 268–278.

Yan, L., Loukoianov, A., Blechl, A., Tranquilli, G., Ramakrishna, W., SanMiguel, P., Bennetzen, J. L., Echenique, V. and Dubcovsky, J. (2004). The wheat VRN2 gene is a flowering repressor down-regulated by vernalization. *Science* **303**, 1640–1644.

Yan, L., Loukoianov, A., Tranquilli, G., Helguera, M., Fahima, T. and Dubcovsky, J. (2003). Positional cloning of the wheat vernalization gene VRN1. *Proc. Natl. Acad. Sci. U.S.A.* **100**, 6263–6268.

Yeung, K. C., Seitz, T., Li, S., Janosch, P., McFerran, B., Kaiser, C., Fee, F., Katsanakis, K. D., Rose, D. W., Mischak, H., et al. (1999). Suppression of Raf-1 kinase activity and MAP kinase signalling by RKIP. *Nature* **401**, 173–177.

Yu, S., Galvao, V. C., Zhang, Y. C., Horrer, D., Zhang, T. Q., Hao, Y. H., Feng, Y. Q., Wang, S., Schmid, M. and Wang, J. W. (2012). Gibberellin Regulates the Arabidopsis Floral Transition through miR156-Targeted SQUAMOSA PROMOTER BINDING-LIKE Transcription Factors. *THE PLANT CELL ONLINE* **24**, 3320–3332.

Yuceer, C., Land, S. B., Kubiske, M. E. and Harkess, R. L. (2003). Shoot morphogenesis associated with flowering in Populus deltoides (Salicaceae). *Am. J. Bot.* **90**, 196–206.

Zuo, Z., Liu, H., Bin Liu, Liu, X. and Lin, C. (2011). Blue Light-Dependent Interaction of CRY2 with SPA1 Regulates COP1 activity and Floral Initiation in Arabidopsis. *Current Biology* **21**, 841–847.

Supplementary Material

SUPPLEMENTARY FIGURES

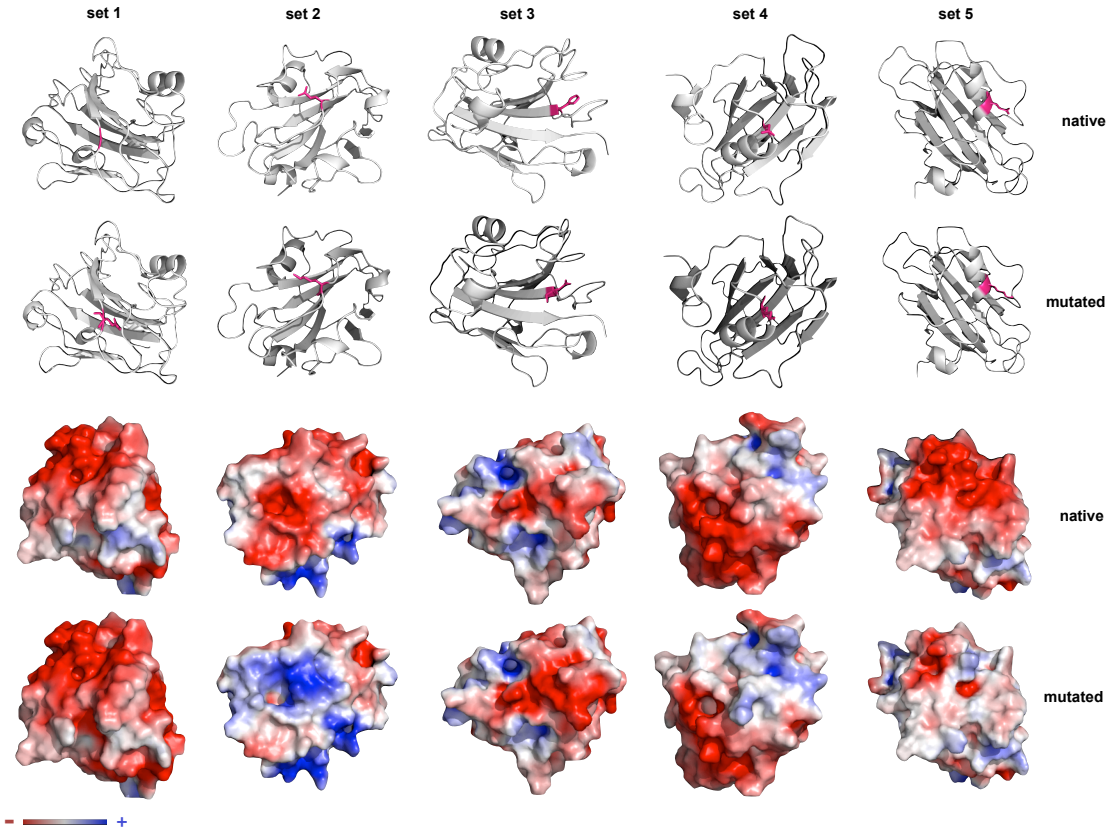

Supplementary Figure 1. Cartoon representation of the native and mutated FT structures and their electrostatic maps from different angles of view. **(A)** 3D modeling of five of the ultraconserved residues (magenta) found in the FT protein and **(B)** their corresponding electrostatic maps calculated by APBS tool showing the surface charge change upon different point mutations are introduced. In this set, (from left to right) mutations from set 2 and 5 were selected for the site-directed mutagenesis due to their profound effect on reverting and neutralizing the surrounding negative charge respectively.

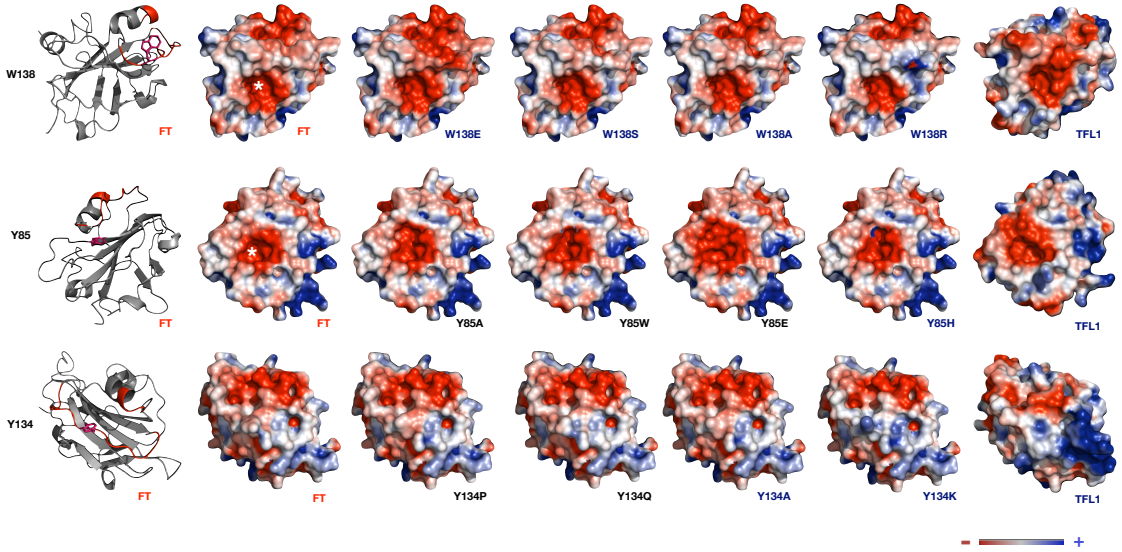

Supplementary Figure 2. Effect of point mutations showing potent effect on conferring mFT floral repressing and I1* forming ability but independent of surface charge change. Electrostatic maps of TFL1 aligned in the same orientations in each case are shown for comparison. Negative and positive electrostatic potential are represented by red and blue color on the electrostatic map respectively. Labels of native and mutated FT retain FT floral promoting and terminal flower forming ability are in red, while those showing floral repressing and I1* forming ability if TFL1 are in blue. Labels of loss-of-function or almost loss-of-function molecules are in black color. Positions of the residues concerned in each case are highlighted in pink, while the invariant loop and FT sequence signature respectively encoded by exon 4B and 4C were highlighted in red in the cartoon structure of FT. Position of the canonical ABP is marked by asterisk on the electrostatic maps at each orientation of native FT (if any).

SUPPLEMENTARY TABLES

Supplemental Table 1. Flowering Time Comparison of Plants Transformed with *FT* Variants Driven by 35S, SUC2 and FD Promoters

mFT *	Total no. of leaves *			I1* §			TF §			n		
	35S †	SUC2 †	FD †	35S	SUC2	FD	35S	SUC2	FD	35S	SUC2	FD
Y85H	24.4±7.0 (15-37)[a]	19.4±5.0 (13-31)	20.5±4.4 (14-27)	Y ¶	Y ¶	Y ¶	N	N	N	19	20	20
Y85W	11.0±2.9 (7-16)	12.4±5.1 (7-18)	12.6±2.1 (9-15)	N	N	N	N	N	N	20	14	20
Y85A	28.5±4.7 (22-32)	27.7±8.0 (17-35)	32.4±8.6 (22-40)	N!	N	N	N	N	N	19	15	18
D71N	4.4±0.5 (4-5)	4.3±0.6 (3-6)	4.6±1.4 (3-7)	N	N	N	Y	Y	Y	20	19	20
D71A	4.0±0.0 (4)	4.1±1.5 (1-4)	4.0±0.0 (4)	N	N	N	Y	Y	Y	19	13	10
P72A	3.9±0.6 (3-5)	3.5±1.3 (3-6)	3.3±1.0 (3-7)	N	N	N	Y	Y	Y	20	14	14
D73A	42.4±8.3 (28-51)	43.3±9.3 (35-56)[b]	39.1±8.1 (30-48)	N	N	N	N	N	N	20	12	14
D73K	43.9±10.5 (29-57)	46.8±9.3 (38-56)[b]	37.4±7.3 (30-46)	N	N	N	N	N	N	9	11	10
P75A	4.5±0.6 (3-5)	5.5±1.3 (4-8)	4.6±0.4 (4-6)	N	N	N	N	N	N	20	9	15
P75L	4.2±0.6 (3-5)	5.2±1.2 (3-7)	5.7±1.8 (3-9)	N	N	N	Y	Y	Y	20	13	13
E146K	5.5±0.8 (4-7)	6.0±3.0 (3-10)	5.9±3.2 (4-11)	N	N	N	Y	Y	Y	19	20	18
E146A	5.7±0.8 (5-8)	6.6±2.1 (4-11)	5.6±2.2 (3-9)	N	N	N	Y	Y	Y	20	19	18
R62D	3.6±0.5 (3-4)	3.7±0.7 (3-5)	4.3±0.9 (2-5)	N	N	N	Y	Y	Y	19	20	14
R130G	4.7±0.7 (4-6)	4.7±2.2 (6-9)	5.1±1.3 (4-8)	N	N	N	N	N	N	19	20	20
R130E	4.6±0.5 (4-5)	4.8±1.7 (3-8)	4.4±2.1 (3-8)	N	N	N	N	N	N	20	12	17
R130A	3.5±0.6 (2-4)	4.5±1.3 (3-6)	4.5±0.5 (3-5)	N	N	N	Y	Y	Y	20	20	15
I150E	6.1±0.9 (4-8)	4.9±0.7 (4-6)	6.2±1.2 (5-8)	N	N	N	Y	Y	Y	20	19	20
Y151N	5.8±1.4 (4-10)	5.1±1.4 (4-9)	6.0±2.2 (5-9)	N	N	N	Y	Y	Y	19	11	8
E109K	48.6±9.7 (32-70)	46.6±7.3 (33-71)	43.6±6.5 (33-69)[c]	Y	Y	Y	N	N	N	20	20	20
E109M	38.9±4.5 (29-45)	37.0±5.7 (30-45)	37.5±7.5 (17-48)	Y	Y	Y	N	N	N	19	2	19
E109A	44.5±5.3 (33-53)	41.1±5.0 (35-48)	40.2±6.8 (33-48)	Y	Y	Y	N	N	N	20	12	19
E109D	5.4±1.4 (4-9)	4.4±2.1 (3-8)	5.6±1.9 (3-8)	N	N	N	Y	Y	Y	18	16	12
Q140D	6.0±1.3 (4-9)	6.5±2.3 (5-11)	7.1±1.9 (4-9)	N	N	N	Y	Y	Y	15	19	19
Q140K	52.2±8.9 (35-75)	55.8±6.3 (39-66)[b]	50.8±7.0 (38-71)	Y	Y	Y	N	N	N	20	19	20
Q140A	6.2±0.7 (5-7)	6.6±2.6 (4-11)	5.7±2.3 (5-12)	N	N	N	Y	Y	Y	20	19	19
Q140R	39.6±7.0 (22-52)[a]	32.8±6.9 (21-68)	36.5±8.4 (26-57)	Y	Y	Y	N	N	N	16	20	18
N152K	56.8±7.7 (41-70)[aa]	49.6±5.4 (38-58)	50.5±5.4 (40-61)[cc]	Y	Y	Y	N	N	N	19	19	20
N152D	5.9±1.0 (5-8)	6.0±1.6 (4-8)	6.2±2.1 (4-9)	N	N	N	Y	Y	Y	19	20	20
N152A	9.1±1.5 (7-11)	8.9±1.9 (5-13)	9.4±2.5 (5-12)	N	N	N	Y	Y	Y	9	16	19

N152Y	3.9±1.2 (2-7)	4.1±0.8 (3-6)	3.9±0.9 (3-6)	N	N	N	Y	Y	Y	16	20	13
L128K	30.0±7.6 (21-47)	29.0±3.6 (25-32)	27.7±3.7 (11-22)^{c}	Y	Y	Y	N	N	N	9	13	19
L128A	19.7±4.9 (13-28)	20.7±7.3 (11-30)	18.9±4.6 (12-25)	N	N	N	N	N	N	15	20	10
L128F	22.3±5.7 (14-30)	19.7±4.3 (13-26)	18.6±6.8 (13-27)	N	N	N	N	N	N	9	18	20
L128I	10.2±2.7 (6-14)	8.5±1.6 (6-12)	9.6±2.6 (7-15)	N	N	N	Y	Y	Y	9	20	20
W138E	65.6±6.0 (49-78)	62.5±4.9 (42-59)	60.1±9.0 (37-72)^{c}	Y	Y	Y	N	N	N	19	19	19
W138A	45.5±11.1 (29-64)	46.6±8.2 (23-50)	46.0±6.9 (21-55)	Y	Y	Y	N	N	N	18	20	16
W138S	55.8±5.4 (45-62)	53.6±7.4 (41-65)^{bb}	61.3±1.5 (60-63)^{cc}	Y	Y	Y	N	N	N	9	20	13
W138R	50.5±4.9 (42-59)	49.5±5.4 (39-59)	47.9±6.1 (41-59)	Y	Y	Y	N	N	N	19	20	20
Y134A	40.5±8.4 (27-55)^{a}	37.9±7.6 (23-52)	39.5±6.9 (29-57)	Y	Y	Y	N	N	N	20	20	11
Y134P	10.6±4.8 (5-14)	9.4±3.2 (5-16)	11.1±4.2 (6-15)	N	N	N	N	N	N	20	20	20
Y134K	42.1±8.5 (29-57)	39.8±7.6 (30-49)	41.6±7.5 (24-58)	Y	Y	Y	N	N	N	20	18	13
Y134Q	9.1±3.4 (5-18)	9.4±2.1 (6-13)	10.3±3.0 (6-12)	N	N	N	N	N	N	19	14	17
G137A	4.3±0.7 (3-5)	4.7±1.2 (3-8)	4.6±1.6 (3-8)	N	N	N	Y	Y	Y	19	20	14
G137E	5.7±0.8 (4-7)	5.7±0.8 (4-7)	6.1±2.9 (5-12)	N	N	N	Y	Y	Y	14	18	16
G137R	4.7±1.2 (3-8)	5.1±1.0 (3-9)	5.6±0.8 (3-6)	N	N	N	Y	Y	Y	20	15	13
G137W	6.9±1.4 (5-10)	7.4±1.8 (4-12)	7.3±2.0 (5-11)	N	N	N	Y	Y	Y	14	17	20

.* Indicators of flowering time and shown as average ± standard derivation (range). All transformants involved were grown under SDs as indicated. **†** 35S, constitutive cauliflower mosaic virus 35S promoter driven; SUC2, phloem companion cell-specific SUC promoter driven; FD, shoot apical meristem-specific promoter driven. Symbol a, b, and c indicates the statistical significance of difference in comparison between 35S and SUC2, SUC2 and FD, and FD and 35S respectively using two-tailed multiple Student *t*-test with Bonferroni correction. Single, double and triple symbols represent $P < 0.05$, $P < 0.01$, and $P < 0.001$ respectively. No symbol means that there was no statistically significant difference among indicated genotypes in each experiment (Student's *t*-test, $P \geq 0.05$). Statistical tests were done on the total number of leaves. § I1*, interim developmental phase I1*; TF, terminal flower. ¶ Only 1-2 shoots corresponding to the I1* phase can be occasionally found in the Y85 mutated transformants.

Mutations *	Total no. of leaves †	I1* §	TF §	n
K29E	4.0±0.6 (3-5)	N	Y	20
K29R	4.2±1.0 (3-7)	N	Y	16
R44A	4.0±0.9 (3-7)	N	Y	20
R44F	4.1±0.3 (4-5)	N	Y	20
P45A	3.7±0.5 (3-4)	N	Y	19
P45F	3.7±0.6 (3-4)	N	Y	13
S46A	6.0±2.4 (4-11)	N	N	12
K51P	3.9±0.6 (3-5)	Y	Y	18
K51A	3.7±0.5 (3-4)	Y	Y	20
K51R	4.5±0.8 (3-7)	Y	Y	20
P52A	3.7±0.5 (3-4)	Y	Y	20
P52E	59.3±2.8 (56-63)	N	N	16
R53I	3.4±0.5 (3-4)	Y	Y	19

Supplementary Table 2. Flowering time of overexpressors of *FT* mutated at cationic pocket center (K29) and cationic groove propagated from R44 to R53. * Each mutation has been tested under the control of the 35S, SUC and FD promoters. No statistically significant difference were found between the datassets and only dataset of 35S promoter was shown. † Indicators of flowering time and shown as average ± standard derivation (range). All transformants involved were grown under SD as indicated. § I1*, interim developmental phase I1*; TF, terminal flower.

Query *	Mammalian †	Yeast †	Viral †	Sequence of highly consensus matches	Sequence of other consensus matches
TCP1	x	x	oo	GHMVSAVPE	
TCP2	o	x	oo, o	STALQFYDL	TSFTDLLNS, QTLTTVAAN, TSFTDLLNS
TCP3	x	x	oo	PTAIQFYDV, SKAVDWLIT, SAIDDLAQL	
TCP4	x	x	o	TSIDELAEL	
TCP5	x	x	oo, o	PTAIQLYDL, SKVIDWLLE, DWLLEAAKD	TVAISNVAA, PAMSSLFPT
TCP6	x	x	x		
TCP7	x	x	x		
TCP8	x	x	oo	AALNSAYSR	
TCP9	x	x	o		PSFSMSLAP
TCP10	x	x	oo, o	EDAMKTFFP	PSMMTLLNS
TCP11	o	x	oo, o	SNWVDVAAD, NWVDVAADD	ETIEWLLSQ, ETIEWLLSQ
TCP12	x	x	oo	DVAANVVES	
TCP13	x	x	oo, o	PTAIQLYDL, SKAVDWLLD, DWLLDAAKE	TTIQSLFPS, STLYSLLHG
TCP14	oo	oo	oo	SSILNVIMD, SILNVIMDG	
TCP15	x	x	oo	AALNAAYRP	
TCP16	x	x	x		
TCP17	oo	x	oo, o	GNVTVAFSN, MTAIQVYDL, SKVIDWLLE, GNVTVAFSN	ETMSSLFPT
TCP18	o	x	oo,o	CELASMWTV	SSINDILIH, SSINDILIH
TCP19	x	x	x		
TCP20	x	x	oo,o	DDAASAVVS, DAASAVVSD	SALASSAAT, ALASSAATS
TCP21	x	x	o		GQVWSFATG
TCP22	x	x	x		
TCP23	x	x	x		
TCP24	x	x	oo, o	ATAIQFYDL, SKAVEWLIN, EWLINAASD	SSFTQLLTG
FT	x	x	x		
TFL1	x	x	oo	GDVLDFFTP	
FD	o	x	oo, o	SIFQDFLKG, TTVTVLYSS, NELELEVAH	NELELEVAH

Supplementary Table 3. Prediction of 9-amino acid transactivation domain (9aa TAD) of TCP family members, FT, TFL1 and FD. The computational search for the 9aa TAD was performed using the online resources from National EMBnet-Node Austria at http://www.at.embnet.org/toolbox/9aatad/ (Piskacek et al., 2007) * Name of TCP members shown to bound with FT via region BPP *in planta* are in red color. **†** Double-circles indicates highly consensus matches found; single-circles indicates other weaker consensus matches found; cross indicates no matches was found. 9aa TAD used in this prediction program includes Gal4, Pho4, Gln3, Gcn4 and Rtg3 (from yeast), HSF (from plant), p53, E2A, HSF, KLF2, NF-IL6, NF- k B, NFAT1 (from mammals) and VP16, EBNA2 (from viruses).

LIST OF OLIGOS

Oligo List 1. Oligos used for the random mutagenesis.

Oligo	Purpose	Target	Forward/Reverse	Sequence (5'-3')	bp
G-20760	Cloning	35S promoter	F	GCGGCGGGGCCCATTCGGTCCCCAGATTAGCCT	33
G-20761	Cloning	35S promoter	R	GCGGCGCCGCGGAGCTCGTCCCCCGTGTTCT	31
G-20762	Cloning	rbcs terminator	F	GCGGCGACTAGTAGCTTTCGTTCGTATCATCGG	33
G-20763	Cloning	rbcs terminator	R	GCGGCGCTGCAGCGATTGATGCATGTTGTCAA	32
G-22312	Cloning	mCitrine	F	CGCCGCGAATTCAAGCTTTCTAGAGCGGCCGCACCCGGGCTCGAGGTGAGCAAGGGCGAGGAG	63
G-22313	Cloning	mCitrine	R	CGCCGCACTAGTTTACTTGTACAGCTCGTCCATGCCG	37
G-20652	Cloning	FT CDS	F	ATGTACCCATACGATGTTCCCGATTACGCTTCTATAAATATAAGAGACCCT	51
G-20653	Cloning	FT CDS	R	ACTTCCTGAACCACTCCCACTTCCAAGTCTTCTTCCTCCGCAGC	44
G-22376	Mutagenesis/ sequencing	FT CDS	F	CGCCGCAAGCTTATGTACCCATACGATGTTCCCGATTACGCT	42
G-22377	Mutagenesis/ sequencing	FT CDS	R	CGCCGCCTCGAGACTTCCTGAACCACTCCCACTTCC	36

Oligo List 2. Oligos used for the site-directed mutagenesis.

Oligo	Purpose	Target	FT mutation	Forward/Reverse	Sequence (5'-3')	bp
G-25689	mutagenesis	FT CDS	-	F	CGCCGCAAGCTTATGTCTATAAATATAAGAGAC	33
G-25690	mutagenesis	FT CDS	-	R	CGCCGCCTCGAGCTAAAGTCTTCTTCCTCCGCA	33
MF1	mutagenesis	FT CDS	T27K	F	AGATCAATCAAGCTAAAGGTT	21
MR1	mutagenesis	FT CDS	T27K	R	AACCTTTAGCTTGATTGATCT	21
MF2	mutagenesis	FT CDS	G57H	F	GTTGAGATTCACGGAGAAGAC	21
MR2	mutagenesis	FT CDS	G57H	R	GTCTTCTCCGTGAATCTCAAC	21
MF3	mutagenesis	FT CDS	N79D	F	AGTCCTAGCGATCCTCACCTC	21
MR3	mutagenesis	FT CDS	N79D	R	GAGGTGAGGATCGCTAGGACT	21
MF4	mutagenesis	FT CDS	H81Y	F	AGCAACCCTTATCTCCGAGAA	21
MR4	mutagenesis	FT CDS	H81Y	R	TTCTCGGAGATAAGGGTTGCT	21
MF5	mutagenesis	FT CDS	Y85W	F	CTCCGAGAATGGCTCCATTGG	21
MR5	mutagenesis	FT CDS	Y85W	R	CCAATGGAGCCATTCTCGGAG	21
MF6	mutagenesis	FT CDS	G98D	F	GCTACAACTGATACAACCTTT	21
MR6	mutagenesis	FT CDS	G98D	R	AAAGGTTGTATCAGTTGTAGC	21
MF7	mutagenesis	FT CDS	Q140D	F	GGGTGGCGCGATAACTTCAAC	21
MR7	mutagenesis	FT CDS	Q140D	R	GTTGAAGTTATCGCGCCACCC	21
MF8	mutagenesis	FT CDS	I150E	F	TTTGCTGAGGAGTACAATCTC	21
MR8	mutagenesis	FT CDS	I150E	R	GAGATTGTACTCCTCAGCAAA	21
MF9	mutagenesis	FT CDS	Y151N	F	GCTGAGATCAACAATCTCGGC	21
MR9	mutagenesis	FT CDS	Y151N	R	GCCGAGATTGTTGATCTCAGC	21
MF10	mutagenesis	FT CDS	N152D	F	GAGATCTACGATCTCGGCCTT	21
MR10	mutagenesis	FT CDS	N152D	R	AAGGCCGAGATCGTAGATCTC	21
MF11	mutagenesis	FT CDS	G171R	F	AGTGGCTGCAGAGGAAGAAGA	21
MR11	mutagenesis	FT CDS	G171R	R	TCTTCTTCCTCTGCAGCCACT	21
MF12	mutagenesis	FT CDS	D71N	F	GTTATGGTGAATCCAGATGTT	21
MR12	mutagenesis	FT CDS	D71N	R	AACATCTGGATTCACCATAAC	21
MF13	mutagenesis	FT CDS	W88R	F	TATCTCCATAGGTTGGTGACT	21
MR13	mutagenesis	FT CDS	W88R	R	AGTCACCAACCTATGGAGATA	21
MF14	mutagenesis	FT CDS	Q127R	F	TTGTTTCGACGCCTTGGCAGG	21
MR14	mutagenesis	FT CDS	Q127R	R	CCTGCCAAGGCGTCGAAACAA	21
MF15	mutagenesis	FT CDS	F142I	F	CGCCAGAACATCAACACTCGC	21
MR15	mutagenesis	FT CDS	F142I	R	GCGAGTGTTGATGTTCTGGCG	21
MF16	mutagenesis	FT CDS	N163D	F	GTTTTCTACGACTGTCAGAGG	21
MR16	mutagenesis	FT CDS	N163D	R	CCTCTGACAGTCGTAGAAAAC	21
MF17	mutagenesis	FT CDS	E167K	F	TGTCAGAGGAAGAGTGGCTGC	21
MR17	mutagenesis	FT CDS	E167K	R	GCAGCCACTCTTCCTCTGACA	21
MF18	mutagenesis	FT CDS	E55V	F	CCAAGAGTTGTAATTGGTGGA	21
MR18	mutagenesis	FT CDS	E55V	R	TCCACCAATTACAACTCTTGG	21
MF19	mutagenesis	FT CDS	F64I	F	CTCAGGAACATCTATACTTTG	21
MR19	mutagenesis	FT CDS	F64I	R	CAAAGTATAGATGTTCCTGAG	21
MF20	mutagenesis	FT CDS	Y85H	F	CTCCGAGAACACCTCCATTGG	21
MR20	mutagenesis	FT CDS	Y85H	R	CCAATGGAGGTGTTCTCGGAG	21

Oligo List 2. Oligos used for the site-directed mutagenesis (continued)

Oligo	Purpose	Target	FT mutation	Forward/Reverse	Sequence (5'-3')	bp
MF21	mutagenesis	FT CDS	E109K	F	GTGTGTTACAAGAATCCAAGT	21
MR21	mutagenesis	FT CDS	E109K	R	ACTTGGATTCTTGTAACACAC	21
MF22	mutagenesis	FT CDS	Q140K	F	GGGTGGCGCAAGAACTTCAAC	21
MR22	mutagenesis	FT CDS	Q140K	R	GTTGAAGTTCTTGCGCCACCC	21
MF23	mutagenesis	FT CDS	E146K	F	AACACTCGCAAGTTTGCTGAG	21
MR23	mutagenesis	FT CDS	E146K	R	CTCAGCAAACTTGCGAGTGTT	21
MF24	mutagenesis	FT CDS	N152K	F	GAGATCTACAAGCTCGGCCTT	21
MR24	mutagenesis	FT CDS	N152K	R	AAGGCCGAGCTTGTAGATCTC	21
MF25	mutagenesis	FT CDS	R35G	F	TATGGCCAAGGGGAGGTGACT	21
MR25	mutagenesis	FT CDS	R35G	R	AGTCACCTCCCCTTGGCCATA	21
MF26	mutagenesis	FT CDS	N39D	F	GAGGTGACTGATGGCTTGGAT	21
MR26	mutagenesis	FT CDS	N39D	R	ATCCAAGCCATCAGTCACCTC	21
MF27	mutagenesis	FT CDS	G40L	F	GTGACTAATCTTTTGGATCTA	21
MR27	mutagenesis	FT CDS	G40L	R	TAGATCCAAAAGATTAGTCAC	21
MF28	mutagenesis	FT CDS	S78N	F	CCAAGTCCTAATAACCCTCAC	21
MR28	mutagenesis	FT CDS	S78N	R	GTGAGGGTTATTAGGACTTGG	21
MF29	mutagenesis	FT CDS	H118R	F	GCAGGAATTCGACGTGTCGTG	21
MR29	mutagenesis	FT CDS	H118R	R	CACGACACGTCGAATTCCTGC	21
MF30	mutagenesis	FT CDS	R119H	F	GGAATTCATCACGTCGTGTTT	21
MR30	mutagenesis	FT CDS	R119H	R	AAACACGACGTGATGAATTCC	21
MF31	mutagenesis	FT CDS	L9H	F	AGAGACCCTCACATAGTAAGC	21
MR31	mutagenesis	FT CDS	L9H	R	GCTTACTATGTGAGGGTCTCT	21
MF32	mutagenesis	FT CDS	G16E	F	AGAGTTGTTGAAGACGTTCTT	21
MR32	mutagenesis	FT CDS	G16E	R	AAGAACGTCTTCAACAACTCT	21
MF33	mutagenesis	FT CDS	D17G	F	GTTGTTGGAGGGGTTCTTGAT	21
MR33	mutagenesis	FT CDS	D17G	R	ATCAAGAACCCCTCCAACAAC	21
MF34	mutagenesis	FT CDS	R24I	F	CCGTTTAATATCTCAATCACT	21
MR34	mutagenesis	FT CDS	R24I	R	AGTGATTGAGATATTAAACGG	21
MF35	mutagenesis	FT CDS	K29E	F	ATCACTCTAGAGGTTACTTAT	21
MR35	mutagenesis	FT CDS	K29E	R	ATAAGTAACCTCTAGAGTGAT	21
MF36	mutagenesis	FT CDS	D42N	F	AATGGCTTGAATCTAAGGCCT	21
MR36	mutagenesis	FT CDS	D42N	R	AGGCCTTAGATTCAAGCCATT	21
MF37	mutagenesis	FT CDS	G58E	F	GAGATTGGTGAGGAAGACCTC	21
MR37	mutagenesis	FT CDS	G58E	R	GAGGTCTTCCTCACCAATCTC	21
MF38	mutagenesis	FT CDS	E59G	F	ATTGGTGGAGGGGACCTCAGG	21
MR38	mutagenesis	FT CDS	E59G	R	CCTGAGGTCCCCTCCACCAAT	21
MF39	mutagenesis	FT CDS	D60N	F	GGTGGAGAAAACCTCAGGAAC	21
MR39	mutagenesis	FT CDS	D60N	R	GTTCCTGAGGTTTTCTCCACC	21
MF40	mutagenesis	FT CDS	S76N	F	GATGTTCCAAATCCTAGCAAC	21
MR40	mutagenesis	FT CDS	S76N	R	GTTGCTAGGATTTGGAACATC	21
MF41	mutagenesis	FT CDS	D92A	F	TTGGTGACTGCCATCCCTGCT	21
MR41	mutagenesis	FT CDS	D92A	R	AGCAGGGATGGCAGTCACCAA	21

Oligo	Purpose	Target	FT mutation	Forward/Reverse	Sequence (5'-3')	bp
MF42	mutagenesis	FT CDS	P94T	F	ACTGATATCACAGCTACAACT	21
MR42	mutagenesis	FT CDS	P94T	R	AGTTGTAGCTGTGATATCAGT	21
MF43	mutagenesis	FT CDS	F101L	F	GGAACAACCCTCGGCAATGAG	21
MR43	mutagenesis	FT CDS	F101L	R	CTCATTGCCGAGGGTTGTTCC	21
MF44	mutagenesis	FT CDS	H118D	F	GCAGGAATTGATCGTGTCGTG	21
MR44	mutagenesis	FT CDS	H118D	R	CACGACACGATCAATTCCTGC	21
MF45	mutagenesis	FT CDS	R130G	F	CAGCTTGGCGGGCAAACAGTG	21
MR45	mutagenesis	FT CDS	R130G	R	CACTGTTTGCCCGCCAAGCTG	21
MF46	mutagenesis	FT CDS	W138E	F	GCACCAGGGGAGCGCCAGAAC	21
MR46	mutagenesis	FT CDS	W138E	R	GTTCTGGCGCTCCCCTGGTGC	21
MF47	mutagenesis	FT CDS	I150F	F	TTTGCTGAGTTTTACAATCTC	21
MR47	mutagenesis	FT CDS	I150F	R	GAGATTGTAAAACTCAGCAAA	21
MF48	mutagenesis	FT CDS	A158D	F	CTTCCCGTGGATGCAGTTTTC	21
MR48	mutagenesis	FT CDS	A158D	R	GAAAACTGCATCCACGGGAAG	21
MF51	mutagenesis	FT CDS	P8A	F	ATAAGAGACGCTCTTATAGTA	21
MR51	mutagenesis	FT CDS	P8A	R	TACTATAAGAGCGTCTCTTAT	21
MF52	mutagenesis	FT CDS	L9A	F	AGAGACCCTGCTATAGTAAGC	21
MR52	mutagenesis	FT CDS	L9A	R	GCTTACTATAGCAGGGTCTCT	21
MF53	mutagenesis	FT CDS	R13A	F	ATAGTAAGCGCTGTTGTTGGA	21
MR53	mutagenesis	FT CDS	R13A	R	TCCAACAACAGCGCTTACTAT	21
MF54	mutagenesis	FT CDS	V14A	F	GTAAGCAGAGCTGTTGGAGAC	21
MR54	mutagenesis	FT CDS	V14A	R	GTCTCCAACAGCTCTGCTTAC	21
MF55	mutagenesis	FT CDS	G16A	F	AGAGTTGTTGCTGACGTTCTT	21
MR55	mutagenesis	FT CDS	G16A	R	AAGAACGTCAGCAACAACTCT	21
MF56	mutagenesis	FT CDS	D17K	F	GTTGTTGGAAAGGTTCTTGAT	21
MR56	mutagenesis	FT CDS	D17K	R	ATCAAGAACCTTTCCAACAAC	21
MF57	mutagenesis	FT CDS	V18A	F	GTTGGAGACGCTCTTGATCCG	21
MR57	mutagenesis	FT CDS	V18A	R	CGGATCAAGAGCGTCTCCAAC	21
MF58	mutagenesis	FT CDS	D20K	F	GACGTTCTTAAGCCGTTTAAT	21
MR58	mutagenesis	FT CDS	D20K	R	ATTAAACGGCTTAAGAACGTC	21
MF59	mutagenesis	FT CDS	D20A	F	GACGTTCTTGCTCCGTTTAAT	21
MR59	mutagenesis	FT CDS	D20A	R	ATTAAACGGAGCAAGAACGTC	21
MF60	mutagenesis	FT CDS	P21M	F	GTTCTTGATATGTTTAATAGA	21
MR60	mutagenesis	FT CDS	P21M	R	TCTATTAAACATATCAAGAAC	21
MF61	mutagenesis	FT CDS	F22A	F	CTTGATCCGGCTAATAGATCA	21
MR61	mutagenesis	FT CDS	F22A	R	TGATCTATTAGCCGGATCAAG	21
MF62	mutagenesis	FT CDS	L28M	F	TCAATCACTATGAAGGTTACT	21
MR62	mutagenesis	FT CDS	L28M	R	AGTAACCTTCATAGTGATTGA	21
MF63	mutagenesis	FT CDS	Y32A	F	AAGGTTACTGCTGGCCAAAGA	21
MR63	mutagenesis	FT CDS	Y32A	R	TCTTTGGCCAGCAGTAACCTT	21
MF64	mutagenesis	FT CDS	G33N	F	GTTACTTATAACCAAAGAGAG	21
MR64	mutagenesis	FT CDS	G33N	R	CTCTCTTTGGTTATAAGTAAC	21

Oligo List 2. Oligos used for the site-directed mutagenesis (continued)

Oligo	Purpose	Target	FT mutation	Forward/Reverse	Sequence (5'-3')	bp
MF65	mutagenesis	FT CDS	R35D	F	TATGGCCAAGACGAGGTGACT	21
MR65	mutagenesis	FT CDS	R35D	R	AGTCACCTCGTCTTGGCCATA	21
MF66	mutagenesis	FT CDS	N39A	F	GAGGTGACTGCTGGCTTGGAT	21
MR66	mutagenesis	FT CDS	N39A	R	ATCCAAGCCAGCAGTCACCTC	21
MF67	mutagenesis	FT CDS	G40A	F	GTGACTAATGCTTTGGATCTA	21
MR67	mutagenesis	FT CDS	G40A	R	TAGATCCAAAGCATTAGTCAC	21
MF68	mutagenesis	FT CDS	L41H	F	ACTAATGGCCACGATCTAAGG	21
MR68	mutagenesis	FT CDS	L41H	R	CCTTAGATCGTGGCCATTAGT	21
MF69	mutagenesis	FT CDS	L41C	F	ACTAATGGCTGCGATCTAAGG	21
MR69	mutagenesis	FT CDS	L41C	R	CCTTAGATCGCAGCCATTAGT	21
MF70	mutagenesis	FT CDS	D42A	F	AATGGCTTGGCTCTAAGGCCT	21
MR70	mutagenesis	FT CDS	D42A	R	AGGCCTTAGAGCCAAGCCATT	21
MF71	mutagenesis	FT CDS	R44F	F	TTGGATCTATTCCCTTCTCAG	21
MR71	mutagenesis	FT CDS	R44F	R	CTGAGAAGGGAATAGATCCAA	21
MF72	mutagenesis	FT CDS	R44A	F	TTGGATCTAGCTCCTTCTCAG	21
MR72	mutagenesis	FT CDS	R44A	R	CTGAGAAGGAGCTAGATCCAA	21
MF73	mutagenesis	FT CDS	P45A	F	GATCTAAGGGCTTCTCAGGTT	21
MR73	mutagenesis	FT CDS	P45A	R	AACCTGAGAAGCCCTTAGATC	21
MF74	mutagenesis	FT CDS	S46A	F	CTAAGGCCTGCTCAGGTTCAA	21
MR74	mutagenesis	FT CDS	S46A	R	TTGAACCTGAGCAGGCCTTAG	21
MF75	mutagenesis	FT CDS	K51A	F	GTTCAAAACGCTCCAAGAGTT	21
MR75	mutagenesis	FT CDS	K51A	R	AACTCTTGGAGCGTTTTGAAC	21
MF76	mutagenesis	FT CDS	K51P	F	GTTCAAAACCCACCAAGAGTT	21
MR76	mutagenesis	FT CDS	K51P	R	AACTCTTGGTGGGTTTTGAAC	21
MF77	mutagenesis	FT CDS	P52A	F	CAAAACAAGGCTAGAGTTGAG	21
MR77	mutagenesis	FT CDS	P52A	R	CTCAACTCTAGCCTTGTTTTG	21
MF78	mutagenesis	FT CDS	R53I	F	AACAAGCCAATCGTTGAGATT	21
MR78	mutagenesis	FT CDS	R53I	R	AATCTCAACGATTGGCTTGTT	21
MF79	mutagenesis	FT CDS	E55N	F	CCAAGAGTTAACATTGGTGGA	21
MR79	mutagenesis	FT CDS	E55N	R	TCCACCAATGTTAACTCTTGG	21
MF80	mutagenesis	FT CDS	E55A	F	CCAAGAGTTGCTATTGGTGGA	21
MR80	mutagenesis	FT CDS	E55A	R	TCCACCAATAGCAACTCTTGG	21
MF81	mutagenesis	FT CDS	G58A	F	GAGATTGGTGCTGAAGACCTC	21
MR81	mutagenesis	FT CDS	G58A	R	GAGGTCTTCAGCACCAATCTC	21
MF82	mutagenesis	FT CDS	D60A	F	GGTGGAGAAGCTCTCAGGAAC	21
MR82	mutagenesis	FT CDS	D60A	R	GTTCCTGAGAGCTTCTCCACC	21
MF83	mutagenesis	FT CDS	D60H	F	GGTGGAGAACACCTCAGGAAC	21
MR83	mutagenesis	FT CDS	D60H	R	GTTCCTGAGGTGTTCTCCACC	21
MF84	mutagenesis	FT CDS	R62D	F	GAAGACCTCGACAACTTCTAT	21
MR84	mutagenesis	FT CDS	R62D	R	ATAGAAGTTGTCGAGGTCTTC	21
MF85	mutagenesis	FT CDS	N63S	F	GACCTCAGGTCCTTCTATACT	21
MR85	mutagenesis	FT CDS	N63S	R	AGTATAGAAGGACCTGAGGTC	21

Oligo	Purpose	Target	FT mutation	Forward/Reverse	Sequence (5'-3')	bp
MF86	mutagenesis	FT CDS	N63E	F	GACCTCAGGGAGTTCTATACT	21
MR86	mutagenesis	FT CDS	N63E	R	AGTATAGAACTCCCTGAGGTC	21
MF87	mutagenesis	FT CDS	Y65A	F	AGGAACTTCGCTACTTTGGTT	21
MR87	mutagenesis	FT CDS	Y65A	R	AACCAAAGTAGCGAAGTTCCT	21
MF88	mutagenesis	FT CDS	M69A	F	ACTTTGGTTGCTGTGGATCCA	21
MR88	mutagenesis	FT CDS	M69A	R	TGGATCCACAGCAACCAAAGT	21
MF89	mutagenesis	FT CDS	D71A	F	GTTATGGTGGCTCCAGATGTT	21
MR89	mutagenesis	FT CDS	D71A	R	AACATCTGGAGCCACCATAAC	21
MF90	mutagenesis	FT CDS	P72A	F	ATGGTGGATGCTGATGTTCCA	21
MR90	mutagenesis	FT CDS	P72A	R	TGGAACATCAGCATCCACCAT	21
MF91	mutagenesis	FT CDS	D73A	F	GTGGATCCAGCTGTTCCAAGT	21
MR91	mutagenesis	FT CDS	D73A	R	ACTTGGAACAGCTGGATCCAC	21
MF92	mutagenesis	FT CDS	P75A	F	CCAGATGTTGCTAGTCCTAGC	21
MR92	mutagenesis	FT CDS	P75A	R	GCTAGGACTAGCAACATCTGG	21
MF93	mutagenesis	FT CDS	S76G	F	GATGTTCCAGGACCTAGCAAC	21
MR93	mutagenesis	FT CDS	S76G	R	GTTGCTAGGTCCTGGAACATC	21
MF94	mutagenesis	FT CDS	P77A	F	GTTCCAAGTGCTAGCAACCCT	21
MR94	mutagenesis	FT CDS	P77A	R	AGGGTTGCTAGCACTTGGAAC	21
MF95	mutagenesis	FT CDS	S78A	F	CCAAGTCCTGCTAACCCTCAC	21
MR95	mutagenesis	FT CDS	S78A	R	GTGAGGGTTAGCAGGACTTGG	21
MF96	mutagenesis	FT CDS	P80A	F	CCTAGCAACGCTCACCTCCGA	21
MR96	mutagenesis	FT CDS	P80A	R	TCGGAGGTGAGCGTTGCTAGG	21
MF97	mutagenesis	FT CDS	H81N	F	AGCAACCCTAACCTCCGAGAA	21
MR97	mutagenesis	FT CDS	H81N	R	TTCTCGGAGGTTAGGGTTGCT	21
MF98	mutagenesis	FT CDS	H81A	F	AGCAACCCTGCTCTCCGAGAA	21
MR98	mutagenesis	FT CDS	H81A	R	TTCTCGGAGAGCAGGGTTGCT	21
MF99	mutagenesis	FT CDS	L82M	F	AACCCTCACATGCGAGAATAT	21
MR99	mutagenesis	FT CDS	L82M	R	ATATTCTCGCATGTGAGGGTT	21
MF100	mutagenesis	FT CDS	R83D	F	CCTCACCTCGACGAATATCTC	21
MR100	mutagenesis	FT CDS	R83D	R	GAGATATTCGTCGAGGTGAGG	21
MF101	mutagenesis	FT CDS	R83A	F	CCTCACCTCGCTGAATATCTC	21
MR101	mutagenesis	FT CDS	R83A	R	GAGATATTCAGCGAGGTGAGG	21
MF102	mutagenesis	FT CDS	E84K	F	CACCTCCGAAAGTATCTCCAT	21
MR102	mutagenesis	FT CDS	E84K	R	ATGGAGATACTTTCGGAGGTG	21
MF103	mutagenesis	FT CDS	E84A	F	CACCTCCGAGCTTATCTCCAT	21
MR103	mutagenesis	FT CDS	E84A	R	ATGGAGATAAGCTCGGAGGTG	21
MF104	mutagenesis	FT CDS	Y85A	F	CTCCGAGAAGCTCTCCATTGG	21
MR104	mutagenesis	FT CDS	Y85A	R	CCAATGGAGAGCTTCTCGGAG	21
MF105	mutagenesis	FT CDS	H87A	F	GAATATCTCGCTTGGTTGGTG	21
MR105	mutagenesis	FT CDS	H87A	R	CACCAACCAAGCGAGATATTC	21
MF106	mutagenesis	FT CDS	W88A	F	TATCTCCATGCTTTGGTGACT	21
MR106	mutagenesis	FT CDS	W88A	R	AGTCACCAAAGCATGGAGATA	21

Oligo List 2. Oligos used for the site-directed mutagenesis (continued)

Oligo	Purpose	Target	FT mutation	Forward/Reverse	Sequence (5'-3')	bp
MF107	mutagenesis	FT CDS	T91V	F	TGGTTGGTGGTCGATATCCCT	21
MR107	mutagenesis	FT CDS	T91V	R	AGGGATATCGACCACCAACCA	21
MF108	mutagenesis	FT CDS	D92N	F	TTGGTGACTAACATCCCTGCT	21
MR108	mutagenesis	FT CDS	D92N	R	AGCAGGGATGTTAGTCACCAA	21
MF109	mutagenesis	FT CDS	I93A	F	GTGACTGATGCTCCTGCTACA	21
MR109	mutagenesis	FT CDS	I93A	R	TGTAGCAGGAGCATCAGTCAC	21
MF110	mutagenesis	FT CDS	P94A	F	ACTGATATCGCTGCTACAACT	21
MR110	mutagenesis	FT CDS	P94A	R	AGTTGTAGCAGCGATATCAGT	21
MF111	mutagenesis	FT CDS	G98N	F	GCTACAACTAACACAACCTTT	21
MR111	mutagenesis	FT CDS	G98N	R	AAAGGTTGTGTTAGTTGTAGC	21
MF112	mutagenesis	FT CDS	F101R	F	GGAACAACCAGGGGCAATGAG	21
MR112	mutagenesis	FT CDS	F101R	R	CTCATTGCCCCTGGTTGTTCC	21
MF113	mutagenesis	FT CDS	F101A	F	GGAACAACCGCTGGCAATGAG	21
MR113	mutagenesis	FT CDS	F101A	R	CTCATTGCCAGCGGTTGTTCC	21
MF114	mutagenesis	FT CDS	G102A	F	ACAACCTTTGCTAATGAGATT	21
MR114	mutagenesis	FT CDS	G102A	R	AATCTCATTAGCAAAGGTTGT	21
MF115	mutagenesis	FT CDS	N103E	F	ACCTTTGGCGAGGAGATTGTG	21
MR115	mutagenesis	FT CDS	N103E	R	CACAATCTCCTCGCCAAAGGT	21
MF116	mutagenesis	FT CDS	N103A	F	ACCTTTGGCGCTGAGATTGTG	21
MR116	mutagenesis	FT CDS	N103A	R	CACAATCTCAGCGCCAAAGGT	21
MF117	mutagenesis	FT CDS	E104K	F	TTTGGCAATAAGATTGTGTGT	21
MR117	mutagenesis	FT CDS	E104K	R	ACACACAATCTTATTGCCAAA	21
MF118	mutagenesis	FT CDS	E104A	F	TTTGGCAATGCTATTGTGTGT	21
MR118	mutagenesis	FT CDS	E104A	R	ACACACAATAGCATTGCCAAA	21
MF119	mutagenesis	FT CDS	C107G	F	GAGATTGTGGGATACGAAAAT	21
MR119	mutagenesis	FT CDS	C107G	R	ATTTTCGTATCCCACAATCTC	21
MF120	mutagenesis	FT CDS	Y108A	F	ATTGTGTGTGCTGAAAATCCA	21
MR120	mutagenesis	FT CDS	Y108A	R	TGGATTTTCAGCACACACAAT	21
MF121	mutagenesis	FT CDS	E109M	F	GTGTGTTACATGAATCCAAGT	21
MR121	mutagenesis	FT CDS	E109M	R	ACTTGGATTCATGTAACACAC	21
MF122	mutagenesis	FT CDS	E109A	F	GTGTGTTACGCTAATCCAAGT	21
MR122	mutagenesis	FT CDS	E109A	R	ACTTGGATTAGCGTAACACAC	21
MF123	mutagenesis	FT CDS	P111A	F	TACGAAAATGCTAGTCCCACT	21
MR123	mutagenesis	FT CDS	P111A	R	AGTGGGACTAGCATTTTCGTA	21
MF124	mutagenesis	FT CDS	S112R	F	GAAAATCCAAGGCCCACTGCA	21
MR124	mutagenesis	FT CDS	S112R	R	TGCAGTGGGCCTTGGATTTTC	21
MF125	mutagenesis	FT CDS	P113A	F	AATCCAAGTGCTACTGCAGGA	21
MR125	mutagenesis	FT CDS	P113A	R	TCCTGCAGTAGCACTTGGATT	21
MF126	mutagenesis	FT CDS	G116A	F	CCCACTGCAGCTATTCATCGT	21
MR126	mutagenesis	FT CDS	G116A	R	ACGATGAATAGCTGCAGTGGG	21
MF127	mutagenesis	FT CDS	I117A	F	ACTGCAGGAGCTCATCGTGTC	21
MR127	mutagenesis	FT CDS	I117A	R	GACACGATGAGCTCCTGCAGT	21

Oligo	Purpose	Target	FT mutation	Forward/Reverse	Sequence (5'-3')	bp
MF128	mutagenesis	FT CDS	H118A	F	GCAGGAATTGCTCGTGTCGTG	21
MR128	mutagenesis	FT CDS	H118A	R	CACGACACGAGCAATTCCTGC	21
MF129	mutagenesis	FT CDS	R119A	F	GGAATTCATGCTGTCGTGTTT	21
MR129	mutagenesis	FT CDS	R119A	R	AAACACGACAGCATGAATTCC	21
MF130	mutagenesis	FT CDS	V120F	F	ATTCATCGTTTCGTGTTTATA	21
MR130	mutagenesis	FT CDS	V120F	R	TATAAACACGAAACGATGAAT	21
MF131	mutagenesis	FT CDS	V120Y	F	ATTCATCGTTACGTGTTTATA	21
MR131	mutagenesis	FT CDS	V120Y	R	TATAAACACGTAACGATGAAT	21
MF132	mutagenesis	FT CDS	F122L	F	CGTGTCGTGCTCATATTGTTT	21
MR132	mutagenesis	FT CDS	F122L	R	AAACAATATGAGCACGACACG	21
MF133	mutagenesis	FT CDS	R126A	F	ATATTGTTTGCTCAGCTTGGC	21
MR133	mutagenesis	FT CDS	R126A	R	GCCAAGCTGAGCAAACAATAT	21
MF134	mutagenesis	FT CDS	Q127A	F	TTGTTTCGAGCTCTTGGCAGG	21
MR134	mutagenesis	FT CDS	Q127A	R	CCTGCCAAGAGCTCGAAACAA	21
MF135	mutagenesis	FT CDS	L128K	F	TTTCGACAGAAGGGCAGGCAA	21
MR135	mutagenesis	FT CDS	L128K	R	TTGCCTGCCCTTCTGTCGAAA	21
MF136	mutagenesis	FT CDS	L128A	F	TTTCGACAGGCTGGCAGGCAA	21
MR136	mutagenesis	FT CDS	L128A	R	TTGCCTGCCAGCCTGTCGAAA	21
MF137	mutagenesis	FT CDS	G129D	F	CGACAGCTTGACAGGCAAACA	21
MR137	mutagenesis	FT CDS	G129D	R	TGTTTGCCTGTCAAGCTGTCG	21
MF138	mutagenesis	FT CDS	G129A	F	CGACAGCTTGCTAGGCAAACA	21
MR138	mutagenesis	FT CDS	G129A	R	TGTTTGCCTAGCAAGCTGTCG	21
MF139	mutagenesis	FT CDS	R130E	F	CAGCTTGGCGAGCAAACAGTG	21
MR139	mutagenesis	FT CDS	R130E	R	CACTGTTTGCTCGCCAAGCTG	21
MF140	mutagenesis	FT CDS	R130A	F	CAGCTTGGCGCTCAAACAGTG	21
MR140	mutagenesis	FT CDS	R130A	R	CACTGTTTGAGCGCCAAGCTG	21
MF141	mutagenesis	FT CDS	Q131A	F	CTTGGCAGGGCTACAGTGTAT	21
MR141	mutagenesis	FT CDS	Q131A	R	ATACACTGTAGCCCTGCCAAG	21
MF142	mutagenesis	FT CDS	T132A	F	GGCAGGCAAGCTGTGTATGCA	21
MR142	mutagenesis	FT CDS	T132A	R	TGCATACACAGCTTGCCTGCC	21
MF143	mutagenesis	FT CDS	V133A	F	AGGCAAACAGCTTATGCACCA	21
MR143	mutagenesis	FT CDS	V133A	R	TGGTGCATAAGCTGTTTGCCT	21
MF144	mutagenesis	FT CDS	Y134A	F	CAAACAGTGGCTGCACCAGGG	21
MR144	mutagenesis	FT CDS	Y134A	R	CCCTGGTGCAGCCACTGTTTG	21
MF145	mutagenesis	FT CDS	A135G	F	ACAGTGTATGGACCAGGGTGG	21
MR145	mutagenesis	FT CDS	A135G	R	CCACCCTGGTCCATACACTGT	21
MF146	mutagenesis	FT CDS	P136A	F	GTGTATGCAGCTGGGTGGCGC	21
MR146	mutagenesis	FT CDS	P136A	R	GCGCCACCCAGCTGCATACAC	21
MF147	mutagenesis	FT CDS	G137E	F	TATGCACCAGAGTGGCGCCAG	21
MR147	mutagenesis	FT CDS	G137E	R	CTGGCGCCACTCTGGTGCATA	21
MF148	mutagenesis	FT CDS	G137A	F	TATGCACCAGCTTGGCGCCAG	21
MR148	mutagenesis	FT CDS	G137A	R	CTGGCGCCAAGCTGGTGCATA	21

Oligo List 2. Oligos used for the site-directed mutagenesis (continued)

Oligo	Purpose	Target	FT mutation	Forward/Reverse	Sequence (5'-3')	bp
MF149	mutagenesis	FT CDS	W138S	F	GCACCAGGGTCGCGCCAGAAC	21
MR149	mutagenesis	FT CDS	W138S	R	GTTCTGGCGCGACCCTGGTGC	21
MF150	mutagenesis	FT CDS	W138A	F	GCACCAGGGGCTCGCCAGAAC	21
MR150	mutagenesis	FT CDS	W138A	R	GTTCTGGCGAGCCCCTGGTGC	21
MF151	mutagenesis	FT CDS	R139A	F	CCAGGGTGGGCTCAGAACTTC	21
MR151	mutagenesis	FT CDS	R139A	R	GAAGTTCTGAGCCCACCCTGG	21
MF152	mutagenesis	FT CDS	Q140A	F	GGGTGGCGCGCTAACTTCAAC	21
MR152	mutagenesis	FT CDS	Q140A	R	GTTGAAGTTAGCGCGCCACCC	21
MF153	mutagenesis	FT CDS	F142A	F	CGCCAGAACGCTAACACTCGC	21
MR153	mutagenesis	FT CDS	F142A	R	GCGAGTGTTAGCGTTCTGGCG	21
MF154	mutagenesis	FT CDS	N143A	F	CAGAACTTCGCTACTCGCGAG	21
MR154	mutagenesis	FT CDS	N143A	R	CTCGCGAGTAGCGAAGTTCTG	21
MF155	mutagenesis	FT CDS	T144A	F	AACTTCAACGCTCGCGAGTTT	21
MR155	mutagenesis	FT CDS	T144A	R	AAACTCGCGAGCGTTGAAGTT	21
MF156	mutagenesis	FT CDS	R145A	F	TTCAACACTGCTGAGTTTGCT	21
MR156	mutagenesis	FT CDS	R145A	R	AGCAAACTCAGCAGTGTTGAA	21
MF157	mutagenesis	FT CDS	E146A	F	AACACTCGCGCTTTTGCTGAG	21
MR157	mutagenesis	FT CDS	E146A	R	CTCAGCAAAAGCGCGAGTGTT	21
MF158	mutagenesis	FT CDS	F147A	F	ACTCGCGAGGCTGCTGAGATC	21
MR158	mutagenesis	FT CDS	F147A	R	GATCTCAGCAGCCTCGCGAGT	21
MF159	mutagenesis	FT CDS	E149G	F	GAGTTTGCTGGAATCTACAAT	21
MR159	mutagenesis	FT CDS	E149G	R	ATTGTAGATTCCAGCAAACTC	21
MF160	mutagenesis	FT CDS	I150H	F	TTTGCTGAGCACTACAATCTC	21
MR160	mutagenesis	FT CDS	I150H	R	GAGATTGTAGTGCTCAGCAAA	21
MF161	mutagenesis	FT CDS	I150A	F	TTTGCTGAGGCTTACAATCTC	21
MR161	mutagenesis	FT CDS	I150A	R	GAGATTGTAAGCCTCAGCAAA	21
MF162	mutagenesis	FT CDS	Y151A	F	GCTGAGATCGCTAATCTCGGC	21
MR162	mutagenesis	FT CDS	Y151A	R	GCCGAGATTAGCGATCTCAGC	21
MF163	mutagenesis	FT CDS	N152A	F	GAGATCTACGCTCTCGGCCTT	21
MR163	mutagenesis	FT CDS	N152A	R	AAGGCCGAGAGCGTAGATCTC	21
MF164	mutagenesis	FT CDS	L153A	F	ATCTACAATGCTGGCCTTCCC	21
MR164	mutagenesis	FT CDS	L153A	R	GGGAAGGCCAGCATTGTAGAT	21
MF165	mutagenesis	FT CDS	P156A	F	CTCGGCCTTGCTGTGGCCGCA	21
MR165	mutagenesis	FT CDS	P156A	R	TGCGGCCACAGCAAGGCCGAG	21
MF166	mutagenesis	FT CDS	V157A	F	GGCCTTCCCGCTGCCGCAGTT	21
MR166	mutagenesis	FT CDS	V157A	R	AACTGCGGCAGCGGGAAGGCC	21
MF167	mutagenesis	FT CDS	F161A	F	GCCGCAGTTGCTTACAATTGT	21
MR167	mutagenesis	FT CDS	F161A	R	ACAATTGTAAGCAACTGCGGC	21
MF168	mutagenesis	FT CDS	Y162A	F	GCAGTTTTCGCTAATTGTCAG	21
MR168	mutagenesis	FT CDS	Y162A	R	CTGACAATTAGCGAAAACTGC	21
MF169	mutagenesis	FT CDS	N163A	F	GTTTTCTACGCTTGTCAGAGG	21
MR169	mutagenesis	FT CDS	N163A	R	CCTCTGACAAGCGTAGAAAAC	21

Oligo	Purpose	Target	FT mutation	Forward/Reverse	Sequence (5'-3')	bp
MF170	mutagenesis	FT CDS	R166K	F	AATTGTCAGAAGGAGAGTGGC	21
MR170	mutagenesis	FT CDS	R166K	R	GCCACTCTCCTTCTGACAATT	21
MF171	mutagenesis	FT CDS	R166A	F	AATTGTCAGGCTGAGAGTGGC	21
MR171	mutagenesis	FT CDS	R166A	R	GCCACTCTCAGCCTGACAATT	21
MF172	mutagenesis	FT CDS	E167A	F	TGTCAGAGGGCTAGTGGCTGC	21
MR172	mutagenesis	FT CDS	E167A	R	GCAGCCACTAGCCCTCTGACA	21
MF173	mutagenesis	FT CDS	S168T	F	CAGAGGGAGACGGGCTGCGGA	21
MR173	mutagenesis	FT CDS	S168T	R	TCCGCAGCCCGTCTCCCTCTG	21
MF174	mutagenesis	FT CDS	G169A	F	AGGGAGAGTGCTTGCGGAGGA	21
MR174	mutagenesis	FT CDS	G169A	R	TCCTCCGCAAGCACTCTCCCT	21
MF176	mutagenesis	FT CDS	G171E	F	AGTGGCTGCGAGGGAAGAAGA	21
MR176	mutagenesis	FT CDS	G171E	R	TCTTCTTCCCTCGCAGCCACT	21
MF177	mutagenesis	FT CDS	G171R	F	AGTGGCTGCAGGGGAAGAAGA	21
MR177	mutagenesis	FT CDS	G171R	R	TCTTCTTCCCCTGCAGCCACT	21
MF185	mutagenesis	FT CDS	P8W	F	ATAAGAGACTGGCTTATAGTA	21
MR185	mutagenesis	FT CDS	P8W	R	TACTATAAGCCAGTCTCTTAT	21
MF186	mutagenesis	FT CDS	L9W	F	AGAGACCCTTGGATAGTAAGC	21
MR186	mutagenesis	FT CDS	L9W	R	GCTTACTATCCAAGGGTCTCT	21
MF187	mutagenesis	FT CDS	V11M	F	CCTCTTATAATGAGCAGAGTT	21
MR187	mutagenesis	FT CDS	V11M	R	AACTCTGCTCATTATAAGAGG	21
MF188	mutagenesis	FT CDS	S12F	F	CTTATAGTATTCAGAGTTGTT	21
MR188	mutagenesis	FT CDS	S12F	R	AACAACTCTGAATACTATAAG	21
MF189	mutagenesis	FT CDS	R13D	F	ATAGTAAGCGACGTTGTTGGA	21
MR189	mutagenesis	FT CDS	R13D	R	TCCAACAACGTCGCTTACTAT	21
MF190	mutagenesis	FT CDS	V14F	F	GTAAGCAGATTCGTTGGAGAC	21
MR190	mutagenesis	FT CDS	V14F	R	GTCTCCAACGAATCTGCTTAC	21
MF191	mutagenesis	FT CDS	V15F	F	AGCAGAGTTTTCGGAGACGTT	21
MR191	mutagenesis	FT CDS	V15F	R	AACGTCTCCGAAAACTCTGCT	21
MF192	mutagenesis	FT CDS	V18F	F	GTTGGAGACTTCCTTGATCCG	21
MR192	mutagenesis	FT CDS	V18F	R	CGGATCAAGGAAGTCTCCAAC	21
MF193	mutagenesis	FT CDS	P45F	F	GATCTAAGGTTCTCTCAGGTT	21
MR193	mutagenesis	FT CDS	P45F	R	AACCTGAGAGAACCTTAGATC	21
MF194	mutagenesis	FT CDS	P52E	F	CAAAACAAGGAGAGAGTTGAG	21
MR194	mutagenesis	FT CDS	P52E	R	CTCAACTCTCTCCTTGTTTTG	21
MF195	mutagenesis	FT CDS	D73K	F	GTGGATCCAAAGGTTCCAAGT	21
MR195	mutagenesis	FT CDS	D73K	R	ACTTGGAACCTTTGGATCCAC	21
MF196	mutagenesis	FT CDS	P75W	F	CCAGATGTTTGGAGTCCTAGC	21
MR196	mutagenesis	FT CDS	P75W	R	GCTAGGACTCCAAACATCTGG	21
MF197	mutagenesis	FT CDS	P80W	F	CCTAGCAACTGGCACCTCCGA	21
MR197	mutagenesis	FT CDS	P80W	R	TCGGAGGTGCCAGTTGCTAGG	21

Oligo List 2. Oligos used for the site-directed mutagenesis (continued)

Oligo	Purpose	Target	FT mutation	Forward/Reverse	Sequence (5'-3')	bp
MF198	mutagenesis	FT CDS	Y85E	F	CTCCGAGAAGAGCTCCATTGG	21
MR198	mutagenesis	FT CDS	Y85E	R	CCAATGGAGCTCTTCTCGGAG	21
MF199	mutagenesis	FT CDS	G102W	F	ACAACCTTTTGGAATGAGATT	21
MR199	mutagenesis	FT CDS	G102W	R	AATCTCATTCCAAAAGGTTGT	21
MF200	mutagenesis	FT CDS	C107R	F	GAGATTGTGAGGTACGAAAAT	21
MR200	mutagenesis	FT CDS	C107R	R	ATTTTCGTACCTCACAATCTC	21
MF201	mutagenesis	FT CDS	G116R	F	CCCACTGCAAGGATTCATCGT	21
MR201	mutagenesis	FT CDS	G116R	R	ACGATGAATCCTTGCAGTGGG	21
MF202	mutagenesis	FT CDS	G116E	F	CCCACTGCAGAGATTCATCGT	21
MR202	mutagenesis	FT CDS	G116E	R	ACGATGAATCTCTGCAGTGGG	21
MF203	mutagenesis	FT CDS	I117W	F	ACTGCAGGATGGCATCGTGTC	21
MR203	mutagenesis	FT CDS	I117W	R	GACACGATGCCATCCTGCAGT	21
MF204	mutagenesis	FT CDS	R119E	F	GGAATTCATGAGGTCGTGTTT	21
MR204	mutagenesis	FT CDS	R119E	R	AAACACGACCTCATGAATTCC	21
MF205	mutagenesis	FT CDS	Q127E	F	TTGTTTCGAGAGCTTGGCAGG	21
MR205	mutagenesis	FT CDS	Q127E	R	CCTGCCAAGCTCTCGAAACAA	21
MF206	mutagenesis	FT CDS	G129R	F	CGACAGCTTAGGAGGCAAACA	21
MR206	mutagenesis	FT CDS	G129R	R	TGTTTGCCTCCTAAGCTGTCG	21
MF207	mutagenesis	FT CDS	Q131E	F	CTTGGCAGGGAGACAGTGTAT	21
MR207	mutagenesis	FT CDS	Q131E	R	ATACACTGTCTCCCTGCCAAG	21
MF208	mutagenesis	FT CDS	T132M	F	GGCAGGCAAATGGTGTATGCA	21
MR208	mutagenesis	FT CDS	T132M	R	TGCATACACCATTTGCCTGCC	21
MF209	mutagenesis	FT CDS	V133H	F	AGGCAAACACACTATGCACCA	21
MR209	mutagenesis	FT CDS	V133H	R	TGGTGCATAGTGTGTTTGCCT	21
MF210	mutagenesis	FT CDS	Y134K	F	CAAACAGTGAAGGCACCAGGG	21
MR210	mutagenesis	FT CDS	Y134K	R	CCCTGGTGCCTTCACTGTTTG	21
MF211	mutagenesis	FT CDS	Y134Q	F	CAAACAGTGCAGGCACCAGGG	21
MR211	mutagenesis	FT CDS	Y134Q	R	CCCTGGTGCCTGCACTGTTTG	21
MF212	mutagenesis	FT CDS	Y134P	F	CAAACAGTGCCAGCACCAGGG	21
MR212	mutagenesis	FT CDS	Y134P	R	CCCTGGTGCTGGCACTGTTTG	21
MF213	mutagenesis	FT CDS	A135Q	F	ACAGTGTATCAGCCAGGGTGG	21
MR213	mutagenesis	FT CDS	A135Q	R	CCACCCTGGCTGATACACTGT	21
MF214	mutagenesis	FT CDS	P136N	F	GTGTATGCAAACGGGTGGCGC	21
MR214	mutagenesis	FT CDS	P136N	R	GCGCCACCCGTTTGCATACAC	21
MF215	mutagenesis	FT CDS	R139E	F	CCAGGGTGGGAGCAGAACTTC	21
MR215	mutagenesis	FT CDS	R139E	R	GAAGTTCTGCTCCCACCCTGG	21
MF216	mutagenesis	FT CDS	C164A	F	TTCTACAATGCTCAGAGGGAG	21
MR216	mutagenesis	FT CDS	C164A	R	CTCCCTCTGAGCATTGTAGAA	21
MF217	mutagenesis	FT CDS	C164E	F	TTCTACAATGAGCAGAGGGAG	21
MR217	mutagenesis	FT CDS	C164E	R	CTCCCTCTGCTCATTGTAGAA	21
MF218	mutagenesis	FT CDS	Q165A	F	TACAATTGTGCTAGGGAGAGT	21

Oligo	Purpose	Target	FT mutation	Forward/Reverse	Sequence (5'-3')	bp
MR218	mutagenesis	FT CDS	Q165A	R	ACTCTCCCTAGCACAATTGTA	21
MF219	mutagenesis	FT CDS	R166E	F	AATTGTCAGGAGGAGAGTGGC	21
MR219	mutagenesis	FT CDS	R166E	R	GCCACTCTCCTCCTGACAATT	21
MF220	mutagenesis	FT CDS	G169E	F	AGGGAGAGTGAGTGCGGAGGA	21
MR220	mutagenesis	FT CDS	G169E	R	TCCTCCGCACTCACTCTCCCT	21
MF225	mutagenesis	FT CDS	T66I	F	AACTTCTATATCTTGGTTATG	21
MR225	mutagenesis	FT CDS	T66I	R	CATAACCAAGATATAGAAGTT	21
MF226	mutagenesis	FT CDS	G102E	F	ACAACCTTTGAGAATGAGATT	21
MR226	mutagenesis	FT CDS	G102E	R	AATCTCATTCTCAAAGGTTGT	21
MF227	mutagenesis	FT CDS	Y85R	F	CTCCGAGAAAGGCTCCATTGG	21
MR227	mutagenesis	FT CDS	Y85R	R	CCAATGGAGCCTTTCTCGGAG	21
MF228	mutagenesis	FT CDS	Y32E	F	AAGGTTACTGAGGGCCAAAGA	21
MR228	mutagenesis	FT CDS	Y32E	R	TCTTTGGCCCTCAGTAACCTT	21
MF229	mutagenesis	FT CDS	Y32K	F	AAGGTTACTAAGGGCCAAAGA	21
MR229	mutagenesis	FT CDS	Y32K	R	TCTTTGGCCCTTAGTAACCTT	21
MF230	mutagenesis	FT CDS	Q34E	F	ACTTATGGCGAGAGAGAGGTG	21
MR230	mutagenesis	FT CDS	Q34E	R	CACCTCTCTCTCGCCATAAGT	21
MF231	mutagenesis	FT CDS	R35K	F	TATGGCCAAAAGGAGGTGACT	21
MR231	mutagenesis	FT CDS	R35K	R	AGTCACCTCCTTTTGGCCATA	21
MF232	mutagenesis	FT CDS	R35E	F	TATGGCCAAGAGGAGGTGACT	21
MR232	mutagenesis	FT CDS	R35E	R	AGTCACCTCCTCTTGGCCATA	21
MF233	mutagenesis	FT CDS	K51E	F	GTTCAAAACGAGCCAAGAGTT	21
MR233	mutagenesis	FT CDS	K51E	R	AACTCTTGGCTCGTTTTGAAC	21
MF234	mutagenesis	FT CDS	K51D	F	GTTCAAAACGACCCAAGAGTT	21
MR234	mutagenesis	FT CDS	K51D	R	AACTCTTGGGTCGTTTTGAAC	21
MF235	mutagenesis	FT CDS	R53E	F	AACAAGCCAGAGGTTGAGATT	21
MR235	mutagenesis	FT CDS	R53E	R	AATCTCAACCTCTGGCTTGTT	21
MF236	mutagenesis	FT CDS	D71E	F	GTTATGGTGGAGCCAGATGTT	21
MR236	mutagenesis	FT CDS	D71E	R	AACATCTGGCTCCACCATAAC	21
MF237	mutagenesis	FT CDS	D71K	F	GTTATGGTGAAGCCAGATGTT	21
MR237	mutagenesis	FT CDS	D71K	R	AACATCTGGCTTCACCATAAC	21
MF238	mutagenesis	FT CDS	D73E	F	GTGGATCCAGAGGTTCCAAGT	21
MR238	mutagenesis	FT CDS	D73E	R	ACTTGGAACCTCTGGATCCAC	21
MF239	mutagenesis	FT CDS	Y85D	F	CTCCGAGAAGATCTCCATTGG	21
MR239	mutagenesis	FT CDS	Y85D	R	CCAATGGAGATCTTCTCGGAG	21
MF240	mutagenesis	FT CDS	Y85K	F	CTCCGAGAAAAGCTCCATTGG	21
MR240	mutagenesis	FT CDS	Y85K	R	CCAATGGAGCTTTTCTCGGAG	21
MF241	mutagenesis	FT CDS	W88E	F	TATCTCCATGAGTTGGTGACT	21
MR241	mutagenesis	FT CDS	W88E	R	AGTCACCAACTCATGGAGATA	21
MF242	mutagenesis	FT CDS	W88D	F	TATCTCCATGACTTGGTGACT	21

Oligo List 2. Oligos used for the site-directed mutagenesis (continued)

Oligo	Purpose	Target	FT mutation	Forward/Reverse	Sequence (5'-3')	bp
MR242	mutagenesis	FT CDS	W88D	R	AGTCACCAAGTCATGGAGATA	21
MF243	mutagenesis	FT CDS	W88K	F	TATCTCCATAAGTTGGTGACT	21
MR243	mutagenesis	FT CDS	W88K	R	AGTCACCAACTTATGGAGATA	21
MF244	mutagenesis	FT CDS	E109R	F	GTGTGTTACAGAAATCCAAGT	21
MR244	mutagenesis	FT CDS	E109R	R	ACTTGGATTTCTGTAACACAC	21
MF245	mutagenesis	FT CDS	E109D	F	GTGTGTTACGACAATCCAAGT	21
MR245	mutagenesis	FT CDS	E109D	R	ACTTGGATTGTCGTAACACAC	21
MF246	mutagenesis	FT CDS	L128E	F	TTTCGACAGGAGGGCAGGCAA	21
MR246	mutagenesis	FT CDS	L128E	R	TTGCCTGCCCTCCTGTCGAAA	21
MF247	mutagenesis	FT CDS	Y134D	F	CAAACAGTGGACGCACCAGGG	21
MR247	mutagenesis	FT CDS	Y134D	R	CCCTGGTGCGTCCACTGTTTG	21
MF248	mutagenesis	FT CDS	Y134R	F	CAAACAGTGAGGGCACCAGGG	21
MR248	mutagenesis	FT CDS	Y134R	R	CCCTGGTGCCCTCACTGTTTG	21
MF249	mutagenesis	FT CDS	Y134F	F	CAAACAGTGTTTGCACCAGGG	21
MR249	mutagenesis	FT CDS	Y134F	R	CCCTGGTGCAAACACTGTTTG	21
MF250	mutagenesis	FT CDS	Y134E	F	CAAACAGTGGAAGCACCAGGG	21
MR250	mutagenesis	FT CDS	Y134E	R	CCCTGGTGCTTCCACTGTTTG	21
MF251	mutagenesis	FT CDS	W138R	F	GCACCAGGGCGGCGCCAGAAC	21
MR251	mutagenesis	FT CDS	W138R	R	GTTCTGGCGCCGCCCTGGTGC	21
MF252	mutagenesis	FT CDS	W138K	F	GCACCAGGGAAGCGCCAGAAC	21
MR252	mutagenesis	FT CDS	W138K	R	GTTCTGGCGCTTCCCTGGTGC	21
MF253	mutagenesis	FT CDS	W138D	F	GCACCAGGGGACCGCCAGAAC	21
MR253	mutagenesis	FT CDS	W138D	R	GTTCTGGCGGTCCCCTGGTGC	21
MF254	mutagenesis	FT CDS	W138Y	F	GCACCAGGGTATCGCCAGAAC	21
MR254	mutagenesis	FT CDS	W138Y	R	GTTCTGGCGATACCCTGGTGC	21
MF255	mutagenesis	FT CDS	Q140R	F	GGGTGGCGCCGGAACTTCAAC	21
MR255	mutagenesis	FT CDS	Q140R	R	GTTGAAGTTCCGGCGCCACCC	21
MF256	mutagenesis	FT CDS	Q140E	F	GGGTGGCGCGAGAACTTCAAC	21
MR256	mutagenesis	FT CDS	Q140E	R	GTTGAAGTTCTCGCGCCACCC	21
MF257	mutagenesis	FT CDS	N141E	F	TGGCGCCAGGAGTTCAACACT	21
MR257	mutagenesis	FT CDS	N141E	R	AGTGTTGAACTCCTGGCGCCA	21
MF258	mutagenesis	FT CDS	N152R	F	GAGATCTACAGGCTCGGCCTT	21
MR258	mutagenesis	FT CDS	N152R	R	AAGGCCGAGCCTGTAGATCTC	21
MF259	mutagenesis	FT CDS	N152E	F	GAGATCTACGAGCTCGGCCTT	21
MR259	mutagenesis	FT CDS	N152E	R	AAGGCCGAGCTCGTAGATCTC	21
MF260	mutagenesis	FT CDS	V18K	F	GTTGGAGACAAGCTTGATCCG	21
MR260	mutagenesis	FT CDS	V18K	R	CGGATCAAGCTTGTCTCCAAC	21
MF261	mutagenesis	FT CDS	P75K	F	CCAGATGTTAAGAGTCCTAGC	21
MR261	mutagenesis	FT CDS	P75K	R	GCTAGGACTCTTAACATCTGG	21
MF262	mutagenesis	FT CDS	P94L	F	ACTGATATCTTAGCTACAACT	21
MR262	mutagenesis	FT CDS	P94L	R	AGTTGTAGCTAAGATATCAGT	21

Oligo	Purpose	Target	FT mutation	Forward/Reverse	Sequence (5'-3')	bp
MF332	mutagenesis	FT CDS	N152Y	F	GAGATCTACTATCTCGGCCTT	21
MR332	mutagenesis	FT CDS	N152Y	R	AAGGCCGAGATAGTAGATCTC	21
MF333	mutagenesis	FT CDS	L128F	F	TTTCGACAGTTTGGCAGGCAA	21
MR333	mutagenesis	FT CDS	L128F	R	TTGCCTGCCAAACTGTCGAAA	21
MF334	mutagenesis	FT CDS	L128I	F	TTTCGACAGATTGGCAGGCAA	21
MR334	mutagenesis	FT CDS	L128I	R	TTGCCTGCCAATCTGTCGAAA	21
MF335	mutagenesis	FT CDS	G137W	F	TATGCACCATGGTGGCGCCAG	21
MR335	mutagenesis	FT CDS	G137W	R	CTGGCGCCACCATGGTGCATA	21
MF336	mutagenesis	FT CDS	G137R	F	TATGCACCATCGGGGCGCCAG	21
MR336	mutagenesis	FT CDS	G137R	R	CTGGCGCCCCGATGGTGCATA	21
EMF49_2	mutagenesis	FT CDS	D7K	F	CGCCGCAAGCTTATGTCTATAAATATAAGAAAGCCTCTTATAGTAAGC	48
EMF50_2	mutagenesis	FT CDS	D7A	F	CGCCGCAAGCTTATGTCTATAAATATAAGAGCTCCTCTTATAGTAAGC	48
EMR175_2	mutagenesis	FT CDS	C170A	R	CGCCGCCTCGAGCTAAAGTCTTCTTCCTCCAGCGCCACTCTCCCTCTG	48
EMR178	mutagenesis	FT CDS	G172R	R	CGCCGCCTCGAGCTAAAGTCTTCTCCTTCCGCA	33
EMR179	mutagenesis	FT CDS	R173A	R	CGCCGCCTCGAGCTAAAGTCTAGCTCCTCCGCA	33
EMR180	mutagenesis	FT CDS	R174A	R	CGCCGCCTCGAGCTAAAGAGCTCTTCCTCCGCA	33
EMR181	mutagenesis	FT CDS	L175R	R	CGCCGCCTCGAGCTACCTTCTTCTTCCTCCGCA	33
EMR182	mutagenesis	FT CDS	L175E	R	CGCCGCCTCGAGCTACTCTCTTCTTCCTCCGCA	33
EMR183	mutagenesis	FT CDS	R173A + R174A	R	CGCCGCCTCGAGCTAAAGTGCTGCTCCTCCGCA	33
EMR184	mutagenesis	FT CDS	R173E + R174E + L175D	R	CGCCGCCTCGAGCTAATCTTCTTCTCCTCCGCA	33
EMR221	mutagenesis	FT CDS	C170P	R	CGCCGCCTCGAGCTAAAGTCTTCTTCCTCCTGGGCCACTCTC	42
EMR222	mutagenesis	FT CDS	G172E	R	CGCCGCCTCGAGCTAAAGTCTTCTCTCTCCGCAGCCACTCTC	42
EMR223	mutagenesis	FT CDS	R173E	R	CGCCGCCTCGAGCTAAAGTCTCTCTCCTCCGCAGCCACTCTC	42
EMR224	mutagenesis	FT CDS	R173E + R174E	R	CGCCGCCTCGAGCTAAAGCTCCTCTCCTCCGCAGCCACTCTC	42

Oligo List 3. Oligos used for the *tfl1-1* complementation.

Oligo	Purpose	Target	Forward/Reverse	Sequence (5'-3')	bp
AF61_2	cloning	gTFL1- 2.2kb upstream	F	CGCCGCCTGCAGCAACCTTGATTTCATCCG	30
AR61	cloning	gTFL1- 2.2kb upstream	R	CGCCGCCTGCAGTTTCTTTTGTTAACTTAGAGGAAAAG	38
AF125	cloning	gTFL1- 4.6kb downstream	F	CGCCGCACTAGTTTTCATGATTGTCATAAACTGC	34
AR125	cloning	gTFL1- 4.6kb downstream	R	CGCCGCGAGCTCGTGCTGGTCGTGGAGACAC	31
SF50	sequencing	gTFL1- 2.2kb upstream	F	CAACCTTGATTTCATCCG	18
SF51	sequencing	gTFL1- 2.2kb upstream	F	ACCAAATCTTAATAAAGC	18
SF52	sequencing	gTFL1- 2.2kb upstream	F	TTTGAGGAATTTTGGTTC	18
SF53	sequencing	gTFL1- 2.2kb upstream	F	CAATAATTGTATCCGGAG	18
SF54	sequencing	gTFL1- 2.2kb upstream	F	CAAAAAGAAAAAGAAAAAG	19
SR10	sequencing	gTFL1- 2.2kb upstream	R	GCCTCTGGTTATTAACTT	18
SF55	sequencing	gTFL1- 4.6kb downstream	F	CATGATTGTCATAAACTG	18
SF56	sequencing	gTFL1- 4.6kb downstream	F	CAAAAAAAAATCTAATAGGC	20
SF57	sequencing	gTFL1- 4.6kb downstream	F	AAATGGATTGGCCATTTT	18
SF58	sequencing	gTFL1- 4.6kb downstream	F	GTTATCTACACATGTGCC	18
SF59	sequencing	gTFL1- 4.6kb downstream	F	GTAGAGTATTAGGGTTTC	18
SF60	sequencing	gTFL1- 4.6kb downstream	F	CTGTCATGCAAAATAAAA	18
SF61	sequencing	gTFL1- 4.6kb downstream	F	CATAGAAAGGCTGTCTAA	18
SF62	sequencing	gTFL1- 4.6kb downstream	F	TTGTGTTACTATGTTGAG	18
SF63	sequencing	gTFL1- 4.6kb downstream	F	ACAATCTTGGTTCTGATT	18
SF64	sequencing	gTFL1- 4.6kb downstream	F	ACTGACCGGTGAGCTGAA	18
SR11	sequencing	gTFL1- 4.6kb downstream	R	CAACTCATCTTTGGCAGT	18
LF6	MCS	-	F	CGCCGCCTGCAGTGCGGCCGCCCCGGGGTCGACCCATGGGGATCCCGCCGC	51
LR6	MCS	-	R	GCGGCGGGATCCCCATGGGTCGACCCCGGGGCGGCCGCACTGCAGGCGGCG	51
AF149	cloning	genomic TFL1/ TFL1 CDS	F	CGCCGCCTGCAGATGGAGAATATGGGAACTAGAGT	35
AR149	cloning	genomic TFL1/ TFL1 CDS	R	CGCCGCACTAGTCTAGCGTTTGCGTGCAGC	30
AF154	cloning	genomic FT/ FT CDS	F	CGCCGCGCGGCCGCATGTCTATAAATATAAGAGACCCTC	39
AR154	cloning	genomic FT/ FT CDS	R	CGCCGCCCATGGCTAAAGTCTTCTTCCTCCGC	32

Oligo List 4. Oligos used for the yeast growth and quantitative ONPG enzyme activity assay.

Oligo	Purpose	Target	Forward/Reverse	Sequence (5'-3')	bp
LF1	MCS	-	F	AATTCGGGCGGCCGCCCATGGGGTACCAAGCTTCCCGGGAGATCTCTGCAGGGGCCCGTCGACACTAGTAG	71
LR1	MCS	-	R	AATTCTACTAGTGTCGACGGGCCCCTGCAGAGATCTCCCGGGAAGCTTGGTACCCCATGGGCGGCCGCCCG	71
AF14	cloning	attR1-2	F	CGCCGCCATATGGGACAAGTTTGTACAAAAAAGCTGAAC	39
AR14	cloning	attR1-2	R	CGCCGCGCGGCCGCACCACTTTGTACAAGAAAGCTGAAC	39
AF55	cloning	attR1-2	F	CGCCGCCATATGGGACAAGTTTGTACAAAAAAGCTGAAC	39
AR55	cloning	attR1-2	R	CGCCGCCTCGAGACCACTTTGTACAAGAAAGCTGAAC	37
AF15	cloning	14-3-3_GRF1	F	CGCCGCGCGGCCGCATGGCGACACCAGGAGCTTCC	35
AR15	cloning	14-3-3_GRF1	R	CGCCGCCTCGAGTTAGGATTGTTGCTCGTCAGC	33
AF16	cloning	14-3-3_GRF2	F	CGCCGCGCGGCCGCATGGCGTCTGGGCGTGAAGAG	35
AR16	cloning	14-3-3_GRF2	R	CGCCGCCTCGAGTCACTGCTGTTCCTCGGTCGG	33
AF17	cloning	14-3-3_GRF3	F	CGCCGCGCGGCCGCATGTCGACAAGGGAAGAGAAT	35
AR17	cloning	14-3-3_GRF3	R	CGCCGCCTCGAGTTACTCGGCACCATCGGGCTT	33
AF18	cloning	14-3-3_GRF4	F	CGCCGCGCGGCCGCATGGCGGCACCACCAGCATCA	35
AR18	cloning	14-3-3_GRF4	R	CGCCGCCTCGAGTTAGATCTCCTTCTGTTCTTC	33
AF19	cloning	14-3-3_GRF5	F	CGCCGCGCGGCCGCATGTCTTCTGATTCGTCCCGG	35
AR19	cloning	14-3-3_GRF5	R	CGCCGCCTCGAGTCACTGCGAAGGTGGTGGTTG	33
AF20	cloning	14-3-3_GRF6	F	CGCCGCGCGGCCGCATGGCGGCGACATTAGGCAGA	35
AR20	cloning	14-3-3_GRF6	R	CGCCGCCTCGAGTCAGGCCTCGTCCATCTGCTC	33
AF21	cloning	14-3-3_GRF7	F	CGCCGCGCGGCCGCATGTCGTCTTCTCGGGAAGAG	35
AR21	cloning	14-3-3_GRF7	R	CGCCGCCTCGAGTCACTGCCCTGTCTCAGCTGG	33
AF22	cloning	14-3-3_GRF8	F	CGCCGCGCGGCCGCATGGCGACGACCTTAAGCAGA	35
AR22	cloning	14-3-3_GRF8	R	CGCCGCCTCGAGTCAGGCCTCATCCATCTGCTC	33
AF23	cloning	14-3-3_GRF9	F	CGCCGCGCGGCCGCATGGGTTCTGGAAAAGAGCGT	35
AR23	cloning	14-3-3_GRF9	R	CGCCGCCTCGAGTTAATTTGATTTACCCCGAGT	33
AF24	cloning	14-3-3_GRF10	F	CGCCGCGCGGCCGCATGGAGAATGAGAGGGAAAAG	35
AR24	cloning	14-3-3_GRF10	R	CGCCGCCTCGAGTTAGTTCTCATCTTGAGGCTC	33
AF25	cloning	14-3-3_GRF11	F	CGCCGCGCGGCCGCATGGAGAACGAGAGAGCGAAG	35
AR25	cloning	14-3-3_GRF11	R	CGCCGCCTCGAGTTAGATTTTGTTTACCTCATC	33
AF26	cloning	14-3-3_GRF12	F	CGCCGCGCGGCCGCATGTCATCATCAGGATCCGAC	35
AR26	cloning	14-3-3_GRF12	R	CGCCGCCTCGAGTCAGTTCTCAGTGGCATCGGC	33
AF27	cloning	14-3-3_GRF13	F	CGCCGCGCGGCCGCATGGAGAATGAGAGAGAAAAG	35
AR27	cloning	14-3-3_GRF13	R	CGCCGCCTCGAGCTAACCGTCTGTCTTATTACC	33
AF28	cloning	14-3-3_GRF14	F	CGCCGCGCGGCCGCATGGAGAATGAACAATCAACG	35
AR28	cloning	14-3-3_GRF14	R	CGCCGCCTCGAGTCACTTACTGTCAAATTCATT	33
AF29	cloning	14-3-3_GRF15	F	CGCCGCGCGGCCGCATGTGTTGTTACTTTGCCACT	35
AR29	cloning	14-3-3_GRF15	R	CGCCGCCTCGAGTTAACTATGCTTTGGTTCCGA	33
AF30	cloning	TCP1	F	CGCCGCGCGGCCGCATGTCGTCTTCCACCAATGAC	35
AR30	cloning	TCP1	R	CGCCGCCTCGAGTTAGTTTACAAAAGAGTCTTG	33

Oligo List 4. Oligos used for the yeast growth and quantitative ONPG enzyme activity assay (continued).

Oligo	Purpose	Target	Forward/Reverse	Sequence (5'-3')	bp
AF31	cloning	TCP2	F	CGCCGCGCGGCCGCATGATTGGAGATCTAATGAAG	35
AR31	cloning	TCP2	R	CGCCGCCTCGAGTCAGTTCTTGCCTTTACCCTT	33
AF32	cloning	TCP3	F	CGCCGCGCGGCCGCATGGCACCAGATAACGACCAT	35
AR32	cloning	TCP3	R	CGCCGCCTCGAGTTAATGGCGAGAATCGGATGA	33
AF33	cloning	TCP4	F	CGCCGCGCGGCCGCATGTCTGACGACCAATTCCAT	35
AR33	cloning	TCP4	R	CGCCGCCTCGAGTCAATGGCGAGAAATAGAGGA	33
AF34	cloning	TCP5	F	CGCCGCGCGGCCGCATGAGATCAGGAGAATGTGAT	35
AR34	cloning	TCP5	R	CGCCGCCTCGAGTCAAGAATCTGATTCATTATC	33
AF35	cloning	TCP6	F	CGCCGCGCGGCCGCATGGTCATGGAGCCCAAGAAG	35
AR35	cloning	TCP6	R	CGCCGCCTCGAGTTATGAACCATTTTCCTCTGC	33
AF36	cloning	TCP7	F	CGCCGCGCGGCCGCATGTCTATTAACAACAACAAC	35
AR36	cloning	TCP7	R	CGCCGCCTCGAGTTAACGTGGATCTTCCTCTCT	33
AF37	cloning	TCP8	F	CGCCGCGCGGCCGCATGGATCTCTCCGACATCCGA	35
AR37	cloning	TCP8	R	CGCCGCCTCGAGTCACTCAGAGCTATTTGAGTT	33
AF38	cloning	TCP9	F	CGCCGCGCGGCCGCATGGCGACAATTCAGAAGCTT	35
AR38	cloning	TCP9	R	CGCCGCACTAGTTCAGTGGTTCGATGACCGTGC	33
AF39	cloning	TCP10	F	CGCCGCGCGGCCGCATGGGACTTAAAGGATATAGC	35
AR39	cloning	TCP10	R	CGCCGCCTCGAGTTAGAGGTGTGAGTTTGGAGG	33
AF40	cloning	TCP11	F	CGCCGCGCGGCCGCATGATTTTTCAGAATGTGTGC	35
AR40	cloning	TCP11	R	CGCCGCACTAGTCTAATGGTGACGGCGTCTACG	33
AF41	cloning	TCP12	F	CGCCGCGCGGCCGCATGTTTCCTTCTCTAGATACC	35
AR41	cloning	TCP12	R	CGCCGCCTCGAGTCAGTAGCAGAGATAATCATA	33
AF42	cloning	TCP13	F	CGCCGCGCGGCCGCATGAATATCGTCTCTTGGAAA	35
AR42	cloning	TCP13	R	CGCCGCCTCGAGTCACATATGGTGATCACTTCC	33
AF43	cloning	TCP14	F	CGCCGCGCGGCCGCATGCAAAAGCCAACATCAAGT	35
AR43	cloning	TCP14	R	CGCCGCCTCGAGCTAATCTTGCTGATCCTCCTC	33
AF44	cloning	TCP15	F	CGCCGCGCGGCCGCATGGATCCGGATCCGGATCAT	35
AR44	cloning	TCP15	R	CGCCGCCTCGAGCTAGGAATGATGACTGGTGCT	33
AF45	cloning	TCP16	F	CGCCGCGCGGCCGCATGGATTCGAAAAATGGAATT	35
AR45	cloning	TCP16	R	CGCCGCCTCGAGTCAAACTGTGGTTGTGGCTGT	33
AF46	cloning	TCP17	F	CGCCGCGCGGCCGCATGGGAATAAAAAAAGAAGAT	35
AR46	cloning	TCP17	R	CGCCGCCTCGAGCTACTCGATATGGTCTGGTTG	33
AF47	cloning	TCP18	F	CGCCGCGCGGCCGCATGAACAACAACATTTTCAGT	35
AR47	cloning	TCP18	R	CGCCGCCTCGAGTCAATACATGTTTTGATAGTT	33
AF48	cloning	TCP19	F	CGCCGCGCGGCCGCATGGAATCGAATCACGAAGGC	35
AR48	cloning	TCP19	R	CGCCGCCTCGAGTTAAGTCTCATGACATGAAGA	33
AF49	cloning	TCP20	F	CGCCGCGCGGCCGCATGGATCCCAAGAACCTAAAT	35
AR49	cloning	TCP20	R	CGCCGCCTCGAGTTAACGACCTGAGCCTTGAGA	33

Oligo	Purpose	Target	Forward/Reverse	Sequence (5'-3')	bp
AF50	cloning	TCP21	F	CGCCGCGCGGCCGCATGGCCGACAACGACGGAGCA	35
AR50	cloning	TCP21	R	CGCCGCACTAGTTCAACGTGGTTCGTGGTCGTC	33
AF51	cloning	TCP22	F	CGCCGCGCGGCCGCATGAATCAGAATTCCTCTGTT	35
AR51	cloning	TCP22	R	CGCCGCCTCGAGTCACTTTTTGTCATCACCACC	33
AF52	cloning	TCP23	F	CGCCGCGCGGCCGCATGGAGTCCCACAACAACAAC	35
AR52	cloning	TCP23	R	CGCCGCCTCGAGTCAAGGAGAACCATCTATAGT	33
AF53	cloning	TCP24	F	CGCCGCGCGGCCGCATGGAGGTTGACGAAGACATT	35
AR53	cloning	TCP24	R	CGCCGCCTCGAGCTATCTCCTTTCCTTTGCCTT	33
AF7	cloning	FD	F	CGCCGCAAGCTTATGTTGTCATCAGCTAAGCAT	33
AR10_2	cloning	FD	R	CGCCGCCTCGAGCTACCTGTTTCCTAGCGCGGGAAC	36
G-25689	cloning	FT	F	CGCCGCAAGCTTATGTCTATAAATATAAGAGAC	33
G-25690	cloning	FT	R	CGCCGCCTCGAGCTAAAGTCTTCTTCCTCCGCA	33
AF56	cloning	ATC	F	CGCCGCGCGGCCGCATGGCCAGGATTTCCTCAGAC	35
AR56	cloning	ATC	R	CGCCGCACTAGTTCAACGGCGTCTAGCGGCGGT	33
AF57	cloning	BFT	F	CGCCGCAAGCTTATGTCAAGAGAAATAGAGCCA	33
AR57	cloning	BFT	R	CGCCGCCTCGAGTTAATAAGAAGGACGTCGTCG	33
AF58	cloning	MFT	F	CGCCGCAAGCTTATGGCGGCTTCTGTTGATCCT	33
AR58	cloning	MFT	R	CGCCGCCTCGAGCTAGCGTCTGCGTGAAGCAGG	33
AF59	cloning	TSF	F	CGCCGCAAGCTTATGTCTTTAAGTCGTAGAGAT	33
AR59	cloning	TSF	R	CGCCGCCTCGAGCTACGTTCTTCTTCCCCCACA	33
AF10	cloning	TFL1	F	CGCCGCAAGCTTATGGAGAATATGGGAACTAGA	33
AR13	cloning	TFL1	R	CGCCGCCTCGAGCTAGCGTTTGCGTGCAGCGGT	33

Oligo List 5. Oligos used for the split luciferase assay.

Oligo	Purpose	Target	Forward/Reverse	Sequence (5'-3')	bp
AF129	cloning	attR1-2	F	CGCCGCGGTACCGGACAAGTTTGTACAAAAAAGCTGAAC	39
AR129	cloning	attR1-2	R	CGCCGCCTGCAGACCACTTTGTACAAGAAAGCTGAAC	37
AF385	cloning	attR1-2	F	TGTTGTGGTACCACAAGTTTGTACAAAAAAGCTGAAC	37
AR387	cloning	attR1-2	R	TGTTGTGTCGACACCACTTTGTACAAGAAAGCTGAAC	37
AF260	cloning	TFL1	F	TGTTGTGGTACCATGGAGAATATGGGAACTAGA	33
AR260	cloning	TFL1	R	TGTTGTGTCGACGCGTTTGCGTGCAGCGGT	30
AF261	cloning	FT	F	TGTTGTGGTACCATGTCTATAAATATAAGAGAC	33
AR261	cloning	FT	R	TGTTGTGTCGACAAGTCTTCTTCCTCCGCAGCC	33

Oligo List 6. Oligos used for genotyping of T-DNA insertion lines.

Oligo	ABRC code	Target	LB	Sequence (5'-3')	bp
LBb1.3	SALK	-	-	ATTTTGCCGATTTCGGAAC	19
LB1	SAIL	-	-	GCCTTTTCAGAAATGGATAAATAGCCTTGCTTCC	34
LB4	SK	-	-	ATACGACGGATCGTAATTTGTCG	23
LB5	GABI	-	-	CCCATTTGGACGTGAATGTAGACAC	25
LB6	Wisc DsLox	-	-	AACGTCCGCAATGTGTTATTAAGTTGTC	28
LB7	FT	-	-	ACCCGACCGGATCGTATCGGT	21
LB8	JIC SM	-	-	TACGAATAAGAGCGTCCATTTTAGAGTGA	29
LP24	SALK_132254.34.50.x	TCP11	LBb1.3	AAATCAGAACCTTCCGAATCG	21
RP24	SALK_132254.34.50.x	TCP11	LBb1.3	CTAAAGACCGTCACACGAAGG	21
LP35	WiscDsLox468E8 (HM)	TCP18	LB6	AAGAACATAAACAAACACAAGGTCC	25
RP35	WiscDsLox468E8 (HM)	TCP18	LB6	TCATCCTACGATCTCGTGTCC	21
LP10	SAIL_1174_D02	TCP4	LB1	TTGGGACCAAAAGATTACGTG	21
RP10	SAIL_1174_D02	TCP4	LB1	ACTATCATCATCAGCATCCGC	21
LP30	SALK_074476.56.00.x	TCP16 5'-UTR	LBb1.3	TCATTTAGGGTCAAATTCCCC	21
RP30	SALK_074476.56.00.x	TCP16 5'-UTR	LBb1.3	GCTGAAAATCCCAAAAACCTC	21
LP29	SALK_011491.56.00.x	TCP15	LBb1.3	AGAACCACGTAAGCCCATCTC	21
RP29	SALK_011491.56.00.x	TCP15	LBb1.3	TCAAATGAACTCCACTACCGC	21
LP38	SALK_088460.34.25.x	TCP20	LBb1.3	CCACCTGCAAGTTCAAACAAC	21
RP38	SALK_088460.34.25.x	TCP20	LBb1.3	TCCGACAAAGAACCAAACAAG	21
LP4	SALK_144731.51.25.x	TCP2	LBb1.3	AACCGGAATTTAACAAATCCG	21
RP4	SALK_144731.51.25.x	TCP2	LBb1.3	CCGAAAGCAGTTGATTCAGC	20
LP14	SK17759	TCP6	LB4	TTTGATTGAGCTTTGGATTGG	21
RP14	SK17759	TCP6	LB4	TCTGCTGCTGATCTTCATGTG	21
LP69	SM_3.29639	TCP5	LB8	TGAATCTGTTTTTCCTCCATCC	22
RP69	SM_3.29639	TCP5	LB8	CTCGAAGCAGCAAAAGATGAC	21
LP44	SAIL_443_F02	TCP23	LB1	TCAACACAAACTCATAGCCCC	21
RP44	SAIL_443_F02	TCP23	LB1	TGAGGCTTTTGCTCAAGACTC	21
LP39	SALK_143403.37.70.x	TCP21	LBb1.3	TGATTGAATGGCAATGATCAC	21
RP39	SALK_143403.37.70.x	TCP21	LBb1.3	TAGTCAACACCGGAGTCAAGC	21
LP23	SALK_050436.54.25.x	TCP10	LBb1.3	AAAAGGTTGAAAGCAAAAGGG	21
RP23	SALK_050436.54.25.x	TCP10	LBb1.3	GATGTTTGTACCACCACCACC	21
LP28	WiscDsLox477-480P20	TCP14	LB6	CCGAAATCTTTTGATTATGGAC	22
RP28	WiscDsLox477-480P20	TCP14	LB6	AGCGGAAATGAGAAGGAAGAG	21
LP6	WiscDsLox441C3	TCP3	LB6	ACCAAGCACGAATCATAGGTG	21
RP6	WiscDsLox441C3	TCP3	LB6	TTTAGGGTTTGGGATTTGGAG	21
LP32	SALK_148580.54.75.x	TCP17	LBb1.3	TCTTTGGATCCTCAGATCTTCC	22
RP32	SALK_148580.54.75.x	TCP17	LBb1.3	ATGTACCTTTGCTCGCATCAG	21

Oligo List 7. Oligos used for TCP/TCP-clade specific amiRNAs.

Oligo	Purpose	amiR_target(s)_off-target(s)	Forward/Reverse	Sequence (5'-3')	bp
mOA	amiR stemloop precursor construction	-	F	TGTTGTAAGCTTCAAACACACGCTCGGACGCAT	33
mOB	amiR stemloop precursor construction	-	R	TGTTGTCTCGAGCATGGCGATGCCTTAAATAAA	33
1KD4	amiR stemloop precursor construction	amiR_TCP8, 14, 15_off transposable element	R	gaAGGATTTTTGACCTCGCTTACtctacatatatattcct	40
1KD3	amiR stemloop precursor construction	amiR_TCP8, 14, 15_off transposable element	F	gaGTAAGCGAGGTCAAAAATCCTtcacaggtcgtgatatg	40
1KD2	amiR stemloop precursor construction	amiR_TCP8, 14, 15_off transposable element	R	gaGTGAGCGAGGTCATAAATCCAtcaaagagaatcaatga	40
1KD1	amiR stemloop precursor construction	amiR_TCP8, 14, 15_off transposable element	F	gaTGGATTTATGACCTCGCTCACtctctcttttgtattcc	40
2KD4	amiR stemloop precursor construction	amiR_TCP8, 14, 22	R	gaATTATGAGCTAGCTCTCGTGGtctacatatatattcct	40
2KD3	amiR stemloop precursor construction	amiR_TCP8, 14, 22	F	gaCCACGAGAGCTAGCTCATAATtcacaggtcgtgatatg	40
2KD2	amiR stemloop precursor construction	amiR_TCP8, 14, 22	R	gaCCGCGAGAGCTAGGTCATAAAtcaaagagaatcaatga	40
2KD1	amiR stemloop precursor construction	amiR_TCP8, 14, 22	F	gaTTTATGACCTAGCTCTCGCGGtctctctcttttgtattcc	40
3KD4	amiR stemloop precursor construction	amiR_TCP7, 21	R	gaATATGATTGAAGGCTCAGTTTtctacatatatattcct	40
3KD3	amiR stemloop precursor construction	amiR_TCP7, 21	F	gaAAACTGAGCCTTCAATCATATtcacaggtcgtgatatg	40
3KD2	amiR stemloop precursor construction	amiR_TCP7, 21	R	gaAAGCTGAGCCTTCTATCATAAtcaaagagaatcaatga	40
3KD1	amiR stemloop precursor construction	amiR_TCP7, 21	F	gaTTATGATAGAAGGCTCAGCTTtctctctttttgtattcc	40
4KD4	amiR stemloop precursor construction	amiR_TCP7, 21	R	gaATGTCCGTAATCCGGCGTTGCtctacatatatattcct	40
4KD3	amiR stemloop precursor construction	amiR_TCP7, 21	F	gaGCAACGCCGGATTACGGACATtcacaggtcgtgatatg	40
4KD2	amiR stemloop precursor construction	amiR_TCP7, 21	R	gaGCGACGCCGGATTTCGGACAAtcaaagagaatcaatga	40
4KD1	amiR stemloop precursor construction	amiR_TCP7, 21	F	gaTTGTCCGAAATCCGGCGTCGCtctctctttttgtattcc	40
5KD4	amiR stemloop precursor construction	amiR_TCP5, 17	R	gaAGCTAGGGTGACTCGGCCTTAtctacatatatattcct	40
5KD3	amiR stemloop precursor construction	amiR_TCP5, 17	F	gaTAAGGCCGAGTCACCCTAGCTtcacaggtcgtgatatg	40
5KD2	amiR stemloop precursor construction	amiR_TCP5, 17	R	gaTAGGGCCGAGTCAGCCTAGCAtcaaagagaatcaatga	40
5KD1	amiR stemloop precursor construction	amiR_TCP5, 17	F	gaTGCTAGGCTGACTCGGCCCTAtctctctttttgtattcc	40
6KD4	amiR stemloop precursor construction	amiR_TCP5, 13, 17	R	gaACTTGAACGTCGTAGAGTGGAtctacatatatattcct	40
6KD3	amiR stemloop precursor construction	amiR_TCP5, 13, 17	F	gaTCCACTCTACGACGTTCAAGTtcacaggtcgtgatatg	40
6KD2	amiR stemloop precursor construction	amiR_TCP5, 13, 17	R	gaTCAACTCTACGACCTTCAAGAtcaaagagaatcaatga	40
6KD1	amiR stemloop precursor construction	amiR_TCP5, 13, 17	F	gaTCTTGAAGGTCGTAGAGTTGAtctctctttttgtattcc	40
7KD4	amiR stemloop precursor construction	amiR_TCP2, TCP24	R	gaAACTGAACGGTCCCCCTGTTAtctacatatatattcct	40
7KD3	amiR stemloop precursor construction	amiR_TCP2, TCP24	F	gaTAACAGGGGGACCGTTCAGTTtcacaggtcgtgatatg	40
7KD2	amiR stemloop precursor construction	amiR_TCP2, TCP24	R	gaTAGCAGGGGGACCCTTCAGTAtcaaagagaatcaatga	40
7KD1	amiR stemloop precursor construction	amiR_TCP2, TCP24	F	gaTACTGAAGGGTCCCCCTGCTAtctctctttttgtattcc	40
8KD4	amiR stemloop precursor construction	amiR_TCP2, TCP24	R	gaAACTGAACGGTCCCCTTGTTAtctacatatatattcct	40
8KD3	amiR stemloop precursor construction	amiR_TCP2, TCP24	F	gaTAACAAGGGGACCGTTCAGTTtcacaggtcgtgatatg	40
8KD2	amiR stemloop precursor construction	amiR_TCP2, TCP24	R	gaTAGCAAGGGGACCCTTCAGTAtcaaagagaatcaatga	40
8KD1	amiR stemloop precursor construction	amiR_TCP2, TCP24	F	gaTACTGAAGGGTCCCCTTGCTAtctctctttttgtattcc	40
9KD4	amiR stemloop precursor construction	amiR_TCP3, TCP4, TCP10	R	gaAGATAAGGCAATCAGCGGTATctacatatatattcct	40
9KD3	amiR stemloop precursor construction	amiR_TCP3, TCP4, TCP10	F	gaATACCGCTGATTGCCTTATCTtcacaggtcgtgatatg	40
9KD2	amiR stemloop precursor construction	amiR_TCP3, TCP4, TCP10	R	gaATGCCGCTGATTGGCTTATCAtcaaagagaatcaatga	40
9KD1	amiR stemloop precursor construction	amiR_TCP3, TCP4, TCP10	F	gaTGATAAGCCAATCAGCGGCATctctctctttttgtattcc	40
10KD4	amiR stemloop precursor construction	amiR_TCP3, TCP4, TCP10	R	gaAACTGGAGTGAAGGGGCCTACtctacatatatattcct	40
10KD3	amiR stemloop precursor construction	amiR_TCP3, TCP4, TCP10	F	gaGTAGGCCCCTTCACTCCAGTTtcacaggtcgtgatatg	40
10KD2	amiR stemloop precursor construction	amiR_TCP3, TCP4, TCP10	R	gaGTGGGCCCCTTCAGTCCAGTAtcaaagagaatcaatga	40
10KD1	amiR stemloop precursor construction	amiR_TCP3, TCP4, TCP10	F	gaTACTGGACTGAAGGGGCCCACtctctctttttgtattcc	40
11KD4	amiR stemloop precursor construction	amiR_TCP6	R	gaACTTAATACAAGTCCAGGTGGtctacatatatattcct	40
11KD3	amiR stemloop precursor construction	amiR_TCP6	F	gaCCACCTGGACTTGTATTAAGTtcacaggtcgtgatatg	40
11KD2	amiR stemloop precursor construction	amiR_TCP6	R	gaCCGCCTGGACTTGAATTAAGAtcaaagagaatcaatga	40
11KD1	amiR stemloop precursor construction	amiR_TCP6	F	gaTCTTAATTCAAGTCCAGGCGGtctctctttttgtattcc	40
12KD4	amiR stemloop precursor construction	amiR_TCP6	R	gaAGTAACCAAACTCTACGATCAtctacatatatattcct	40
12KD3	amiR stemloop precursor construction	amiR_TCP6	F	gaTGATCGTAGAGTTTGGTTACTtcacaggtcgtgatatg	40

Oligo List 7. Oligos used for TCP/TCP-clade specific amiRNAs (continued).

Oligo	Purpose	amiR_target(s)_off-target(s)	Forward/Reverse	Sequence (5'-3')	bp
12KD2	amiR stemloop precursor construction	amiR_TCP6	R	gaTGGTCGTAGAGTTAGGTTACAtcaaagagaatcaatga	40
12KD1	amiR stemloop precursor construction	amiR_TCP6	F	gaTGTAACCTAACTCTACGACCAtctctctttttgtattcc	40
13KD4	amiR stemloop precursor construction	amiR_TCP5, 8, 17_off 8, 14, 22	R	gaAGGATTTTTGACCTAGCGTTCtctacatatatattcct	40
13KD3	amiR stemloop precursor construction	amiR_TCP5, 8, 17_off 8, 14, 22	F	gaGAACGCTAGGTCAAAAATCCTtcacaggtcgtgatatg	40
13KD2	amiR stemloop precursor construction	amiR_TCP5, 8, 17_off 8, 14, 22	R	gaGAGGGCTAGGTCATAAATCCAtcaaagagaatcaatga	40
13KD1	amiR stemloop precursor construction	amiR_TCP5, 8, 17_off 8, 14, 22	F	gaTGGATTTATGACCTAGCGCTCtctctctttttgtattcc	40
14KD4	amiR stemloop precursor construction	amiR_TCP5, 8, 17_off TCP9, 21	R	gaAGAAAAAGTCTAGCCGCGTACtctacatatatattcct	40
14KD3	amiR stemloop precursor construction	amiR_TCP5, 8, 17_off TCP9, 21	F	gaGTACGCGGCTAGACTTTTTCTtcacaggtcgtgatatg	40
14KD2	amiR stemloop precursor construction	amiR_TCP5, 8, 17_off TCP9, 21	R	gaGTGCGCGGCTAGAGTTTTTCAtcaaagagaatcaatga	40
14KD1	amiR stemloop precursor construction	amiR_TCP5, 8, 17_off TCP9, 21	F	gaTGAAAAACTCTAGCCGCGCACtctctctttttgtattcc	40
15KD4	amiR stemloop precursor construction	amiR_TCP2, 24, 5, 17_off TCP13	R	gaAGTGTCTTTCTTTGCCTCTAAtctacatatatattcct	40
15KD3	amiR stemloop precursor construction	amiR_TCP2, 24, 5, 17_off TCP13	F	gaTTAGAGGCAAAGAAAGACACTtcacaggtcgtgatatg	40
15KD2	amiR stemloop precursor construction	amiR_TCP2, 24, 5, 17_off TCP13	R	gaTTGGAGGCAAAGATAGACACAtcaaagagaatcaatga	40
15KD1	amiR stemloop precursor construction	amiR_TCP2, 24, 5, 17_off TCP13	F	gaTGTGTCTATCTTTGCCTCCAAtctctctttttgtattcc	40
16KD4	amiR stemloop precursor construction	amiR_TCP2, 5, 17	R	gaATAATCGTTCTTGAGGGTTCTtctacatatatattcct	40
16KD3	amiR stemloop precursor construction	amiR_TCP2, 5, 17	F	gaAGAACCCTCAAGAACGATTATtcacaggtcgtgatatg	40
16KD2	amiR stemloop precursor construction	amiR_TCP2, 5, 17	R	gaAGGACCCTCAAGATCGATTAAtcaaagagaatcaatga	40
16KD1	amiR stemloop precursor construction	amiR_TCP2, 5, 17	F	gaTTAATCGATCTTGAGGGTCCTtctctctttttgtattcc	40
17KD4	amiR stemloop precursor construction	amiR_TCP2, 24, 5_off TCP17	R	gaACTTTGCGACCGAATGCTTGTtctacatatatattcct	40
17KD3	amiR stemloop precursor construction	amiR_TCP2, 24, 5_off TCP17	F	gaACAAGCATTCGGTCGCAAAGTtcacaggtcgtgatatg	40
17KD2	amiR stemloop precursor construction	amiR_TCP2, 24, 5_off TCP17	R	gaACGAGCATTCGGTGGCAAAGAtcaaagagaatcaatga	40
17KD1	amiR stemloop precursor construction	amiR_TCP2, 24, 5_off TCP17	F	gaTCTTTGCCACCGAATGCTCGTtctctctttttgtattcc	40
18KD4	amiR stemloop precursor construction	amiR_TCP2, 24, 14, 15, 22_off 5, 17	R	gaAGTGTCTTTCTTTGCCTCTAAtctacatatatattcct	40
18KD3	amiR stemloop precursor construction	amiR_TCP2, 24, 14, 15, 22_off 5, 17	F	gaTTAGAGGCAAAGAAAGACACTtcacaggtcgtgatatg	40
18KD2	amiR stemloop precursor construction	amiR_TCP2, 24, 14, 15, 22_off 5, 17	R	gaTTGGAGGCAAAGATAGACACAtcaaagagaatcaatga	40
18KD1	amiR stemloop precursor construction	amiR_TCP2, 24, 14, 15, 22_off 5, 17	F	gaTGTGTCTATCTTTGCCTCCAAtctctctttttgtattcc	40
19KD4	amiR stemloop precursor construction	amiR_TCP2, 14, 22_off 5, 17	R	gaATAATCGTTCTTGAGGGTTCTtctacatatatattcct	40
19KD3	amiR stemloop precursor construction	amiR_TCP2, 14, 22_off 5, 17	F	gaAGAACCCTCAAGAACGATTATtcacaggtcgtgatatg	40
19KD2	amiR stemloop precursor construction	amiR_TCP2, 14, 22_off 5, 17	R	gaAGGACCCTCAAGATCGATTAAtcaaagagaatcaatga	40
19KD1	amiR stemloop precursor construction	amiR_TCP2, 14, 22_off 5, 17	F	gaTTAATCGATCTTGAGGGTCCTtctctctttttgtattcc	40
20KD4	amiR stemloop precursor construction	amiR_TCP9, 19	R	gaAAGTTCCCTTAACCGATATTGtctacatatatattcct	40
20KD3	amiR stemloop precursor construction	amiR_TCP9, 19	F	gaCAATATCGGTTAAGGGAACTTtcacaggtcgtgatatg	40
20KD2	amiR stemloop precursor construction	amiR_TCP9, 19	R	gaCAGTATCGGTTAACGGAACTAtcaaagagaatcaatga	40
20KD1	amiR stemloop precursor construction	amiR_TCP9, 19	F	gaTAGTTCCGTTAACCGATACTGtctctctttttgtattcc	40
21KD4	amiR stemloop precursor construction	amiR_TCP9, 19	R	gaACCGAATGGTTTCGCCGTTGGtctacatatatattcct	40
21KD3	amiR stemloop precursor construction	amiR_TCP9, 19	F	gaCCAACGGCGAAACCATTCGGTtcacaggtcgtgatatg	40
21KD2	amiR stemloop precursor construction	amiR_TCP9, 19	R	gaCCGACGGCGAAACGATTCGGAtcaaagagaatcaatga	40
21KD1	amiR stemloop precursor construction	amiR_TCP9, 19	F	gaTCCGAATCGTTTCGCCGTCGGtctctctttttgtattcc	40
22KD4	amiR stemloop precursor construction	amiR_TCP22, 23	R	gaAGCGATGTTAGCTGGCTGTGCtctacatatatattcct	40
22KD3	amiR stemloop precursor construction	amiR_TCP22, 23	F	gaGCACAGCCAGCTAACATCGCTtcacaggtcgtgatatg	40
22KD2	amiR stemloop precursor construction	amiR_TCP22, 23	R	gaGCGCAGCCAGCTATCATCGCAtcaaagagaatcaatga	40
22KD1	amiR stemloop precursor construction	amiR_TCP22, 23	F	gaTGCGATGATAGCTGGCTGCGCtctctctttttgtattcc	40
23KD4	amiR stemloop precursor construction	amiR_TCP22, 23	R	gaACCTAGCAGTTGACCTCCTAGtctacatatatattcct	40
23KD3	amiR stemloop precursor construction	amiR_TCP22, 23	F	gaCTAGGAGGTCAACTGCTAGGTtcacaggtcgtgatatg	40
23KD2	amiR stemloop precursor construction	amiR_TCP22, 23	R	gaCTGGGAGGTCAACAGCTAGGAtcaaagagaatcaatga	40
23KD1	amiR stemloop precursor construction	amiR_TCP22, 23	F	gaTCCTAGCTGTTGACCTCCCAGtctctctttttgtattcc	40
24KD4	amiR stemloop precursor construction	amiR_TCP8, 23	R	gaAAAAGTACAGAAGTTCGCTGCtctacatatatattcct	40
24KD3	amiR stemloop precursor construction	amiR_TCP8, 23	F	gaGCAGCGAACTTCTGTACTTTTtcacaggtcgtgatatg	40

Oligo	Purpose	amiR_target(s)_off-target(s)	Forward/Reverse	Sequence (5'-3')	bp
24KD2	amiR stemloop precursor construction	amiR_TCP8, 23	R	gaGCGGCGAACTTCTCTACTTTAtcaaagagaatcaatga	40
24KD1	amiR stemloop precursor construction	amiR_TCP8, 23	F	gaTAAAGTAGAGAAGTTCGCCGCtctctctttttgtattcc	40
25KD4	amiR stemloop precursor construction	amiR_TCP8, 23 _off T14, 15	R	gaAAAAGTACAGAAGTTCGCTGGtctacatatatattcct	40
25KD3	amiR stemloop precursor construction	amiR_TCP8, 23 _off T14, 15	F	gaCCAGCGAACTTCTGTACTTTTtcacaggtcgtgatatg	40
25KD2	amiR stemloop precursor construction	amiR_TCP8, 23 _off T14, 15	R	gaCCGGCGAACTTCTCTACTTTAtcaaagagaatcaatga	40
25KD1	amiR stemloop precursor construction	amiR_TCP8, 23 _off T14, 15	F	gaTAAAGTAGAGAAGTTCGCCGGtctctctttttgtattcc	40
26KD4	amiR stemloop precursor construction	amiR_TCP8, 22	R	gaAGCATACCAATTCGCCGTTCCtctacatatatattcct	40
26KD3	amiR stemloop precursor construction	amiR_TCP8, 22	F	gaGGAACGGCGAATTGGTATGCTtcacaggtcgtgatatg	40
26KD2	amiR stemloop precursor construction	amiR_TCP8, 22	R	gaGGGACGGCGAATTCGTATGCAtcaaagagaatcaatga	40
26KD1	amiR stemloop precursor construction	amiR_TCP8, 22	F	gaTGCATACGAATTCGCCGTCCCtctctctttttgtattcc	40

Acknowledgments

First of all, I would like to express my sincere gratitude to my supervisor, Prof. Dr. Detlef Weigel, for his tremendous help, patience and guidance throughout my Ph.D study. From Prof. Weigel, I learned about how amazing plant science can be and how to become a respectful scientist. I am certain that the study and research experience in Weigel lab is going to benefit me life-long. Sincere thanks to Prof. Weigel for giving me such an invaluable opportunity to join his lab - vielen Dank!

My gratitude must also go to the thesis evaluation committee and panel members of my progress assessment committee, Prof. Dr. Friedrich Schöffl and Dr. Markus Schmid, for their insightful advice and comments on my research findings. In addition, I would like to acknowledge my research advisors in Germany, including Dr. Sascha Laubinger, Dr. Jiawei Wang, Dr. Yasushi Kobayashi, Dr. Rebecca Schwab, and Dr. Roosa Laitinen for providing critical advice in defining my research directions and for kindly teaching various technical skills without asking for credit or reward.

Also, I would like to thank a number of current and previous members of Weigelworld, especially Eunyoung, Sang-Tae, Yalong, Jun, Jian-Feng, Xi, Chang, Caomong, Beth, George, Pablo, Nacho, David, Carmen, Lisa, Cris, Eshita, Diep, Johannes, Steffen, Dr. Christine Dreyer, Jathish, Vinicius, Dan, Danielle, Claude, Jorge, Mike, Jonas, Dino, and Subhashini, etc., for their generous sharing of research expertise and laughter.

Further, my true appreciation of their help should also extend to the administrative and technical staffs of Department 6, including Huelya, Frank, Josip, Anette, Monika, Manuela, Christa, Andrea, and the cleaning staffs consisting Gertrund, Evi, Hedda, Lydia, Tamara, and Alex, for their extremely efficient work making my large-scale cloning, dipping and assays possible.

Last but not least, I would like to thank every member in the Weigelworld for giving me such a wonderful experience in Tuebingen.

§

Dedicated to
my parents, grandparents
who inspire and support me in my research career,
and to my my wife and son
for being the cheerleading squad I have needed.

This work is also dedicated to the memory of
my respectful uncle, Louis Chan (-2010) and my two beloved cats, Toffee (-2008) and Toast (-2009),
who passed away during my Ph.D. study in Germany.

§